MICRO AND MACROSCOPIC ANALYSIS OF CROWD BEHAVIOR

Submitted in partial fulfilment of the requirements

for the award of the degree of

DOCTOR OF PHILOSOPHY
in
CIVIL ENGINEERING

by

POOJARI YUGENDAR

(Roll No: 715002)

Supervisor

Dr. K. V. R. RAVI SHANKAR

Assistant Professor

TRANSPORTATION DIVISION

DEPARTMENT OF CIVIL ENGINEERING

NATIONAL INSTITUTE OF TECHNOLOGY

WARANGAL- 506 004 (T.S.) INDIA

MARCH 2020

NATIONAL INSTITUTE OF TECHNOLOGY
WARANGAL

CERTIFICATE

This is to certify that the thesis entitled "**MICRO AND MACROSCOPIC ANALYSIS OF CROWD BEHAVIOR"** being submitted by **Mr. POOJARI YUGENDAR** for the award of the degree of **DOCTOR OF PHILOSOPHY** to the Faculty of **Civil Engineering** of **NATIONAL INSTITUTE OF TECHNOLOGY, WARANGAL** is a record of bonafide research work carried out by him under my supervision and it has not been submitted elsewhere for award of any degree.

Dr. K. V. R. RAVI SHANKAR
Thesis Supervisor
Assistant Professor
Department of Civil Engineering
National Institute of Technology, Warangal
Warangal (T.S.) – INDIA

APPROVAL SHEET

This Thesis entitled "**MICRO AND MACROSCOPIC ANALYSIS OF CROWD BEHAVIOR**" by **Mr. POOJARI YUGENDAR** is approved for the degree of Doctor of Philosophy.

Examiners

_____

_____

_____

Supervisor

_____

Chairman

_____

Date: _____

DECLARATION

This is to certify that the work presented in the thesis entitled **"MICRO AND MACROSCOPIC ANALYSIS OF CROWD BEHAVIOR"** is a bonafide work done by me under the supervision of **Dr. K. V. R. RAVI SHANKAR** and was not submitted elsewhere for the award of any degree. I declare that this written submission represents my ideas in my own words and where others ideas or words have been included, I have adequately cited and referenced the original sources. I also declare that I have adhered to all principles of academic honesty and integrity and have not misrepresented or fabricated or falsified any idea / data / fact /source in my submission. I understand that any violation of the above will be a cause for disciplinary action by the Institute and can also evoke penal action from the sources which have thus not been properly cited or from whom proper permission has not been taken when needed.

_____

(POOJARI YUGENDAR)

(Roll No: **715002**)

Date: _____

Dedicated to

My Beloved Family

ACKNOWLEDGEMENTS

First and foremost, I have to thank my parents **Sri Poojari Ilaiah** and **Poojari Parvatamma**, for their love and support throughout my life. Thank you both for giving me strength to chase my dreams. My Sisters, Brothers-in-law and Nephews deserve my wholehearted thanks as well.

With great pleasure and proud privilege, I manifest my heartier thankfulness to my research supervisor, **Dr. K. V. R. Ravi Shankar,** Assistant Professor, Department of Civil Engineering, for his valuable suggestions, sagacious guidance, scholarly advice and comprehensive critical remarks in bringing out this research work with artistry.

I am perspicuous to divulge my sincere gratefulness to **Prof. M. Chandrasekhar,** Head, Department of Civil Engineering and Chairman, Doctoral Scrutiny Committee for his enlightening guidance and immense help rendered in bringing out this work.

I am grateful to **Prof. C. S. R. K. Prasad**, **Dr. Arpan Mehar**, Department of Civil Engineering and **Prof. D. V. S. S. Siva Sarma,** Department of Electrical Engineering, members of Doctoral Scrutiny Committee, for their guidance and help during the investigation.

I am also thankful to **Dr. Venkaiah Chowdary**, **Dr. S. Shankar**, the faculty members of Transportation Division, NITW.

It is my pleasure to acknowledge **D. Abhigna**, research scholar and my well-wisher for her patience, continuous support and understanding during my research work.

I thank **Prof. K. Ramachandra Rao**, IIT Delhi for the technical support given during the period of research work.

I thank my friends and fellow research scholars K. Mahaboob Peera, Utsav Vishal, Syed Hussain, Harinder, Arjun Kumar, J. Jaya Krishna, S. Eswar, K. Aditya, Prashanth Sekhar Lokku, S. Srikanth, G. Pallavi, L. Govinda, S. Chakravarthi, K. Srikanth, Sravan Kumar, Githender Transportation students for their direct or indirect suggestions throughout the period of my research work.

I thank my friends and fellow research scholars T Chaitanya, K Hanuma, M Venu, N. Venkatesh, K Srikanth, Raji Rajeshwari, Oggu Praveen, B Murali, Guru Prathap Reddy, Harsha Praneeth Pavani for their direct or indirect suggestions throughout the period of my research work.

I thank my B. E friends R. Venkatram, B. Anil, K. Vishnu, S. Naresh, U. Naresh, A. Chandra Sekhar for their help during the period of my research work.

I am thankful to Mr. P. Ashok Kumar, Mr. P. Rajendra Prasad, Mr. Md. Hussain, Mr. Y. Mahesh Kumar, Administrative staff for the help during the research period.

I want to thank Mr. Gaffar, Mr. Ramesh Lab Technicians in transportation laboratory for the constant support during my research work.

Finally I thank everyone, who contributed either directly or indirectly in successful completion of this work.

- ***POOJARI YUGENDAR***

ABSTRACT

Development of cities across the globe is unstoppable and it's very difficult to carefully plan cities. In this situation, understanding pedestrian movements is very essential for design facilities with respect to safety, security, level of service and low cost. Religious occasions, congregations at carnivals, political rallies, and crowd at terminals are occasions pertaining to crowd congregations. These congregations act as serious intimidations for the crowd, because a large number of people moving in limited space results in crowd stampedes. Most of the crowd crushes occurr in developing countries during large congregations and more people die when compared with developed countries (Andrade et al. 2006). Prassana Kumar et al. (2015) stated that on an average more than 70 people per year lost their lives due to stampedes in India. Indian states of Maharashtra and Andhra Pradesh are in top the list of more than 300 deaths in the 15 years (2001-15). Hence, it is very important to study crowd behavior to increase public safety. Understanding crowd behavior and the tools required to forecast crowd behavior are necessary in planning and design facilities such as bus terminals, train platforms, etc.

Three locations were selected for the study: Location-1 is situated in Vijayawada, Andhra Pradesh, India, whereas Location-2 is situated in Medaram, Telangana, India and Location-3 is situated in NIT, Warangal, Telangana. Data was collected by placing digital camera on top of the building. The videos were taken from a high-raise point near the location to avoid occlusion problem during tracking. Camera stands were used to ensure the videos recorded were steady, without any disturbance that might affect the frames at various stages of analysis. Markings were made on the road sections. Distance measurements were made using a standard tape such that the speeds could be cross-checked while extracting data using software.

Various parameters extracted from the video include people count, density, speed of individual persons, and crowd flow. Number of persons in a frame was counted using background subtraction technique. Speed and tracking of each individual were extracted using TRACKER software. Pixel coordinates were converted to real coordinates using the method of Wolf and Dewitt (2000).

In microscopic analysis, parameters like age, gender, group size, child carrying, child holding, and people with and without luggage were considered. For statistical analysis, ANOVA and Pearson correlation tests were performed using SPSS. From these tests, it was

concluded that, there was a significant effect of age, gender, density and luggage on the crowd walking speed. Gender has more significant effect on speed followed by luggage and age. MLR, ANN, ANFIS models were developed for the modelling of crowd speed using the above mentioned factors in the study. The developed model was validated using RMSE (Route Mean Square Error) and MAE (Mean Absolute Error) values. Based on RMSE and MAE values, ANFIS model was observed to be better-fitted model when compared to other models. Gender, density and luggage have a negative effect on speed of the crowd while age has a conflicting effect on speed of the crowd. The increase in number of female persons in the crowd leads to speed reduction. Generally, the speed of the female person is low compared to male. Density is found to have an adverse effect on speed, whereas, at low crowd density, the speed of the crowd was high due to fewer interactions between persons and more space for overtaking. The speed was observed to be low at high crowd density because of more interactions between persons and little space for overtaking. Further, it was observed that luggage has an adverse effect on crowd speed. The speed of people with luggage is low when compared to people without luggage. Children and the old people were negatively associated with crowd speed. Also, as the number of children and the old people increases, it was found that the speed of crowd decreased. Additionally, younger and elder persons were positively associated with crowd speed. As the number of younger and elder persons increased, the speed of the crowd was observed to be higher.

In macroscopic analysis, flow parameters such as free flow speed (U_f), optimum speed (U_o), jam density (K_j), optimum density (K_o) and maximum flow (Q_m) were estimated from the fundamental relationships. Flow–density and speed–flow relationships were then calibrated from the speed–density relationship. To determine the crowd characteristics, two single-regime speed–density models were used Model I - Greenshield's (L) and Model II - Underwood (E). Model I gave the minimum MAPE and RMSE values, which implies that Model-I gives better prediction than Model II for crowd movement. In real conditions, it is not possible to model the entire traffic mass as a single regime due to the existence of both uncongested and congested flow. A multi-regime model concept is thus essential to represent different flow conditions. For two-regime model, the speed–density relationship is developed for two regimes by introducing a breakpoint to distinguish between two different regimes. This breakpoint is identified by K-means clustering analysis using SPSS software. The final selection of the breakpoints was determined using a visual approach. Four models i.e., Model I, II, III and IV representing L-L, L-E, E-L, and E-E were used to determine the crowd characteristics in two-regime model. The minimum MAPE and RMSE values of the crowd

characteristics (speed, density and flow) were obtained using Model III (E-L). Three-regime models consider uncongested flow, transitional flow and congested flow regimes. In three-regime models, the speed–density relationship is developed for three regimes by introducing breakpoints to distinguish between three different regimes. Four models i.e., Model I, II, III and IV representing L-L-L, E-E-E, E-E-L, and E-L-E were used to determine the crowd characteristics in three-regime model. Model-II (E-E-E), with the lowest MAPE and RMSE values when compared to all the four models, provided the best predictions. MAPE and RMSE values of the best multi-regime models were less than that of the best single-regime model. Therefore, multi-regime models provide better predictions than single-regime model. Of the multi-regime models, MAPE and RMSE values of three-regime models were less when compared to two-regime model, which implies that the three-regime model gives better predictions than two-regime models.

In capacity analysis, buffer space is introduced in this study to study the influence of overtaking within the crowd while evacuation. Therefore, this study is divided into two cases: presence of buffer space and absence of buffer space. The height and length of the bottleneck are constant. Five varied widths of bottlenecks which consisted of 80, 100, 120, 140, and 160 centimeters repectively were chosen. In this experiment, 30 and 50 individuals were involved in two different compositions. The evacuees were divided into two groups and assigned different walking responsibilities for every test (move slowly, and move fast). The groups were diverse and comprised male and female. Since the entire group of 50 was of same age group, the group was divided so as to incorporate the effect of age variation within the group. One group of evacuees was designated by the colour of their caps (white). Whereas, persons without caps represent normally acting participants, while the persons with caps follow specific instructions.

The first step in density estimation was the conversion of video into frames, and the next step was to divide the entire area (50 m^2) into equal number of grids having a grid size of 0.5 × 1 meter. Further, using the manual count method, the number of persons in each grid was noted, and finally, the average values of densities (people/area) for all frames in each grid were computed. The whole study area was divided into grids, in order to calculate the density in each grid because it was not uniform throughout the study area. This also gives us an idea of the path/ route of evacuation chosen by most individuals at the time of evacuation. In crowd analysis, another issue involves the tracking of people and finding the location of the same person in a series of images. For this a free open source software TRACKER was used, which tracks persons semi-automatically.

From the experimental study, total time, time gaps, flow, specific flow and densities were extracted. It was observed that the total time decreased as the bottleneck width increased, for both compositions in cases with and without buffer space. The buffer space effect in the reduction of total time was more in case of 50 persons, when compared to 30 persons. It was observed that flow increased as the width of the bottleneck increased, and this increase in flow is due to the formation of dynamic layer, as noted by some researchers in their studies. It was observed that, specific flow was decreasing as the width of the bottleneck increases and specific flows were more for without buffer space as compared to with buffer space. Trajectories were plotted in order to know the route choice of each individual throughout the evacuation period in the study area. It can be identified that lateral occupancy of persons is more in the case of without buffer space as compared to with buffer space, for both compositions (N = 30 & 50).

Arching phenomenon was observed at the entry of exits; this was apparent when a crowd with highly anticipated speed tries to pass through a door in limited amount of time because of which the exit gets congested, and the crowd becomes arc-shaped. It can be observed that densities were decreasing as the width of the bottleneck increased. Density value was observed to be higher for groups of fifty, when compared to groups of thirty people for the same width of bottleneck. High densities were observed near the bottleneck opening when the flow gushing in goes beyond the capacity of the bottleneck, leading to jamming at the bottleneck. It can be observed that, flow of crowd increases as the width of bottleneck increases and this increase is stepwise, and not linear. When the crowd enters the bottleneck, formation of lanes occurs inside the bottleneck as width increases due to zipper effect. For a width of 80 cm, formation of lanes is absent. As the width increases from 80 cm to 100 cm, two lanes were formed and these lanes were continued and laterally expanded up to a width of 140 cm. For a width of 160 cm, it can be clearly observed that three lanes were formed. It can also be observed that the distance between these lanes does not influence bottleneck width (B).

Five types of distributions (i.e., exponential, displaced exponential, Gamma, displaced Gamma and semi-random) were tested to cover the random, intermediate and composite headways. Five types of distributions mentioned above have been compared with the observed data and tested with goodness of fit (χ^2 test). It was found that, among five types of distributions, semi-random distribution is observed to be the best fit for the observed data. The percentage of constrained headways (ϕ) observed in case of 50 persons was more than that of 30 persons. This implies that free flow decreases with increase in number of persons.

In order to estimate the capacity of bottleneck, Buckley model is used. It can be observed that, capacity of bottleneck increases as the width of the bottleneck increases and this increase in capacity is because of the dynamic layer formations due to zipper effect. It can also be observed that, capacity of bottleneck with buffer space is more compared to capacity without buffer space. The obtained capacities were compared with capacities from different experimental studies done in relation to pedestrian flows at bottlenecks. For comparison, Kretz and Muller studies were considered because of their similarity with this study. Capacities obtained in this study were lower than that of capacities obtained from Kretz and Muller. The reason behind the reduction in capacities was Kretz and Muller didn't consider the formation of dynamic layers, hence the effective utilization of width concept was absent, resulting in larger capacities in their study.

Further, the same experimental study area and participants were used for the estimation of capacity of doors. Five varied widths of the doors consisting of 80, 100, 120, 140, and 160 centimeters were chosen for single doors and doors of 100 cm width selected for double doors. Parameters such as total time, time gaps, and densities were extracted and analyzed in terms of various relations such as time gap versus door width, total time versus door width, and flow versus door width. Crowd trajectories and density plots were drawn for different door widths. Capacities were estimated both for single and double doors and comparison of capacities for different door widths was performed. Average time gaps and total times were observed to decrease as the width of the door increased, for cases with and without buffer space. In case of single and double doors, the total time was more in case of 50 persons than for 30 persons. Observations from trajectories have revealed a phenomenon called arching. In case of double doors, it was observed that evacuees were choosing the congested door rather than an uncongested one due to herding behavior. Herding behavior occurred when people were not making individual decisions but behaving as a group. In the evacuation scenario, herding behavior means that, the evacuees choose the most congested exit rather than the uncongested exit. Evacuees think that the congested exit is the most popular choice.

Contents

List of Tables

List of Figures

Notations

MLR	Multiple Linear Regression
ANN	Artificial Neural Networks
ANFIS	Adaptive Neuro Fuzzy Inference System
RMSE	Route Mean Square Error
MAE	Mean Absolute Error
U_f	Free flow speed
U_0	Optimum speed
K_j	Jam density
K_o	Optimum density
Q_m	Maximum flow
L	Greenshield
E	Underwood
MAPE	Mean Absolute Percentage Error
Φ	Percentage of constrained headways
MHT	Multiple Hypothesis Tracking
SVMs	Support Vector Machines
HMM	Hidden Markov Model
MDL	Minimum Description Length
SVR	Support Vector Regression
CNN	Convolutional Neural Networks
LOS	Level of Service
FPR	False Positive Rate
(u, v)	Pixel coordinates
(x, y)	Real coordinates
L_1–L_8	Transformation coefficients
N	Number of persons
A	Area
Q	Flow
K	Density
U	Speed
M	Male
F	Female

CC	Child Carrying
CH	Child Holding
G	Group
MSE	Mean Of Squared Error
Location-1	Location at Krishnapushkaralu
Location-2	Location at Medaram
L1	Three legged intersection at Medaram
L2	Straight stretch at Medaram
MFD	macroscopic flow diagrams
R^2	Coefficient of determination
B	Bottleneck width
C	Capacity
2a	average dynamic layer width
C_1	Capacity per lane
SFPE	Society of Fire Protection Engineers
PM	Predtechenskii and Milinskii
WM	Weidman
HG	Hoogendoorn
E_i	Expected value
O_i	Observed value

1. INTRODUCTION

1.1 General

Religious occasions, congregations at carnivals, political rallies, and crowd at terminals are occasions for crowd congregations. These congregations act as serious intimidations for crowd because a large number of people moving in limited space results in crowd stampedes. In large gatherings, the security of the event is of the highest importance. In high density crowd, abnormal behavior is observed due to large interactions between individuals which lead to a stampede (Farkas et al. 2000). For example, in a t mass gathering event as in Mecca, stampedes occurr every year though authorities constructed walkways and provided traffic controls to avoid stampedes. In India, a similar type of crowd crushes occurrs during Hindu religious gatherings like Khumba mela (Moonen et al. 2011). People using these facilities show different behavior based on awareness of the facility, anticipated walking speed, awareness of congestion, and tendency to herding. Adverse crowd crushes happened at such crowded areas which lead to accidents resulting in fatalities and injuries. These accidents occurr mainly due to panic among the crowd trying to evacuate the facility. The researchers were very interested in enhancing facility designs to reduce interactions between crowd and also simplify the crowd movement in public spaces. There is more attention given to plan these facilities taking into account possible emergencies for the evacuation. The research work reported here is micro and macroscopic analysis of crowd behavior and evacuation planning.

1.2 Crowd definition

Walking is a basic mode of movement and is related to all other modes of transportation. A pedestrian is defined as a person travelling on foot. “A crowd is a large number of people congregated at a precise location for a measurable time period, with common goals and showing common behaviors” (musse et al. 1997).

1.3 Crowd characteristics

The key criteria to determine a collection of individuals who can be treated as crowd are: size, density, time, collectivity, and novelty. The number of persons gathered should be large and distributed over the entire area. Each individual gathered at a location should have a definite

purpose and must have spent measurable time period. People in the crowd should share common goals, interest and acts in a coherent manner

1.4 Types of Crowd

Berlonghi (1995) studied and identified eleven different types of crowds.

1.4.1 Ambulatory crowd: People who are entering or leaving a location, walking to or from parking places.

1.4.2 Disability crowd: People who are limited by their lack of ability to walk, see, hear, or speak fully.

1.4.3 Spectator crowd: A crowd comming to a location and watching an event.

1.4.4 Expressive crowd: People who are singing, cheering, chanting, celebrating, etc.

1.4.5 Participatory crowd: People who are are participating in the event and perform actual activities. Examples are professional performers, athletes.

1.4.6 Demonstrator crowd: A crowd with a familiar frontrunner setup an event to chant. Slogans or protest against something or someone.

1.4.7 Aggressive crowd: A crowd which ignores instructions from officials and becomes abusive, threatening, and potentially unlawful.

1.4.8 Dense crowd: Persons whose physical movement quickly falls because of high crowd density, causing severe wounds and loss of life because of asphyxia.

1.4.9 Rushing or looting crowd: The main aim of the crowd is to obatin something. Example, hastening to get autographs of filmstars, people rushing to reserve seats in buses and trains etc., or even commit theft.

1.4.10 Violent crowd: A crowd which is aggressive and frightening with no thought for the rights of others.

1.4.11 Escaping crowd: A crowd trying to escape from dangerous conditions.

1.5 Crowd behavior

Crowd behavior is the behavior that is shown by individuals who gather in a crowd. Generally, crowd behavior can be divided into two categories:

- Normal behavior
- Abnormal behavior

1.5.1 Normal behavior

In normal behavior, every person tries to reach their destination as early as possible using the smallest amount of energy and time.

1.5.2 Abnormal behaviour

In abnormal behaviour, each person in the crowd will tend to show some kind of panic or aggressive behaviour.

1.6 Crowd based on motion

According to the motion of the crowd, crowd scenes can be divided into two categories: structured crowd and unstructured crowd. In structured crowded scenes, crowd moves systematically in common direction and the flow path does not vary frequently. In unstructured crowded scenes, people in the crowd are move in different or random directions at different times.

1.7 Object detection

Object detection can be done by three techniques:

- Background subtraction
- Optical flow
- Spatio temporal filtering

1.7.1 Background subtraction

Background subtraction is one of the popular method to detect moving objects from the difference between the current frame and a background frame. There are limited approaches to perform background subtraction, which are Gaussian mixture, non-parametric background, temporal differencing, warping background and hierarchical background models.

1.7.2 Optical flow

Optical flow is a vector-based technique that estimates motion by matching points on objects over image frames ((Candamo et al. 2010), (Xiaofei et al. 2010), and (Efros et al. 2003)). Individual moving objects are also identified using this method even though the camera is in motion. This algorithm is very complicated and involves complex computation. This method is robust and detects multiple objects and their motions simultaneously. Crowd analysis can be done for high density crowd using optical flow method.

1.7.3 Spatio temporal filtering

Spatio - temporal filtering method uses several adjacent frames to subtract and get different images based on time series image. This method is not applicable for objects not moving and won't be used in real time applications ((Lee, 2005) and (Ridder et al. 1995)). In spatio temporal filtering method, motion is recognized based on spatio temporal analysis. The motion of the person in the image sequence is described via 3D spatio temporal data volume (Zhong et al. 2004, Piroddi et al. 2006).

1.8 Crowd analysis

Crowd analysis is classified into three types:

- People counting or density estimation
- Tracking
- Crowd behaviour understanding models

1.8.1 People counting or density estimation

The crowd density estimation at public places is a great challenge and very important for public safety and security. Generally, human crowd density estimation methods are classified into two main categories:

- Direct methods
- Indirect methods

1.8.1.1 Direct methods

In these methods, definite classifiers are used to detect part and count each person in the crowds directly to obtain human crowd density.

1.8.1.2 Indirect methods

In indirect methods the crowd density can be obtained using three different methods:

- Pixel-based analysis
- Texture-based analysis
- Object-based analysis

1.8.1.2.1 Pixel based analysis

In pixel based analysis, the number of persons in image is estimated by using very low level features. Background subtraction models and edge detection models are used to analyze the

individual pixels.This method is generally used to estimate the density instead of people counting.

1.8.1.2.2 Texture based analysis

In texture based analysis, image patches are analyzed by their texture content using texture modeling. Texture analysis tries to compute instinctive qualities by terms such as coarse grain, even, smooth, or uneven based on pixel intensities. This method extracts high level features and is typically used to estimate the number of persons in the image instead of detecting each person in the image.

1.8.1.2.3 Object -level analysis

In object level analysis, each individual person is identified in an image. This method gives better results when compared with other two methods. This method can be applied to detect and count each individual person in an image or video in lower density crowds. This method can not be applied to higher density crowd because of severe obstructions and litter.

1.8.2 Tracking

Detecting the position of the same person in a series of images is called tracking. Tracking in crowd scenes can be done using three techniques, namely, point tracking, kernel-based tracking and silhouette-based tracking. Figure 1.1 shows the different crowd tracking methods.

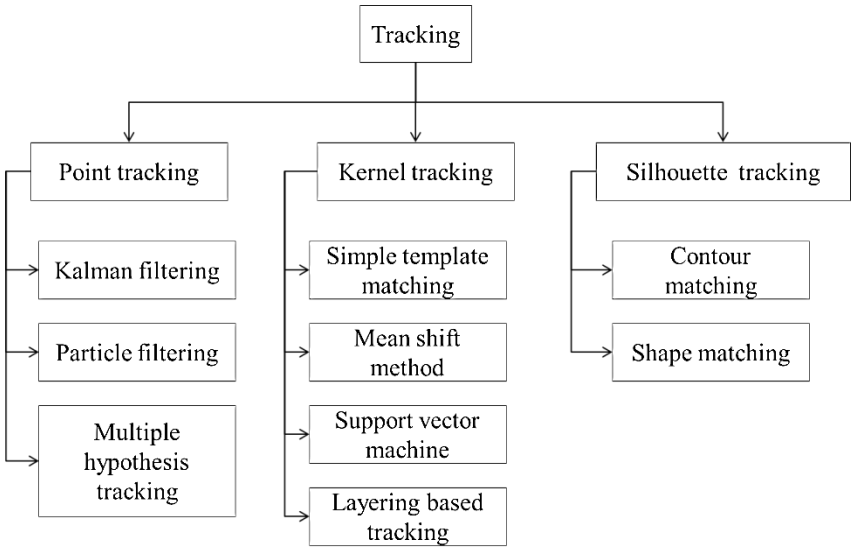

Figure 1.1 Flow chart of tracking methods

1.8.2.1 Point tracking

Point tracking method detects persons in successive images denoted by points. The connotation of the points is based on the previous object state which can include object location and motion. There are three methods to track object based on point tracking, these are being:

- Kalman filtering,
- Particle filtering
- Multiple Hypothesis Tracking (MHT)

1.8.2.1.1 Kalman filtering

Kalman filter calculates the persons in terms of present, past, and future positions. It can also track persons even though the model is not perfect (Joshan et al. 2012).

1.8.2.1.2 Particle filtering

Particle filtering creates all the models for one variable before moving to the following variable (Liang et al. 2007). This method can be used to track persons even when variables are generated dynamically and there are limitlessly many variables.

1.8.2.1.3 Multiple Hypothesis Tracking (MHT)

Multiple hypotheses tracking (MHT) is an iterative algorithm where iteration starts with a set of existing track hypotheses (Lee, 2005). MHT can track multiple objects and handle obstructions.

1.8.2.2 Kernel based tracking

Kernel tracking is typically done by locating the moving object that is denoted by an evolving object area, from one frame to subsequent frame (Joshan et al. 2012). There are four methods to track persons based on kernel based tracking, and these are:

- Simple template tracking
- Mean-shift tracking
- Support vector machine
- Layering based tracking

1.8.2.2.1 Simple template matching

In simple template matching, first the reference image is verified with the frame that is separated from the video and then further tracking process can be performed for single object within the video and overlapping of object is completed partly.

1.8.2.2.2 Mean shift tracking

In mean-shift algorithm, the shape of the objetcs tracked is defined by histograms (Samuel et al. 2004). Image features like color, looks etc. are chosen to express object and then matching is performed continuously in series images. This algorithm first finds the area of a video which is most similar to a formerly developed model. The image area to be tracked is denoted by a histogram.

1.8.2.2.3 Support vector machine

Support vector machines (SVMs) method is used for classification, regression and outlier detection (Kim et al. 2010). SVM provides a set of positive and negative training values in which the positive values contain details of the tracked person, and the negative values contain details other than that of the person being tracked.

1.8.2.2.4 Layering based tracking

Layer based tracking method is to track multiple objects within the crowd. In this method, every layer contains shape depiction, motion, and layer appearance based on intensity values.

1.8.2.3 Silhouette-based tracking

In silhouette-based object tracking, a persons region is identified in every frame using an object model created by the previous frames (Joshan et al. 2012). There are two methods to track persons based on silhouette-based object tracking these being:

- Contour tracking
- Shape matching

1.8.2.3.1 Contour tracking

Contour tracking method is an iterative progress that involves moving a primary contour in the preceding frame to its new position in the present frame (Joshan et al. 2012). This contour development needs a definite amount of the object in the current frame superimposing with the object region in the previous frame. Contour Tracking can be done using two different methods. In the first method, contour shape and motion are modeled using state space models.

In the second method, contour energy is reduced by direct minimization procedures such as gradient descent. This method is more flexible to handle different object shapes.

1.8.2.3.2 Shape tracking

Shape matching involves finding matching outlines detected in two consecutive frames. Shape matching performance is similar to template based tracking in kernel approach.

Different tracking methods are compared based on accuracy and computational time and are tabulated in Table 1.1.

Table 1.1Comparison of object tracking methods

Method		Accuracy	Computational time	Comments
Point tracking	Kalman filter	Moderate	Low to moderate	Track points in noisy images
	Particle filter	High	Moderate to high	It performs well in complex background.
	Multiple hypothesis tracking	Low to moderate	Low	Deals with entries and exits of new objects.
Kernel tracking	Simple template matching	Low	Low to moderate	Deals with particle occlusion
	Mean shift method	Moderate	Low	It can be used for real time applications due to less calculations
	Support vector machine	Moderate	Moderate	It can handle partial occlusions.
	Layering based tracking	Moderate to high	Moderate	Track multiple objects
Silhouette tracking	Contour matching	Moderate to high	Moderate	Object shape is indirectly modeled.
	Shape matching	High	High	It requires training.

1.8.3 Crowd behavior understanding models

There are two main methods for crowd behavior analysis:

- Object-based approach
- Holistic-based approach

1.8.3.1 Object -based approach

In this method, a crowd is treated as a group of individual persons. In this method crowd behavior is analyzed through detecting individuals. This method can fail in higher density crowd because tracking each person in the crowd is very difficult. This method is valid for low and medium density crowd.

1.8.3.2 Holistic-based approach

In this method, crowd is considered a single unit and crowd flows can be calculated. This method is mostly applicable to densely crowded scenes.

1.9 Normal pedestrian behaviour

The behaviour of the pedestrian crowds have been empirically studied for the past decades. The methods used for the evaluation were based on direct observation, photographs, and time-lapse films. Apart from the following behavioral investigations, the intention of these studies was to frame computer animated realistic applications, for the game industry, design elements of pedestrian facilities, or planning guidelines for architectural building and urban design. In a common environment, pedestrians tend to have some basic attributes. For example, people always try to reach their destination in a short interval of time. People choose the shortest way even though it is crowded and avoid diversions.

1.10 Crowd behavior in abnormal situations

Most of the normal behaviour disappears when evacuees face an abnormal situation. For example, in a building, if there is any emergency, the crowd will behave in a different manner. When evacuees try to exit the building as fast as possible, the anticipated velocity of evacuees increases which leads to some typical establishments. As chaos increases, they find the most suitable and shortest way and neglect their comfort zone. They also lose their capability to direct themselves in the surroundings which leads to herding behavior. They also start to show new behavior like jostling which leads to death and injuries in crowd crushes.

1.11 Need for the study

In recent years, development of cities across the globe has become unstoppable and it’s very difficult to plan cities. In this situation, understanding pedestrian movements is very essential for design facilities with respect to safety, security, level of service and low cost. Religious occasions, congregations at carnivals, political rallies, and crowd at terminals are the occasions pertaining to crowd congregations. These congregations act as serious intimidations

for crowd because a large number of people moving in limited space results in stampedes. Most of the crowd crushes occurr in developing countries during large congregations and more people died in such contries compared with developed countries. So it is very important to study crowd behavior to increase public safety, etc. Hence knowledge about behavior of pedestrian and the tools required to predict this behavior are essential in the planning and design of pedestrian facilities, such as bus stations, train platforms, shopping malls etc.

1.12 Objectives of the study

The objectives of the research work are as follows:

a. To evaluate the microscopic analysis of crowd behavior using multiple linear regression (MLR), artificial neural networks (ANN), and adaptive neuro fuzzy inference system (ANFIS).
b. To evaluate the macroscopic analysis of crowd behavior using multi-regime modeling.
c. To evaluate the evacuation scenarios for corridors and doors.

1.13 Organisation of the Report

The thesis work is presented in 7 chapters and the chapters are organized as follows

Chapter 1 gives a brief background of the topic of study including its significance, the need for the study and the specific objectives of the research work.

Chapter 2 This chapter discusses literature review. Literature review explains studies conducted related to bottlenecks, evacuation, walking behaviour, tracking, density estimations etc.

Chapter 3 This chapter deals with the methodology adopted for this study and data collection at different mass gathering locations and subsequent extraction of pertinent parameters required for preliminary analysis. The methodology of the present study and its discussion are shown with the help of flow chart.

Chapter 4 This chapter discusses the microscopic analysis using characteristics like age, gender, group size, child holding, child carrying, people with luggage and without luggage are considered.

Chapter 5 deals with the macroscopic analysis of crowd behavior using single and multi-regime modeling.

Chapter 6 focuses on analysing the effect of composition and bottleneck width on crowd behaviour. The inclusion of buffer space on crowd dispersion is analysed. Capacities of corridors and doors are estimated for different widths.

The summary and conclusions of the study, major research contribution, limitations of the study and scope for further research are presented in **Chapter 7.**

2. LITERATURE REVIEW

2.1 General

Over the past few decades, researchers across the world have been keenly focusing on crowd density estimation, crowd tracking, and crowd behaviour analysis based on holistic-based approach. However, the individual behavior of people in the crowd has been ignored. The present study focuses on individual people behavior considering their physical factors which influences overall crowd speed and flow. This chapter presents a comprehensive review of research covering the studies related to object detection, tracking, behavior understanding models, single and multi regime models, ANN, ANFIS, headway distributions, capacity of corridors, capacity of doors, etc.

2.2 Studies on object detection

Object detection method is performed by background subtraction, optical flow and spatio temporal filtering.

2.2.1 Literature related to background subtraction

Background subtraction is a popular method to detect moving objects based on the difference between the current frame and background frame. There are limited approaches to perform background subtraction, which include Gaussian mixture, non-parametric background, temporal differencing, warping background and hierarchical background models.

2.2.1.1 Literature related to Gaussian mixture model

(Stauffer et al. 1999) presented an adaptive Gaussian mixture model, which changes dynamic scenes caused by illumination changes. Jabri et al. (2000) presented a new method to detect and locate people in video sequences based on background subtraction modeling which uses color and edge data. Confidence maps-gray-scale images were introduced to represent the background subtraction results. Slow illumination changes, scene disorder and camera noise are tolerated and run in real time. Stenger et al. (2001) presented a new framework for Hidden Markov Model (HMM) topology and parameter estimation in online. The parameter estimation was done based on state splitting approach. Several state splitting criteria were compared based on variance. MDL (Minimum Description Length) criterion has less variance compared to others. Theoretical validation was also done on both online and real experiments. Lee (2005) proposed an effective learning algorithm to enhance the convergence rate without

compromising model firmness. This is attained by substituting the global as well as static retention factor for each Gaussian at every frame. Substantial developments were observed on both artificial and real video data. Heikkila et al. (2005) presented a new approach to detecting moving objects from a video series. Texture based method was used for background subtraction and modified local binary pattern (LBP) operator was used to extract texture features. This method can tolerate substantial illumination changes in natural scenes and computational time is also very fast. Shimada et al. (2006) proposed a new algorithm to estimate the background model with a mixture of Gaussians in non-stationary scenes. In this method, a number of Gaussians in each pixel can increase and decrease. This algorithm can reduce the computational time without losing quality of background modeling.

Wang et al. (2006) presented a method for improving video-based surveillance where detection and tracking are addressed concurrently and evaluated in both visible and thermal video sequences. Support vector regression (SVR) along with online learning scheme was used to develop a background model to accurately detect the initial locations of the targets. Zhang et al. (2006) presented a new method to detect moving cast shadows in the scene and this mwthod was a success in indoor and outdoor conditions. Five types of orthogonal transform (Discrete Fourier Transform (DFT), Discrete Cosine Transform (DCT), Singular Value Decomposition (SVD), Haar Transform (HaarT) and Hadamard Transform (HT)) are used to transform image block and the block shows no illumination changes. These transforms are used to classify moving shadows and foreground objects. Zhiqiang et al. (2006) presented a background updating system based on optical flow and apply a refinement algorithm based on color features to eliminate the shadows. This method can update background exactly and quickly and the shadow can be removed efficiently. Lin et al. (2009) proposed an online algorithm to construct a background model for tracking. Background model is developed based on two-level estimate that combines bottom-up and top-down information. Inter block consistency is maintained by introducing global constancy check to remove noises in the local updates.

Gopala Krishna et al. (2011) presented a background subtraction method for detecting multiple moving objects and feature-based method for tracking. The moving objects identified are also counted, by indexing them individually. This method is effective and accurate in different types of background scenes and several situations including indoor and outdoor scenes. Chate et al. (2012) presented a broad survey on moving object detection and tracking, object shape illustrations and feature selection for tracking. Various object detection and tracking approaches were compared and analyzed. Aldhaheri et al. (2014) proposed a new approach for detecting and classifying moving objects (humans and vehicles) from a video

stream. The moving objects are detected using a background subtraction algorithm which is implemented in MATLAB. Edge detection of moving objects was done using Canny or Prewitt action. Edge detection and bounding boxes were used before the classification step to simplify the classification. The moving objects were classified by the height-width ratio of the bounding box around the moving object in each frame. The speed of the moving object was estimated from successive frames in the video stream. This algorithm is simple and accurate and easy to implement. Mohan et al. (2014) presented and compared two methods (object detection and segmentation) for moving objects in a video stream. Object detection was done using background subtraction while segmentation was done by edge detection and thresholding. Background subtraction method is better compared to thresholding method based on PSNR values (Peak Signal to Noise Ratio).

2.2.1.2 Literature related to non parametric background model

Elgammal et al. (2000) developed a new and novel non-parametric background subtraction model and this model runs in both gray level and color images. It can be applied where background is messy but contains small motions, and estimates the pixel intensity density values from sample history values. This method attains very sensitive detection with very low false alarm rates. Li et al. (2004) proposed a new method for detecting foreground objects from complex environments using background subtraction modeling. Foreground objects are detected through foreground and background appearance is categorized by the principle features, statistics and background classification under Bayesian framework. Lanza et al. (2011) developed an efficient and robust background subtraction approach to perform in the presence of disturbance such as illumination changes (gradual, sudden), camera gain and exposure variations, and noise. A non parametric online probabilistic clustering was done to segment the image with respect to fixed background. Kim et al. (2012) presented a new and robust background subtraction algorithm for temporally dynamic texture scenes. Fuzzy Color Histogram (FCH) was adopted to minimalize color differences created by background motions. This method is effective and accurate in dynamic texture scenes. Han et al. (2004) introduced mode propagation method which is an efficient method for successive density approximation. This method is accurate and effective and is successfully applied to background subtraction modeling and useful for computer vision applications.

2.2.1.3 Literature related to temporal differencing

Lipton et al. (1998) developed a robust method to extract, classify, and track moving objects from a real time video. Pixel wise difference between two successive image frames were used to detect moving objects and a classification metric was applied to classify these objects based

on a temporal consistency constraint while temporal differencing and template matching were used to track the objects. This method removes background clutter, and tracks objects continually over large distances. Weinland et al. (2006) introduced Motion History Volumes (MHV) for human actions and presented algorithms for calculating and comparing different actions performed by different people in background subtracted video cameras. Position and comparisons were done using Fourier transforms and this illustration can be used to study and identify basic human action classes independent of gender and body size. Tsai et al. (2009) proposed a background subtraction method using an Independent Component Analysis (ICA) to segment foreground objects (stationary, moving) in indoor environments. This method contains two stages, training and detection. In the training stage statistical independence is measured from relative frequency distributions based on the estimations of joint and marginal probability density functions. In the detection stage, foreground image is separated from reference background image using the trained de-mixing vector. This method is simple, effective, fast computing, and highly tolerant of illumination changes. Cheng et al. (2011**)** presented a new and robust background subtraction method for detecting moving objects. This approach contains three modules: block alarm module, background modeling module, and object extraction module. The block alarm module efficiently checks each block using temporal differencing pixels of the Laplacian distribution model. Background modeling module is used to recognize sudden changes in illumination using a combination of a two stage background training procedure. The object extraction module detects moving objects using a binary moving object mask, which is done by threshold value.

2.2.1.4 Literature related to Warping background

Ko et al. (2010) presented a warping background model that separates background motion and foreground objects. The background is modeled as a set of warping layers and these layers visible to the motion of a blocking layer at ant given time. Foreground regions cannot be modeled by warping of these layers.

2.2.1.5 Literature related to Hierarchical background model

Kim et al. (2005) proposed a real-time algorithm for detecting foreground objects using background subtraction. Layered detection and adaptive codebook updating are used to improve the algorithm and perturbation detection rate analysis is applied for evaluating the performance. This method works well on moving backgrounds and lighting changes. Chen et al. (2006) developed an efficient two-level hierarchical background method that combines pixel-based and block-based methods into a single framework. In hierarchical model, a new descriptor is proposed for block-based background modeling. This method performs better

than single-level approaches. Quan et al. (2013) presented a hierarchical background subtraction algorithm which comprises block-based stage and pixel based stage. In block-based stage, backgrounds are detected via block-based code book to reduce memory consumption and pixel-based stage was selected to improve detection accuracy by introducing spatial and temporal relations in MRF (Markov Random Fields)-MAP (Maximum a posteriori) framework. This method has the highest detection rate and consumes low memory.

2.2.2 Literature related to Optical flow

Efros et al. (2003) introduced a new and robust motion descriptor based on optical flow measurements for moving figure in a spatio-temporal volume. This descriptor classifies the actions in a nearest-neighbor framework and also creates new action sequences. Jeon et al. (2008) proposed a tracking method with four parameters and the advantage of this method is it has lower complexity than KLT (Kanade-Lucas-Tomasi) and calculates four parameters values directly. This proposed method works very well for feature tracking and can track local features. Candamo et al. (2010) described image processing techniques for automatic behavior recognition methods in video streams. Recognition methods include single person, multiple person interactions, person-vehicle interactions, and person-facility interactions. An algorithm's weaknesses, possible research directions and a summary of literature survey in motion detection, classification of moving objects, and tracking were discussed. Aslani et al. (2013) developed a moving detection and tracking method based on optical flow estimation to gather useful information from stationary cameras in digital videos. Median filter was used to remove the noise and unwanted objects were removed by applying thresholding algorithms in morphological operations.

2.2.3 Literature related to Spatio temporal filtering

Niyogi et al. (1994) described a new algorithm for walking figure's individual walking figures can be identified by applying standard pattern recognition techniques to the contour signals. A typical pattern is observed when a person walks parallel to the image plane. Kale et al. (2002) presented an HMM based approach to identify gait. A lower dimensional observation vector is derived from the shape of the walking person. A continuous HMM is trained for each person over several such lower dimensional vector sequences. Gait recognition is performed for HMM model generated observation sequence by log-probability evaluation. Wang et al. (2002) presented a new and simple gait recognition method based on statistical shape analysis. Background subtraction method is used to divide spatial silhouettes from the background. Shape changes of these silhouettes over time are denoted as related formations and then analyzed using the procrust shape analysis method. Zhong et al. (2004) proposed an

unsupervised technique for detecting unusual action in a huge video data. The video is divided into equal sections which classify the extracted features into prototypes. A correspondence relationship between samples and video segments is identified which fulfills the transitive end constraint. Laptev (2005) developed a point detector to find local image features in space-time where difference of image values is high in space and variation in motion over time. Dollar et al. (2005) presented a new spatio-temporal interest point detector and analyzed a number of cuboid descriptors. Behavior recognition is shown in terms of spatio-temporal features. BenAbdelkader et al. (2001) presented a new correspondence-free motion based method to recognize individual gaits. New gait is recognized via standard pattern classification by using k-nearest neighbor rule and Euclidian distance.

2.3 Literature related to object tracking

Broadly object tracking techniques can be classified as point tracking; kernel based tracking, and silhouette based tracking**.**

2.3.1 Literature related to Point Tracking

There are three methods to track object based on point tracking these are Kalman filtering, particle filtering, and Multiple Hypothesis Tracking (MHT).

2.3.1.1 Literature related to Kalman filter

Welch et al. (2006) provided practical introduction to discrete Kalman filter and it includes an explanation and some discussion of the basic discrete Kalman filter. Ali et al. (2009) presented a robust moving object detection method to detect humans and vehicles. This model consists of average background model which is used to subtract foreground images from background and adaptive threshold model which is used to concurrently update the system to environmental changes. Li et al. (2010) presented a fully automatic multi-object tracking algorithm using Kalman filter. Kalman filter motion model is established to choose centroid and tracking. Split or merge is recognized based on detection and the cost function can be used to solve the problems after split. This algorithm is more efficient for tracking multiple moving objects in complicated conditions. Azari et al. (2011) developed a new method for multiple object tracking (MOT) to solve occlusion problem. Kalman filter is used to track each object in normal condition and for each track appearance a model is considered. An appropriate distance function is presented for applying General Nearest Neighbor (GNN) method to identify segmentation errors and occlusions.

2.3.1.2 Literature related to Particle filter

Sarkka et al. (2007) developed a novel and robust Rao-Blackwellized particle filtering based algorithm for tracking targets. Probabilistic stochastic process models are used in this method to frame target conditions, data relations, and birth and death processes. Particle filtering is implemented to track the targets and this is improved by using Rao-Blackwellization. Wei et al. (2007) proposed a new algorithm based on mean shift and particle filter to track moving objects in video scenes. Mean shift algorithm tracks the moving objects through iterations based on gradient descent and particle filter track objects in non Gauss and non linear case. Kim et al. (2010) proposed a new region based tracking method for the detection of multiple moving objects. Object detection is done by using background subtraction and object tracking is done by particle filter. Yang et al. (2005) proposed a new efficient and robust object tracking algorithm based on particle filter and it identifies tracked objects using color and edge orientation histogram features. Several improvements accelerate the algorithm which generates integral images for efficiently computing the color and edge orientation histograms and the observation likelihood is computed to allow the computation quickly. This algorithm is effective and robust against clutter. Okuma et al. (2004) presented a model to detect objects by Adaboost and track the objects using mixture particle filters. Multiple object tracking is achieved by forming the proposal distribution using mixture model for the particle filter and the detections generated by Adaboost. The combination of two methods is simple and fully automatic.

2.3.1.3 Literature related to Multiple Hypothesis Tracking (MHT)

Streit et al. (1994) proposed a probabilistic multi-hypothesis tracking algorithm (PMHT) to track objects in a video stream. The probability that each measurement belongs to each track is estimated using Maximum Likelihood (ML) algorithm which is derived using the method of Expectation-Maximization (EM). Blackman (18, 2004) summarized the basic principles behind MHT, motivations and alternative applications. Interacting multiple model (IMM) method is used to combine multiple filter models with MHT are discussed and the advantages of MHT over single hypothesis approach are studied. Zhang et al. (7, 2010) presented a combined algorithm based on adaptive background subtraction for moving object detection and adaptive background updating for subtracting moving objects from complex situations. Gaussian model is combined with temporal difference to update the background and background subtraction method to extract moving objects from the background model. Noise and stationary parts are removed using median filter and mathematical morphology processes.

2.3.2 Literature related to Kernel Tracking

There are four methods to track persons based on kernel based tracking; they are simple template tracking, mean shift tracking, support vector machine, and layering based tracking.

2.3.2.1 Literature related to Simple Template Tracking

Yi et al. (2010) proposed a new combined algorithm based on running average background modeling and temporal difference method to detect moving objects from difficult background video streams. Running average method is used to detect foreground image using background subtraction when the background image is dynamically updating and temporal difference method is used to get a difference image. Median filter is used to eliminate noise in the combined image. Saravanakumar et al. (2010) developed a new approach to track multiple objects based on detection, motion estimation, and background subtraction. This method is most effectively to remove shadows and occlusions. A reference frame is considered as background information and when a new object enters the frame, the foreground information is identified using the reference frame. Morphological operations are used for removing the shadows.

2.3.2.2 Literature related to Mean Shift Algorithm

Comaniciu et al. (2002) developed a new mean shift-based algorithm to track objects in complex environments. The relation between mean shift algorithm to Nadaraya-Watson estimator is established using kernel regression and robust M- estimators. This algorithm is applicable to gray level or color images. Image segmentation and smoothing can be done using this algorithm.

2.3.2.3 Literature related to Support vector machines (SVM)

Shai (2004) presented a robust hybrid method which consists of Support Vector Machine (SVM) classifier and optic-flow-based tracker to give Support Vector Tracking (SVT) mechanism. A coarse-to-fine approach is used to measure the motion between consecutive frames by building pyramids using support vectors. Kim et al. (2010) proposed a novel approach Support Vector Machines (SVMs) method for classification, regression and outlier detection. SVM provides a set of positive and negative training values in which the positive values consist of tracked image object, and negative values consist of all remaining things that are not tracked.

2.3.2.4 Literature related to Layer based tracking

Tao et al. (2002) introduced a dynamic motion layer representation and iterative algorithm for tracking objects in video surveillance. The generalized expectation maximization (EM) algorithm is used to estimate and model the shape, motion, and layer appearance in a maximum a posteriori (MAP) framework. Near real time tracker is developed using Gaussian shape prior for tracking vehicles. The iterative algorithm is used for continuous object tracking over time. This method is simple and performs better compared to correlation-based tracker and a motion change-based tracker.

2.3.3 Literature related to Silhouette tracking

There are two methods to track persons based on silhouette-based object tracking: contour tracking and shape matching.

2.3.3.1 Literature related to Contour Tracking

Ronfard et al. (1994) presented a modified approach for contour tracking which uses local computations instead of edge detection. A region based energy criterion is introduced for active contours and optimization scheme is used for accounting for internal and external energy. This optimization technique (heuristic) is used to fill the gap between snakes and split and merge regions. Isard et al. (1998) developed a new CONDENSATION algorithm which is a statistical factored sampling algorithm for static and stochastic model for object motion. This algorithms track rigid and no rigid motion are more effective compared to Kalman filter. Bertalmio et al. (2000) presented a new algorithm based on Partial Differential Equations (PDEs) for image segmentation and tracking. Image segmentation is done by using Partial Differential Equation and tracking is done by projecting the velocities. Projecting velocities was introduced in image analysis to obtain systems of coupled PDEs. Bahadur (2010) reviewed number of algorithms implemented on moving object detection and tracking (D&T) and also the performance, comparison and evaluation of all D&T methods.

2.3.3.2 Literature related to Shape Matching

Huttenlocher et al. (1993) developed a model based method for tracking moving objects in complex images. The moving object image is divided into two parts which are two dimensional motion and two dimensional shape respectively. There is a shape change when the object moves from one frame to next and no change in motion for the object between successive frames. Sato et al. (2004) presented a temporal spatio-velocity (TSV) transform which is a combination of a windowing operation and a Hough transform over a spatio-

temporal image to extract pixel velocities from binary image sequences. The TSV transform delivers an effective way to remove noise by focusing on constant velocities, and creates noise-free blobs.

2.4 Literature related to Crowd behavior understanding models

Davies et al. (1995) presented a few image processing techniques for collecting data about monitoring crowds. Crowd behavior and tracking is done by using global pixel intensity values. Julio et al. (2005) developed a model to understand human motion, group detection and classification using Voronoi Diagrams. In each frame, the position of each person is represented as a Voronoi Diagram to determine sociological and psychological parameters. The formations of groups are detected and analyzed using individual characteristics computed based on these parameters. Andrade et al. (2006) proposed an automatic algorithm for detection of abnormal activities in crowd by using projections of eigenvectors in a sub space to assess normal crowd behaviour. The motion tracks in an image are identified using spectral clustering. Rabaud and Belongie (2006) presented a modified KLT tracker to extract a large number of features and identified moving objects in a image using trajectory set clustering method. Trajectories were proposed based on spatio-temporal training and integrated using object descriptor for separation of motions from videos. Brostow and Cipolla (2006) developed an unsupervised Bayesian clustering algorithm for detection of individual moving objects. Image features were tracked and grouped into clusters probabilistically without any supervised learning. This clustering was done based on space-time closeness and trajectory consistency through image space. Ali and Shah (2007) presented a new framework based on Lagrangian Particle Dynamics for the crowd flow separation and flow uncertainty detection. Moving crowd creates a flow area and this area is covered with a grid of particles using numerical integration method. Flow map is used to track the grid of particles through the flow by setting up a Cauchy Green Deformation tensor. This tensor calculates the amount by which the adjacent particles have separated over the length of the integration.

Wei and Qin (2007) proposed a moving object tracking algorithm based on mean shift and particle filter in video scenes. Mean shift algorithm tracks moving objects based on gradient descent and no linear tracking is done by particle filter. Cheriyadat and Radke (2008) presented a novel approach for automatically detecting prevailing motions by optical flow which is clustering low level feature point tracks. This method is more accurate, reliable and tolerant to occlusions. Wang et al. (2009) presented a new robust unsupervised learning algorithm to model actions and interactions in complex crowded scenes using hierarchical Bayesian models. Low level features, simple events, and interactions are connected using

hierarchical Bayesian models. Kratz and Nishino (2009) proposed a new method to represent unreliable restricted motion patterns in highly crowded scenes using 3D Gaussian distributions of spatio-temporal gradients. Distribution-based HMM was used to capture the temporal relation between spatio-temporal patterns and spatial relation by a coupled HMM. For analyzing highly dense crowds, spatio-temporal motion patterns are more suitable.

2.5 Literature related to Single regime models

May and Keller (1967) analyzed the deterministic microscopic and macroscopic traffic-flow models. Microscopic and macroscopic traffic flow theories and their relationships are explained and a comprehensive matrix is developed using steady state flow equations. Analytical techniques are developed to evaluate theories based on experimental data and develop deterministic models based on non-inter car following models. Fruin (1970) developed six types of LOS for the design of walkways and stairways based on qualitative and quantitative factors using maximum capacity ratings. The relation between volume and speed was established based on time-lapse photography for different pedestrian densities. These LOSs can be useful for designing pedestrian facilities or evaluating existing facilities. The LOS for walkways and stairways are mentioned in Table 2.1 and Table 2.2.

Table 2.1 Fruin level of service for walkways

LOS	Density (P/m^2)	Space (m^2/P)	Flow rate (P/min/m)	Average speed (m/s)	Capacity (v/c ratio)
A	≤ 0.27	≥ 3.24	≤ 23	≥ 1.3	0.0 to 0.3
B	0.31 to 0.43	3.24 to 2.32	23 to 33	1.27	0.3 to 0.4
C	0.43 to 0.72	2.32 to 1.39	33 to 49	1.22	0.4 to 0.6
D	0.72 to 1.08	1.39 to 0.93	49 to 66	1.14	0.6 to 0.8
E	1.08 to 2.17	1.39 to 0.46	66 to 82	0.76	0.8 to 1.0
F	> 2.17	< 0.46	Variable	≤ 0.76	Variable

Table 2.2 Fruin level of service for stairways

LOS	Density (P/m^2)	Space (m^2/P)	Flow rate (P/min/m)
A	≤ 0.53	≥ 1.9	≤ 16
B	0.53 to 0.71	1.4 to 1.9	16 to 23
C	0.71 to 1.11	0.9 to 1.4	23 to 33
D	1.11 to 1.43	0.7 to 0.9	33 to 43
E	1.43 to 2.5	0.4 to 0.7	43 to 56
F	> 2.5	< 0.4	Variable

Polus et al. (1983) studied the characteristics of pedestrian flow on sidewalks in the center of the city of Haifa, Israel. Male pedestrian speeds were found to be more compared to female pedestrian speeds and all speeds were found to be inversely related to densities. Single and three-regime speed–density models were calibrated and it was observed that the three regime model is the best predicted model compared to single-regime model. Level of service was proposed and ranges were defined for pedestrian traffic, which is mentioned in Table 2.3.

Table 2.3 LOS for Pedestrian

Flow description	LOS		Density (P/m^2)	Area (m^2/P)	Flow (P/m/min)	Recommendations
Free	A		≤ 0.60	≥ 1.67	0-40	Residential, public parks
Restricted	B		0.61-0.75	1.66-1.33	40-50	Public buildings, shopping centers
Dense	C	C1	0.75-1.25	1.33-0.80	50-75	High rise office buildings,
		C2	1.26-2.00	0.80-0.50	75-95	Sport centers, central transit stations
Jammed	D		Further studied			Not recommended

Tanaboriboon and Guyano (1989) proposed an LOS for pedestrian walkway facilities in Bangkok and compared them with the United States. The pedestrian flows observed were more compared to United States but the pedestrian space occupancies are less. The developed LOS and comparison of LOS are tabulated in Table 2.4 and Table 2.5.

Table 2.4 Pedestrian LOS for walkways in Bangkok

LOS	Space	Flow	Flow description
A	≥ 2.38	≤ 28	Free, no conflicts
B	1.60-2.38	28-40	Free, minimum restrictions
C	0.98-1.60	40-61	Restricted, minor conflicts, lower mean speeds
D	0.65-0.98	61-80	Restricted, major conflicts, difficulty in passing
E	0.37-0.65	81-101	Flow reached capacity, speed restricted severely
F	≤ 0.37	≥ 101	Flow break down, extreme restriction of flow

Table 2.5 LOS Comparison

LOS	Bangkok		U.S	
	Space	Flow	Space	Flow
A	≥ 2.38	≤ 28	≥ 3.2	≤ 23
B	1.60-2.38	28-40	2.30-3.20	23-33
C	0.98-1.60	40-61	1.40-2.30	33-49
D	0.65-0.98	61-80	0.90-1.40	49-66
E	0.37-0.65	81-101	0.50-0.90	66-82
F	≤ 0.37	≥ 101	≤ 0.50	≥ 82

Lam et al. (1995) developed speed-density-flow relationships on indoor and outdoor walkways, crosswalks (signalized, light rail transit), and stairways based on pedestrian flow characteristics in Hong Kong. Speed, density, and flow data were collected and speed-density-flow relationships were developed for each pedestrian facility and compared with other international studies. These relationships can be useful for the development of pedestrian standards. Tanaboriboon et al. (1986) studied pedestrian characteristics in Singapore and compared them with other international studies. The mean walking speed was 74 m/min which is less compared to the pedestrian speed in U.S (81 m/min) and the flow (89 ped/m/min) was observed to be more compared to that of U.S (81 ped/m/min). Daamen and Hoogendoorn (2006) estimated free speed distributions for pedestrians using modified

Kaplan-Meier approach from laboratory environments. The proposed method can be useful for large scale laboratory experiments and different conditions of traffic simulations (uni-directional, bi-directional and crossing). The maximum free speed was observed in case of crossing flows (1.66 m/s) and minimum observed in the case of narrow bottleneck (1.44 m/s). Laxman et al. (2010) studied and analyzed pedestrian flow characteristics in India under heterogeneous traffic conditions and compared the data with other international studies. The free flow speed was observed to be higher than China and Singapore and lower than Germany. The pedestrian speed was influenced by age, gender and luggage. Male pedestrian walking speed was more compared to female pedestrians and also the walking speed of children (10-15 years) wad observed to be more compared to other age groups. The speed of a luggage carrying person was low compared to that of a person without luggage and it was found to reduce by 85%.

Ardekani et al. (2011) developed nine different speed density models for a freeway in Texas. In nine models, four models were conventional models, these being Greenshields, Greenberg, Underwood, and Drake models. In the same way, the remaining five models were modified conventional models which are modified underwood model with Taylor series expansion, a modified Greenberg model, a Polynomial model, a Quadratic model and the Drake model with Taylor series. The Drake model and the Underwood model with Taylor expansion series give the best prediction on estimating free flow speed and density. Rahman et al. (2013) analyzed pedestrian flow characteristics using weighted regression method and traditional ordinary least square (OLS) method on sidewalks in Dhaka, Bangladesh. Speed-flow and flow-density relationships were developed using these methods and compared with collected (observed) data and validated using root mean square error (RMSE). The observed pedestrian flow characteristics were compared with other international studies. Rastogi et al. (2013) studied pedestrian flow characteristics on different types of facilities under mixed traffic conditions in different cities of India. The pedestrian facilities were classified based on width, flow condition (uni-directional, bi-directional), absence of pedestrian facility, and effective width reduction. The maximum flow rate and optimum density was reduced when the width of the facility increases because there is more space available for the pedestrian. Speed-density relationship on sidewalks fit Underwood model and Greenshield's (linear) model on a no exclusive pedestrian facility. At lower density, the free flow speed was not affected by bi-directional flow but at higher density, free flow speed reduced. Free flow speed and maximum flow reduced when there was bottleneck in a facility.

2.6 Literature related to multi-regime models

Drake et al. (1967) studied available hypothesis using statistical tests for free-flow data. Optimal break points were located based on maximum likelihood method in multi-regime models. The mean free speed prediction based on Greenshields model was better compared to other models (Greenberg, Underwood, and Edie). The three-regime model gave best prediction on optimum speed, maximum flow and jam density but mean free speed prediction was poor. Edie model gave the best prediction of all traffic flow parameters except R^2 value which was second lowest. Ceder and May (1990) developed macroscopic and microscopic speed-density models for the best prediction. Single and two-regime models were analyzed using 45 sets of data, in which 32 data sets were used for model development and 13 data sets for validation purpose. Virkler and Elayadath (1994) analyzed seven established popular models (Greenshields, Underwood, Greenberg, Edie, Bell-shaped curve, two-regime linear, and three-regime linear) related to vehicular traffic flow which were tested for pedestrian data and speed-density-flow relationships. The performance of each model was validated using statistical tests and visual perception. Three-regime models were found to be statistically insignificant compared to two-regime models. Edie model was found to be the best predicted model compared to all other models. Ramadan et al. (2016) developed relationships between traffic stream parameters on intercity roads in Egypt. Traffic data was collected from three different sections during weekdays and weekends in different times of the day. Traffic stream models were developed using collected data (flow, density, and speed) and checked for single and multi-regime models using statistical tests. Three-regime model was found to be the best predicted model compared to single-regime model.

2.7 Artificial Neural Network (ANN)

Dougherty (1995) presented the review of literature on neural networks related to transportation. Neural network model was compared with other techniques. Florio and Mussone (1995) developed a flow-density relationship for vehicles using ANN based on data collected over Italian motorway and they also performed NN to predict the vehicular flow on the same stretch. Zhao et al. (2000) presented a new and robust stereo-based segmentation and network based recognition for identifying pedestrians in video scenes. This algorithm has three phases; in the first phase, the image was segmented into sub-image object candidates and in the second phase, sub-image object candidates were converted to sub-images using merging and splitting. In the third phase, sub-images are used as input parameters in a trained

neural network for pedestrian detection. Smith and Demetsky (1994) presented a new method to predict the short term traffic conditions in real time using neural networks based on operational traffic management data. This model performed well during peak conditions compared to traditional prediction models. Annunziato et al. (2003) compared developed methods with traditional back-propagation algorithm when weights are optimized off-line and online to develop real-time models for short time traffic prediction. This approach is very effective and more accurate to predict traffic volume in a short time.

Szarvas et al. (2005) presented new algorithm to detect pedestrians by using convolutional neural network (CNN) classifier. This method is more accurate compared to others because it inevitably optimized the feature illustration to the detection task and standardized the neural network. The proposed classifier false positive rate (FPR) is less than $1/5^{th}$ of support vector machine (SVM) classifier using Hilar-wavelet features. The computational demand of CNN classifier is lower than that of SVM. Sharma et al. (2005) reviewed the application of ANN in vehicular pollution modeling under urban condition. The basic feature of ANN modeling and the performance of ANN based vehicular emission models was defined. Zheng et al. (2006) presented a combined neural network model for the prediction of freeway traffic flow in a short time. The Bayesian combined neural network model (BCNN) is a combination of two single predictors, the back propagation and the radial basis function.

Murat and Baskin (2006) developed ANNDEsT (Artificial Neural Network Delay Estimation of Traffic flows) model for the estimation of vehicle delay for non-uniform delay type. Three-way split method was used to avoid over fitting problem and coefficient of determination, Mean Absolute Error (MAE) and Akaike Information Criteria (AIC) values were used for selecting the final network. This model was compared with HCM, Webster and Akcelik delay methods. ANNDEsT model given better results compared to other models for over saturation conditions (non-uniform). Salvo et al. (2007) investigated the effect of various parameters on average speed of the bus by using neural network and AVMS data (Automatic Vehicle Monitoring System). The numerous parameters of each vehicle such as load condition and vehicle condition were considered. The collected AVMS data consists of bus location, geometrical parameters and traffic rules. The comparison between Radial Basis Function network (RBF) and Multi layer perception (MLP) was done. The input parameters used in these neural networks are two types; geometrical parameters (number of lanes, width of lane, reserved lane) and traffic conditions (traffic flow rate, number of intersections with or without traffic lights, number of bus stops/kilometer, legal or illegal parking). RBF performed better compared to MLP in all stretches. Ng et al. (2013) presented a convolutional neural network for gender classification of pedestrians. In this method, hierarchical and multilayered neural

networks are combined into a single framework which is known as convolutional neural network to extract the features and classification. This algorithm can recognize pedestrians and classify the gender with an accuracy of 80.4%.

Arora and Mosahari (2012) presented a single layer ANN modeling for the prediction of noise due to traffic in Agra-Firozabad runway in India. 95 data sets were used in this model for noise prediction. In this analysis, 80% data was used for testing and the remaing 20% data was used for validation. Levenberg-Marquardt algorithm (LMA) was found to be the best with a minimum mean squared error (MSE). It was observed that, traffic flow, speed of heavy vehicles and percentage of heavy vehicles were the main causes of noise pollution. Kumar et al. (2013) predicted traffic flow using ANN based on previous traffic data. Traffic volume, speed, density, time and day of the traffic data are input variables. In this study, speed of each type of vehicles is considered separately but in past studies average speeds of all types of vehicle flow were considered. ANN performed better for the prediction of traffic flow even though time interval increased from 5 minutes to 15 minutes. Kumar et al. (2015) predicted traffic flow using ANN based on previous traffic data. The input parameters used in this model are speed, density, traffic volume, time and the day of the week. In this study, each type of vehicle speed is considered separately but in the past studies which combined average speeds of vehicle flow were considered. The model was validated using field data collected on rural highway. Masip (2015) presented a new method for the detection of pedestrians using convolutional neural networks (CNNs). A novel framework was created using CNN architecture and a fast linear classifier and the results were very accurate when compared to Histogram of Oriented Gradients (HOG) pedestrian detector.

Alex and Isaac (2016) developed a delay models using simulation model TRAFFICSIM for heterogeneous traffic in India. This model was developed for signalized intersections to estimate the delay by varying traffic composition. LOS at signalized intersection is explained by using delay and flow ration in heterogeneous conditions. The effect of percentage of three wheelers and buses was also considered while developing LOS. Dogan et al. (2016) estimated delay and stops at signalized intersections (4-legged) using ANN. In this model, input parameters are approach volumes, cycle length, and presence and absence of left turn used. In the same way, output parameters are average delay and number of stops used in the model. The simulation is run 196 times for produced data. This model is most effective and accurate to estimate the delays and stops at intersections. Fouladgar et al. (2017) proposed a deep learning based algorithm for the traffic flow prediction in northern California. In this algorithm, each node predicts its own congestion state in real-time with reference to the

neighboring network node congestion. Euclidean loss function is introduced in this model to get higher performance which can avoid the impact of unbalanced dataset. This method is more suitable for newly constructed locations. Alex et al. (2017) presented a new method to detect and recognize the motion of pedestrians in real situations by using convolutional neural networks (CNN). In this study, for better results, the results obtained using CNN were used as input parameters for the modified method. The modified CNN networks such as AlexNet, GoogleNet, and ResNet were best performing CNN with 90% accuracy.

2.8 Adaptive Neuro-Fuzzy Inference system (ANFIS)

Zadeh (1965) was the first person to introduced the fuzzy logic concept. After Zadeh, many researchers developed models using the fuzzy logic approach in different areas. The primary use of fuzzy logic approach is its attractive features like simplicity and natural structure. Pappis and Mamdani (1977) applied fuzzy logic controller in an intersection (two one way streets). In this analysis, a fuzzy controller was constructed based on linguistic instructions and the model was validated using the instructions. Average delay of vehicles at intersection is considered for the purpose of comparison and the results obtained from fuzzy controller are compared with vehicle actuated controller. It was shown that the average delay of vehicles was determined using fuzzy logic controller and these were less compared to vehicle actuated controller. Teodorovlc and Kikuchi (1990) applied ANFIS model for traffic assignment between two alternate routes on highway links. In this analysis, travel time on each route was treated as a fuzzy number and the rules were framed based on the degree of preference for each route. This analysis was done to each driver on each link and traffic was assigned to each route. Jang (1992) presented a temporal back-propagation methodology for creating self-learning fuzzy controllers. In this methodology, adaptive network as a building block and back propagation method was used to reduce the difference between actual and desired values. The upturned pendulum was used to validate the efficiency of the proposed method and the strength of the developed fuzzy controller. Sun (1994) presented a new model for data compression, pattern recognition and decision analysis using ANFIS. In this analysis, parameters were identified using Jang's model and Kalman filters were used to increase the performance. Parameters were classified with the help of modified Jang's model in which parameterized t-norms and mean operators were used for a simpler model. The idea of weight of importance was introduced for feature selection.

Wang (1996) presented a new method to extract fuzzy rules from given data. The membership functions were determined by calculating the variance and fuzzy rules were carried out by using fuzzy neural network. The algorithm designed consists of two parts in which optimal

number of fuzzy rules are determined in first part and the accuracy of the system is enhanced in second part using back-propagation. Sayers (1997) presented an application of fuzzy logic in traffic signals at intersections to take decisions to control the traffic. Ouyang and Lee (2000) presented a hybrid system to determine fuzzy rules from a given data. The developed algorithm consists of two stages, i.e., data partition and rule extraction. The data set is divided into numerous clusters based on similarity in first stage. In the second stage, a fuzzy IF-THEN rule is extracted from each cluster. The membership functions of the corresponding rule are determined by statistical techniques. The results show that the developed algorithm performed very quickly to generate fuzzy rules with a low mean square error. Rojas et al. (2000) presented a methodology to automatically identify the structure and optimization of parameters using a three-phase approach to construct a fuzzy system. Pomares et al. (2002) presented a new method to get the structure of a complete rule-based fuzzy system. The optimal topology of the fuzzy system was determined using target approximation error. The number of membership functions was also calculated using this error.

Murat and Uludag (2008) developed a route choice model of transportation networks in urban areas using fuzzy logic model (FLM) and logistic regression model (LRM) and compared them with base data. In their study, four parameters of traffic, namely, traffic safety, travel time, congestion and environmental changes were used and compared with accuracy percentage. Average accuracy of FLM was higher than LRM model. Yeh et al. (2011) proposed a new robust method for developing type 2 fuzzy rules for a given data comprising input and output. Fuzzy clustering method was used to divide the given data into clusters based on similarity. The membership function of each cluster was defined with mean and deviations. The fuzzy rules (type-2 fuzzy Takagi-Sugeno-Kang (TSK)) were determined for each cluster. Fuzzy neural network was constructed and the related parameters were distinguished using hybrid learning algorithm which includes particle swarm optimization (PSO) and a least squares estimation (LSE). Askerbeyh and Mustafa (2011) developed a new system based on fuzzy logic to simulate isolated traffic junction. Different fuzzy algorithms are used to check the performance of two traffic junctions. It was shown that fuzzy logic controller performed better and was more accurate compared to others. Kumar et al. (2013) used fuzzy logic model for mode choice modeling based on trip characteristics of travelers. In this study, different types of modes (2W, 3W, car, bus, cycle, metro, LRT) were used for one link. Public transport share was also estimated along with private vehicles. Yusupbekov et al. (2016) developed a new algorithm based on adaptive fuzzy-logic traffic control systems (AFLTCS) in heavy road traffic flows. In their study, simulation model based on adaptive

fuzzy-logic traffic control systems (AFLTCS) was developed for handling road traffic. The algorithm thus designed was compared with simulation model to test the efficiency.

2.9 Literature related to headway distributions

Mondal and Gupta (2018) carried out a study on discharge headway at signalized intersection for heterogeneous traffic. For analysis 3 cites from different parts of India were selected and data collection was carried out in 5 different signalized intersections. The analysis of discharge headway was carried out by means of plotting box and whisker plot. In order to quantify the discharge headway, continuous distribution model was used to analyse the headway distribution at the queue condition. Kolmogorov-Smirnov test was done to find the most suitable distribution model for analysis and from K-S test, it is clear that log-normal distribution is suitable for the analysis. Multi regime was fitted for different variable condition, where vehicle type and green time are key factors which affect the headway. Multi Linear Regression analysis was used to develop a model for discharge headway along with consideration of two independent variables. The outcome obtained from the study may be beneficial only for micro simulation model condition. To better understand the discharge headway, more data and other factors need to be considered to improve the performance of the model.

Ren et al. (2015) explored studied whether the assumptions made in HCM 2000 for analyzing the headway distribution were suitable for single lane roundabout entry capacity or not. Initially, the study was carried out manually and further analysis of headway distribution was done and then it was fitted with Gaussian distribution which is most suitable distribution for the collected samples. Based on the results from the analysis, some adjustments were proposed for HCM model while in the adjustment, linear function was established. The modified one provides better result than existing condition. Aghabayk et al. (2014) analyzed the behavior of pedestrians in different conditions (turning and crossing). Also some studies have been carried out in merging area, but the fact is condition will be seen to be common in places such as exit points of stadium and railway station. In this study the key focus is on merging area limited to T-junction and stair case. Understanding the behavior and characteristics of pedestrian in merging movement under crowded conditions are the main objective of their study.

Moinuddin et al. (2017) developed a mathematical model for speed, flow and headway relationship for heterogeneous traffic condition. Analysis was carried out to find the suitable distribution for different flow condition. Also estimation of capacity from speed & flow

relationship was considered. For the analysis, data was collected from 4 different study sections. Analysis of headway data near theater complex was carried out using normal distribution, since it has relatively high flow. For other 3 locations, which have low flow, flow analysis was carried by means of exponential distribution. Moridpour (2014) analysed the headway distribution for heavy vehicles and passenger cars under heavy traffic condition. To evaluate headway characteristics, time headway was separately evaluated for each vehicle type. Analysis of headway distribution for heavy vehicle and passenger vehicles was carried out for different traffic flow rate. Based on the analysis, a mathematical model was framed to estimate the parameters of headway distribution. From the study, lognormal distribution model fitted well to the time headway. Milan et al. (2018) studied in detail territorial social forces acting on the pedestrian in term of headway distribution and spectral rigidity. Analysis was carried out by probabilistic distribution of time headway between pedestrians for both theoretical and experimental condition. Though the analysis carried out by different distribution model, the study was restricted to unidirectional motion, where overtaking is not considered. From the study, pedestrian flow seems to show a higher level of synchronization than vehicular flow.

Prahara and Prasetya (2018) studied the impact of different modes in developing countries. In most of the developing countries, motorbike is the dominant mode of transport. Thus, the traffic characteristics of motorcycle dominated traffic was analysed and it differs from common traffic condition. The study was carried out by recording traffic movement in the selected study area for a particular time period. Further, speed-flow relationship was framed for analysing the macroscopic characteristics and then headway data was fitted to the negative exponential distribution along with the proposed theory for small vehicle.

Rupali Roy & Pritam Saha (2018) analysed the effect of heterogeneous distribution of time headways of two-lane roads. Also slow moving vehicles lead to frequent formation of platoons, which in turn increase the chance of risk while overtaking. The proportion of shorter headway increases in highly skewed observation for the selected area where the traffic flow is medium; analysis was carried out using log-logistic distribution. Based on the result obtained from the analysis comparison was made with other studies. From the following study, further initiatives were aimed at establishing a robust method of modeling headways on two-lane roads with mixed traffic. Sadeghpour et al. (2016) analysed data to determine the distribution of pedestrian arrival headways at signalized intersections and calculated the pedestrian average waiting time (delay) which affects green time. Field study was conducted at six intersections where pedestrian flows were low, moderate and high in Istanbul. Chi-squared

and Kolmogorov-Smirnov tests were used to investigate and determine the distribution of pedestrians' arrival headways. It was found that Gamma distribution is the best-fitted distribution for pedestrian arrival headway.

2.10 Literature related to Evacuation

2.10.1 Literature related to Capacity of bottlenecks

Weidmann (1993) studied the walking behaviour of pedestrians and observed the factors which affect the walking speeds of pedestrians, such as age, gender, size, and health, luggage, trip length, and purpose, type, grade and shelter of infrastructure, ambient, and weather condition. Tajima et al (2001) investigated pedestrian stream flow at a bottleneck under open boundaries using the lattice-gas model of biased random walkers. Hoogendoorn et al (2003) observed that capacity increases stepwise. When the crowd entered the bottleneck, formation of dynamic lanes occurs inside the bottleneck due to zipper effect. The distance between dynamic lanes is independent of the bottleneck width (B). The zipper effect is a self-organization phenomenon leading to optimization of the available space and velocity inside the bottleneck. The capacity increases only when an additional lane can develop which generally occurs in a stepwise way with increasing width. Daamen et al (2005) observed speeds of pedestrians obtained from previous studies in uncongested corridors and found an average speed of 1.34 m/s with a standard deviation of 0.37 m/s. It was observed that, age-related factors are influential in the study of walking behaviour also in addition to age itself. Movement conditions affecting the pedestrian's speed include purpose, presence of attractions, trip length, weather conditions, and the type of infrastructure and surface conditions (Lee 2005).

Seyfried et al. (2006) presented a modified one dimensional social force model to analyze the velocity-density relation on the fundamental diagrams. The mean value of the velocity mainly depends on the interaction between persons. Kretz et al (2006) experimented with crowd flow through bottlenecks and presented the results in the form of total times, flows, specific flows, and time gaps. The necessity of these parameters on the bottleneck width was evaluated. A continuous decrease of specific flow was observed with increasing width of bottleneck when only one person could pass bottleneck. Specific flow was observed to be constant for larger bottlenecks. Nagai et al (2006) investigated the evacuation processes of pedestrians, and crawlers by evacuating pedestrians from the corridor with an exit based on experiment and simulation. For the simulation, lattice gas simulation was used, where a biased random walker

simulates each pedestrian. It was found that the experimental results are consistent with the simulation results. Liddle et al (2009) investigated influence of the bottleneck width on the specific flow and observed that the specific flow is independent of widths varying from 0.6 m to 2.5 m. The specific flow was observed to be nearly 1.9 $(m*s)^{-1}$ in a normal situation.

Seyfried et al (2009) performed an experimental study on crowd behaviour at bottlenecks, and observed that the flow always depends on the bottleneck width. Seyfried et al. (2008) performed experiments with 250 persons under laboratory conditions and the trajectories of each person were measured with high accuracy to analyze the flow through bottlenecks. There was a huge deviation in different methods analyzing the flow through bottlenecks. The changing population demographics can influence pedestrian characteristics when compared with other studies. Chattaraj et al. (2009) presented fundamental diagrams for two different lengths of corridor from different cultures (German, Indian) and the results obtained were compared using statistical tests (t-test, z-test). The Indian person's speed was found to be less affected by density compared with that of the German. From statistical analysis, it was found that, cultural differences exist in the pedestrian's fundamental diagrams. Seyfried et al. (2010) presented experimental results for congested pedestrian traffic using experiential data based on individual trajectories. Trajectories were extracted for each person by providing individual scale which shows pedestrian congestions based on go and stop conditions. The velocity-density relation and phase separation were replicated. Steffen and Seyfried (2010) presented a new method for calculating pedestrian microscopic characteristics by using pedestrian trajectories. Pedestrian density was measured using Voronoi diagrams to reduce the density scatter. The speed and direction of each pedestrian was measured based on position differences between times with identical phases of stepwise movement.

Chraibi and Seyfried (2010) presented modified spatially continuous force based model to analyze the pedestrian movements in one and two dimensional space. The fundamental diagram was measured for narrow and wide corridors. Real life video of crowd stampedes and panicking ants data were used to develop a simulation model showing potential problems and consequences of turning movements during collective dynamics (Nirajan et al 2011). Using this tool, it is possible to develop evacuation strategies and design solutions that can prevent stampedes. Zhang et al. (2011) performed experiments with 350 persons in straight and T-junction corridors under laboratory condition and four different measurement methods were used to investigate the influence of these methods on pedestrian fundamental diagrams. The trajectories of each person were extracted using PeTrack software. It was found that Voronoi diagram method is the best method for designing pedestrian fundamental diagram. Liddle et

al. (2011) performed experiments with 180 persons to measure density and speed more accurately using Voronoi diagrams. Spatio-temporal variations of the persons at bottlenecks were analyzed using this method. It was observed that, density is not constant with time and density peak moves into bottleneck when the bottleneck width increases. Panicking ant's data and crowd dynamics simulation model data were used to describe how right-angled egress paths work ineffectively compared with straight egress paths during collective panic egress (Dias et al 2012). The total egress behavior of a crowd was influenced by exit choice behavior. A discrete choice model was proposed to represent pedestrian exit choice decisions during evacuation (Duives et al 2012).

Saboia & Goldenstein 2012 studied crowd behaviour at bottlenecks and observed that faster-is-slower pattern refers to clogging at locations close to the exit. The average speed of pedestrians leaving the exit decreases when they attempt to walk faster and consequently egress time increases. Zhang et al. (2012) performed experiments of bi-directional flow with 350 persons in straight corridors under laboratory condition and four different measurement methods were used to investigate the influence of these methods on the pedestrian fundamental diagrams. The trajectories of each person were extracted using PeTrack software. It was found that, Voronoi diagram method is the best method for the pedestrian fundamental diagram. At densities below 2.0 m^{-2}, there is no significant difference in fundamental diagrams. The maximum flow of 2.0 ms^{-1} was observed for uni-directional flow and 1.5 ms^{-1} observed for bi-directional flow.

Zhang and Seyfried (2013) presented experiments with different intersecting angles for bi-directional flow. The Veronoi diagrams method was used to measure speed-density relations. Several flow types were compared and it was found that there is no effect of intersecting angle on fundamental diagrams. It shows that different types of flow have the same influence on transport system. Das et al (2014) conducted a series of experiments at angled corridors to understand the walking characteristics of individuals at different speeds. Cao et al. (2016) studied the effect of age (young, old, and mixed) on pedestrian movements. The trajectories of each person were extracted using PeTrack software. Traffic jams observed more often in mixed group compared to others because of large variation of motions. The three groups have three different fundamental diagrams which cannot be combined into one diagram. Different age groups and speeds of the pedestrians in a crowd were main reasons for non-homogenety in density and also one reason that influence pedestrian movement. It was found that density of crowd composition was not the only factor leading to jams. Nicolas et al. (2017) studied pedestrian movements through a narrow door (72 cm) in which a fraction of participants (c_s) behaves selfishly and others behave politely. Experiments were conducted under laboratory

conditions with normal walking and fast moving persons using quasi-stationary regime. It was found that; flow rate was higher for larger c_s and with more fast moving persons. The flow was observed to be systematic for polite crowds while for higher c_s the flow observed was unsystematic.

2.10.2 Literature related to Capacity of doors

Daamen and Hoogendoorn (2010) presented the factors affecting the capacity of door during evacuation. In their study, the factors considered were width of door, population composition, presence and absence of an open door and evacuation condition. The average capacities of doors for all widths were observed to be lowest for low stress levels and highest for high stress levels. The capacities observed were to be low for persons with disabilities. The presence of an open door has negative effect on door capacity. In their experiments, faster is slower phenomenon failed due to higher urgency which led to higher speeds, which in turn led to higher capacity. Weifeng and Hai (2011) developed a new model based on cellular automaton to study the visibility during evacuations. In the model, smoke effect was considered because visibility can affect human behavior during evacuations and empirical formula was used in the proposed model to estimate the visibility range. The walking speeds of the evacuees decreases with increase in smoke density.

Jo et al. (2014) presented the features of pedestrian movement around doors connected to corridors. The change in flow rates through a door connected to a corridor was analyzed to verify the safe evacuation for the design. The flow rate at the door decreased when the corridor was crowded. The flow rates were observed to be same in simulation and experiment. Lovreglio et al. (2014) presented a behavior model based on discrete choice model to predict the probability of a person showing herding behavior in exit choice during emergency evacuation situations. The model was developed based on the data collected through an on line survey. It was shown that the evacuees are influenced by both people near the exit and their socio-economic characteristics. Lovreglio et al. (2016) investigated the effect of Herding Behavior (HB) in exit choice during emergency situations and developed a behavior model (binary logit model) to predict the occurrences of HB in exit choice. The developed model consists of environmental factors and personal factors and also random human behavior but most of the existing models consider panic level of the evacuee.

2.11 Summary of literature review

From the review of literature regarding object detection, background subtraction technique is simple and accuracy is moderate but computational time is low. Optical flow algorithm is

very complicated and computational time is very high and accuracy is moderate. Spatio-temporal filtering method is not applicable for stationary objects and cannot be used for real time applications. This algorithm works in low resolution scenarios but suffers from noise issues while accuracy is only moderate. In this study, background subtraction technique was used for object detection.

From the review of literature regarding object tracking, point tracking computational time is low and accuracy is moderate. This algorithm can track points in noisy images. Kernel tracking can be used for real time applications due to low computation time and accuracy is moderate. Silhouette tracking can detect an objects shape indirectly by training and computational time is more but accuracy is high. These algorithms fail when crowd size is very high and obstructions are present. In this study, TRACKER software was used for object tracking. The detailed explanation of TRACKER software is mentioned in Methodology.

From the review of literature regarding behavior understanding models, in object based approach tracking individual persons in high density crowd is very difficult and this method is applicable only to low to moderate density crowd. Holistic based approach ignores individual information in crowd and this method is mostly applicable to high density crowd. A lot of studies were done on crowd behaviour based on holistic approach (i.e., crowd is treated as a single entity.) few number studies were carried out on object based approach (i.e., crowd is treated like a collection of individuals). In this study, object-based and holistic-based approaches were both studied.

From the review of literature regarding capacity of bottlenecks, it can be said that many researchers have studied the crowd behaviour at bottlenecks in terms of density, flows and capacity estimation etc. Pedestrian flow at bottlenecks continuously depends on the width of the bottlenecks. Some studies shows that linear dependence between the width and capacity of bottleneck but in a contrary way, some researchers showed that capacity increases stepwise as the width increases. Pedestrians prefer to increase (or decrease) their walking speed with increasing (or decreasing) their step length more than their step frequency. Many factors affect the walking speeds of pedestrians, such as age, gender, size, health, characteristics of the trip, properties of the infrastructure, environmental characteristics and along with these factors, the walking speed also depends on pedestrian density. In this study, capacity of bottlenecks was analysed based on the effect of composition and bottleneck width. The inclusion of buffer space on crowd dispersion was also analysed.

3. METHODOLOGY AND DATA COLLECTION

3.1 General

The detailed methodology for the present research work is discussed in this chapter. As mentioned in the previous chapters, crowd flow characteristics vary with demographic factors of each individual, environmental factors, and geometric factors. The subsequent sections of this chapter deal with different stages considered in the current methodology. This chapter also deals with the process adopted for data collection at different mass gathering locations and subsequent extraction of the pertinent parameters required for preliminary analysis. The data thus extracted is used for developing the fundamental crowd flow diagrams, MLR, ANN, and ANFIS models for microscopic analysis and single, multi-regime modeling for the macroscopic analysis. Further the capacity of bottlenecks, doors, and stairways are calculated for safe evacuation.

3.2 Methodology

The methodology adopted for the present study was executed in different stages and the coreesponding flow chart is presented in Figure 3.1. Various steps in the methodology are described in detail in subsequent sections.

3.2.1 Site selection

The present study is intended to analyse the behaviour of the crowd at major mass gatherings instead of confining the study to particular stretches. To analyse this, three major crowd events were considered for the data collection.

3.2.2 Data collection

Data collection was performed using video graphic survey. The camera was mounted on the specific selected location to cover the entire area with out any obstructions.

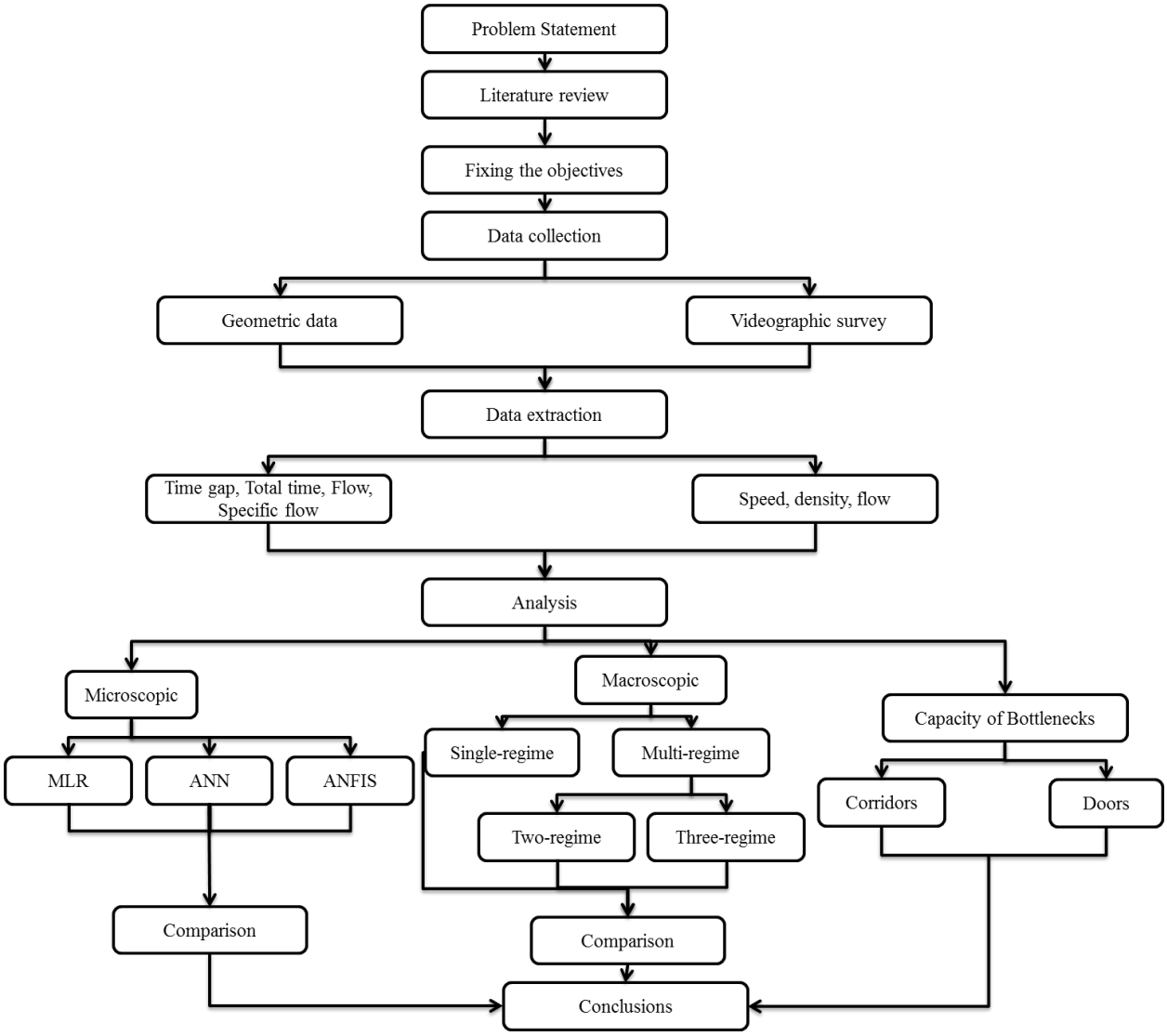

Figure 3.1 Proposed flow chart of study methodology

3.2.3 Data extraction

Data extraction was done using MATLAB and TRACKER software. The extracted data was classified into categories to observe the flow behavior as well as individual behavior.

3.2.4 Crowd characteristics

Crowd characteristics include gender, age, child holding, child carrying, people carrying luggage. These factors affect effective parameters like speed, density and flow of the crowd.

3.2.5 Speed of the crowd

People in the crowd move at different speeds due to heterogeneity (gender, age, luggage, etc.). Speed is extracted using TRACKER software.

3.2.6 Density of the crowd

Density is estimated using two methods: automatic and manual. In automatic method, pixel-based method was used to assess crowd density. In manual method, total area is divided into grids and number of persons in each grid for all frames is calculated.

3.2.7 Microscopic analysis

In this analysis, effect of factors like age, gender, group size, child holding, child carrying, people with luggage and without luggage on crowd speed are considered. MLR, ANN and ANFIS models were developed between crowd speed and significant factors were observed from the statistical analysis. The developed model is validated using RMSE and MAE values.

3.2.8 Macroscopic analysis

A model was developed based on better fitness of predicted data to actual observed data. Single and multi-regime models were used in this study to characterize crowd traffic in different regimes, such as uncongested flow, transitional flow, and congested flow.

3.2.9 Capacity of bottlenecks

The variation of flow behavior of the crowd with reference to bottleneck widths (corridors, doors) at different compositions (density) considering both with and without buffer space is studied and evaluated in this section. Double doors were provided to observe any herding behavior during the evacuation.

The data collection, extraction and preliminary analysis of the present work will be discussed in the next section.

3.3 Data collection

3.3.1 Krishna Pushkaralu

The first event was Krishna Pushkaralu which occurs every twelve years, there being a religious congregation at each main river in India. Approximately 35 million people took a holy dip in Krishna river during Krishna Pushkaralu held in August, 2016. Due to irregular movements of the individuals, mob formations are more in these types of events. Figure 3.2 shows the crowd study area during Krishna Pushkarams. Mid block section was selected at Vijayawada, Andhra Pradesh, India during Krishna pushkaralu. Organized flows were observed at mid block section.

Figure 3.2 Crowded study area during Krishna pushkaralu

3.3.2 Medaram festival

The second major event is Medaram Festival (Sammakka Sarakkajatara, Location-2) which is the biggest tribal congregation in India held once every two years. Devotees from different corners of the state arrive in large numbers for the four-day festival. During the festival in February 2017, approximately 2.8 million devotees participated in this event. Figure 3.3 shows the crowd study area at Medaram. Two locations were selected to observe different flow patterns of the crowd at Medaram festival. The behaviour of each person in a crowd is affected by movement of the persons around them. L1 is a three-legged intersection which is located near temple entrance. The crowd movement is diversified at this location because of crowd merging from three directions to the temple entrance. L2 is a mid-block section located between the temple and bus stand. The crowd movement is directional but not properly regulated at this location because of roadside vendors and shops.

Figure 3.3 Crowded study area at medaram

3.3.3 Evacuation experimental

The evacuation experiment was set up in front of the transportation division-NIT Warangal. A digital camera was fixed at the top of the building. The experimental study area is 10 m by 5m as shown in Figure 3.4. The height and width of the bottleneck was constant and the length of the bottleneck was 1.5 m. The holding areas made sure that there was same initial density of the crowd for each run. The distance from the first holding area to the entrance of the bottleneck was 3 meters. Five different widths of bottlenecks 80, 100, 120, 140, and 160 centimeter repectively were experimented. The sample snaps of the experiment setup have been shown in Figure 3.5. Double doors (100 cm) were provided to observe any herding behavior during the evacuation.

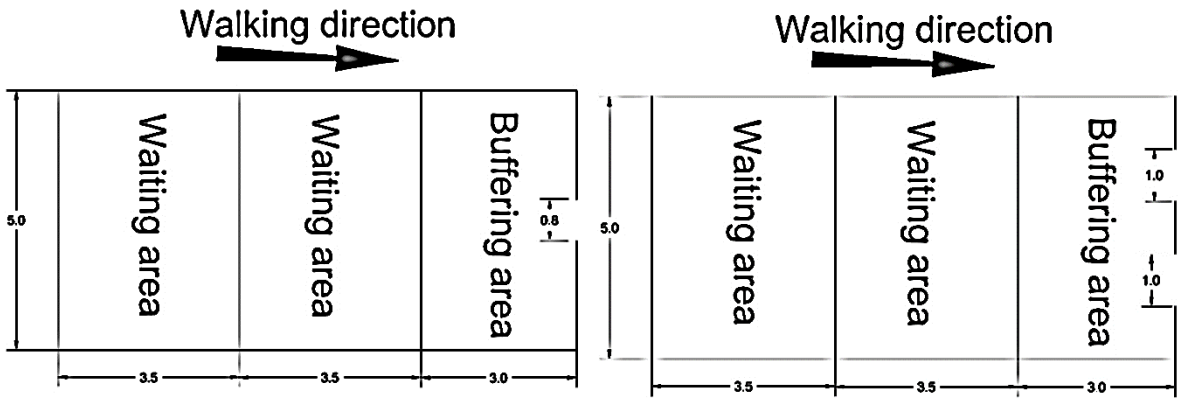

Figure 3.4 Experimental setup

a) Crowd flow without buffer space

b) Crowd flow with buffer space

Figure 3.5 Sample snaps during evacuation study

In this experiment, 50 individuals were involved. The participants were divided into two groups, which were given separate walking tasks for each experiment (walk slowly, walk fast, etc.). The groups were heterogeneous and consisted of men and women of different ages. The group participants were indicated by the colour of their caps (white). The persons without caps are ordinarily behaving pedestrians, while the persons with caps follow specific instructions (walk aggressively, walk slowly, etc.). Figure 3.6 shows the normal, slow and fast walking evacuees in this study.

Figure 3.6 Different types of evacuees

Note: A = Normal walking speed, B = walk Slowly, C = walk aggressively

3.3.4 Data extraction

3.3.4.1 Crowd density estimation

3.3.4.1.1 Manual

The first step in density estimation was the conversion of video into frames, and the next step was to divide the entire area (50 meter^2) into an equal number of grids having grid size of 0.5 × 1 meter. The last step was to count the number of persons in each grid by manual counting method, and finally the average values of densities for all frames were obtained. Figure 3.7 shows the study area divided into grids.

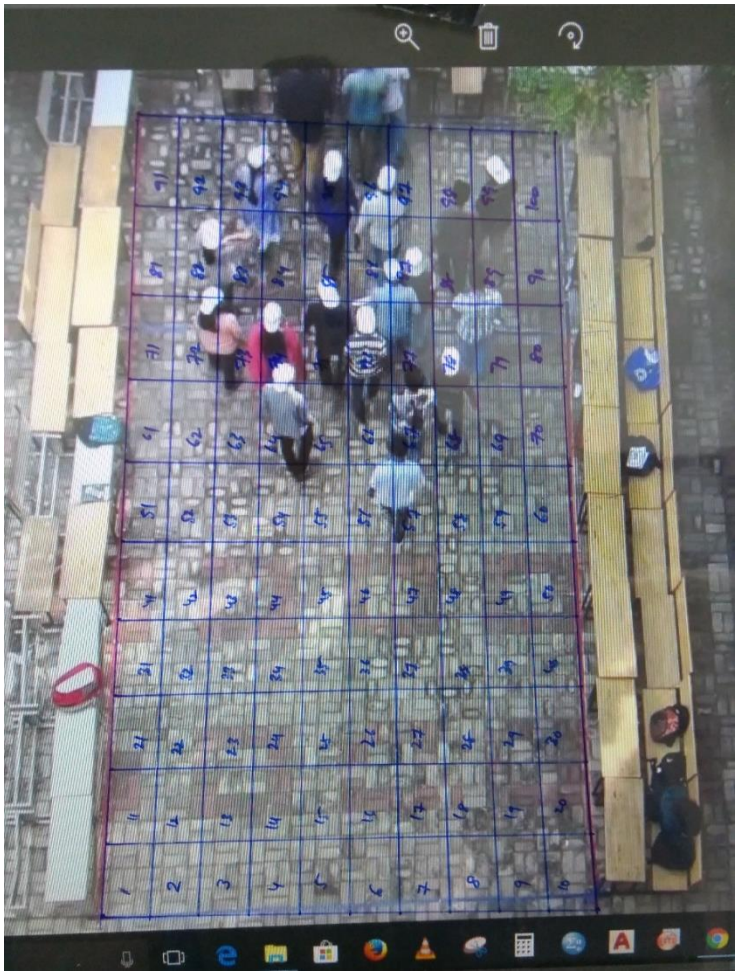

Figure 3.7 Study area divided into grids

3.3.4.1.2 Automatic

In this study, pixel-based method was used to assess the crowd density. The number of people in a frame can be counted using foreground/background segmentation. Figure 3.8 shows the flow diagram for estimating the density of crowd Figure 3.9 shows the background subtraction at Krishna pushkaralu (sample).

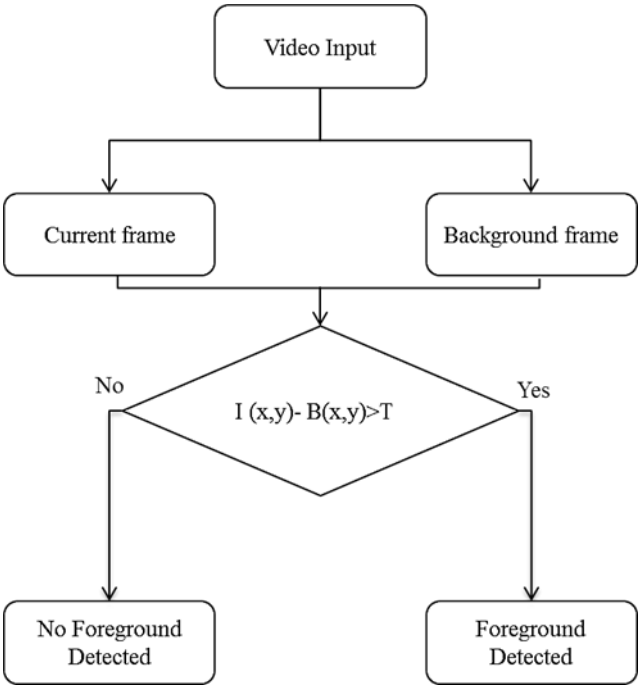

Figure 3.8 Crowd density estimation flow chart

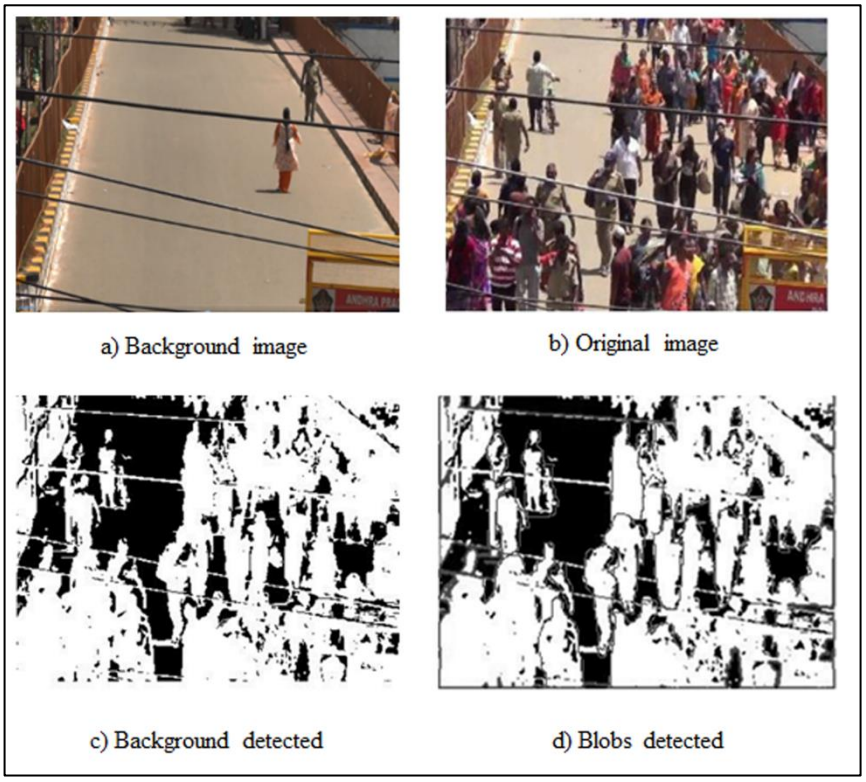

Figure 3.9 Crowd density estimation using background subtraction technique

The first step of density estimation using pixel level analysis is separating the foreground objects from the background in the frames. After removing the background from the frame, the removed foreground objects are automatically recognized as the blobs. The number of

blobs represents the number of people in that frame. The ratio of the number of people to the area gives crowd density.

3.3.4.2 Crowd tracking

Tracking refers to locating an object (or multiple objects) over a sequence of images. For extracting the speed, the video is imported into the TRACKER software, where the video is converted into frames. Then, the coordinate axis of the frames needs to be fixed. The lower left corner of the video image was selected as the coordinates of origin. The next step of the analysis is to create and assign a separate point mass for each and every person. This assigned point mass can be used to store and display the characteristics (coordinates, speed, acceleration) of a person. Figure 3.10 shows the image tracking the persons in the frame at Medaram.

Figure 3.10 Images representing the sample tracking of persons in the frame at Medaram

3.3.4.3 Conversion Image Coordinate to the Real World coordinates

The pixel coordinates obtained from the video cannot represent a person's movements in real-world situations because the camera angle while recording was not perpendicular to the ground. Hence, conversion of pixel coordinates to real-world coordinates is required for getting the real world trajectories of individuals. A direct linear conversion algorithm was applied based on Wolf and Dewitt (2000) to minimize the effect of swaying and height difference. The relevant conversion formulas are as follows (Eqs. (3.1) and (3.2)):

$$u + \frac{L_1 x + L_2 y + L_3}{L_7 x + L_8 y + 1} = 0 \quad (3.1)$$

$$v + \frac{L_4 x + L_5 y + L_6}{L_7 x + L_8 y + 1} = 0 \quad (3.2)$$

Where (u, v) are the pixel coordinate, (x, y) are the real world coordinate and L_1–L_8 are transformation coefficients. Eight real world reference points were selected and measured in the experiment sites along with the corresponding pixel coordinates. Four points were used to compute the conversion coefficients and the remaining four points used to check the errors.

3.3.4 Calculation of crowd movement variables

Basic terminology which is helpful to understand the study with ease is provided in this section.

3.3.4.1 Travel distance

For each person the travel distance can be calculated as

Travel distance = $\sqrt{(y_{k+1} - y_k)^2 + (x_{k+1} - x_k)^2}$

Where, k is the number of observations for each persons starting with 1.

3.3.4.2 Average walking speed (meter/second)

The average time that person in a crowd walks through a certain distance within an area is calculated as follows:

$$U = \frac{L}{\sum_{i=1}^{N} \frac{t_i}{N}} \quad (3.3)$$

Where L represents walking distance, N represents the number of persons in the observed crowd, and t_i represents the walking time of person i.

3.3.4.3 Average density (person/square meter)

The quantity of crowd within a unit area is called density.

$$K = N/A \quad (3.4)$$

Where K represents average density, N represents the number of persons in the crowd within the area A.

3.3.4.4 Crowd volume (person/meter/second)

The quantity of crowd that is going through a section within a unit time period is:

$$Q = K \times U \quad (3.5)$$

Where Q represents the crowd flow, K represents the average density of the crowd, and U represents the average speed of crowd.

3.3.5 Crowd characteristics

The flow parameters may change with respect to gender and age too. So the velocities, flows, and densities of the individuals in the crowd have been found to serve the objectives considered. The data is extracted for different gender, age groups with luggage and without luggage. The crowd attribute classification criteria are tabulated in Table 3.1.

Table 3.1 Crowd attributes classification

Attribute	**Classification**	
Gender	Male Female	
Age	<15 years	Child
	15-40 years	Youth
	40-65 years	Middle age
	>65 years	Old
Luggage	Carrying luggage No luggage	
Child Holding	Yes No	
Child carrying	Yes No	
Group	2 >2	

3.3.6 Crowd composition

The crowd composition of different attributes of study areas is shown in Figure 3.11 to Figure 3.22.

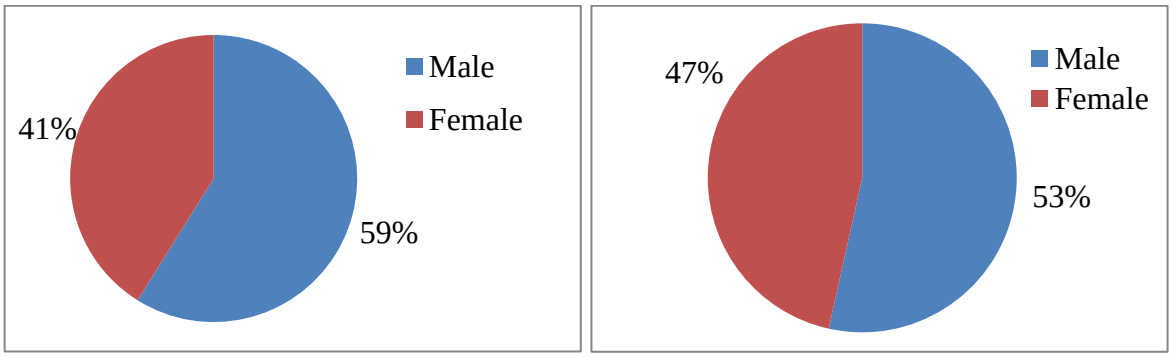

A) Medaram **B) Krishna Pushkaralu**

Figure 3.11 Gender composition

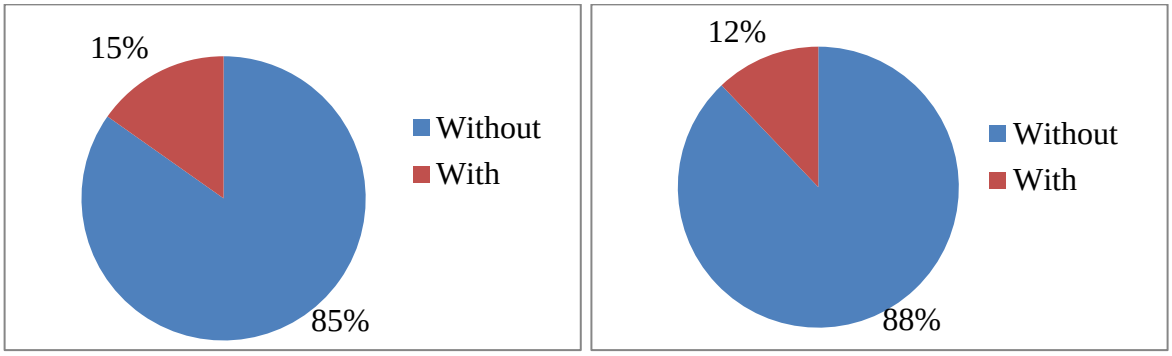

A) Medaram **B) Krishna Pushkaralu**

Figure 3.12 Luggage composition

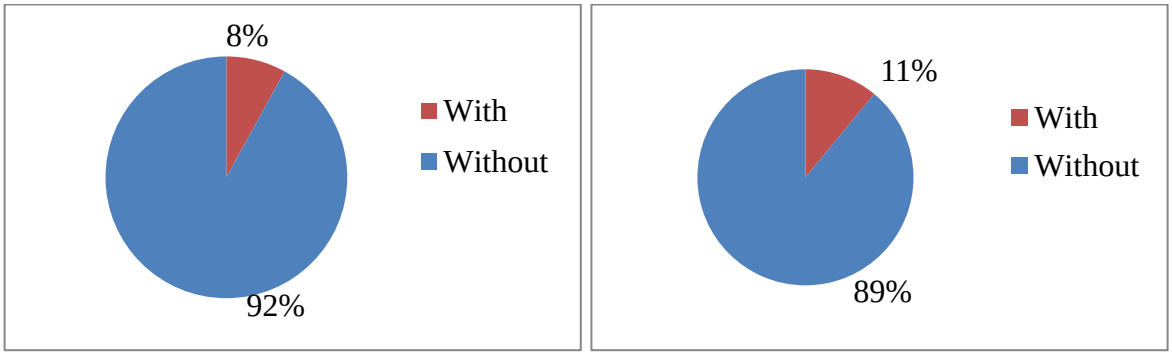

A) Medaram **B) Krishna Pushkaralu**

Figure 3.13 Child carrying composition

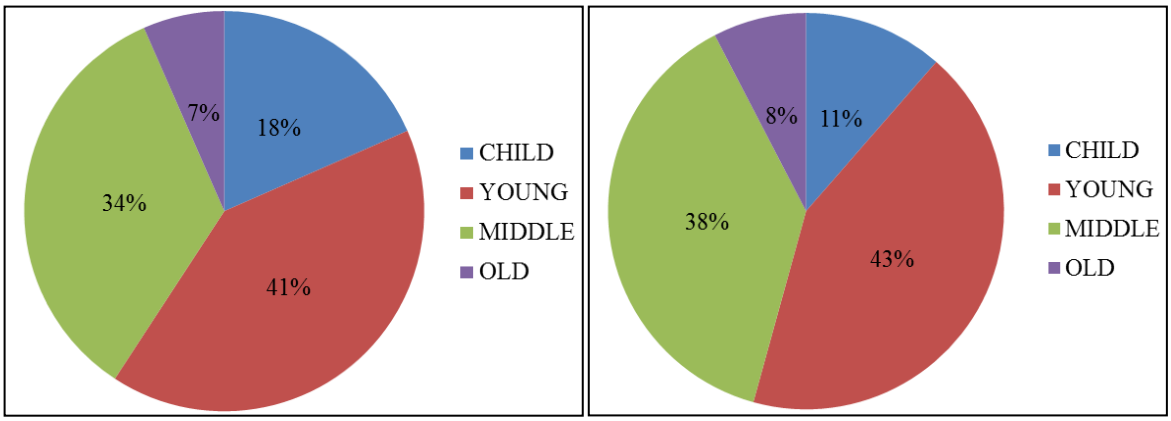

A) Medaram **B) Krishna Pushkaralu**

Figure 3.14 Age composition

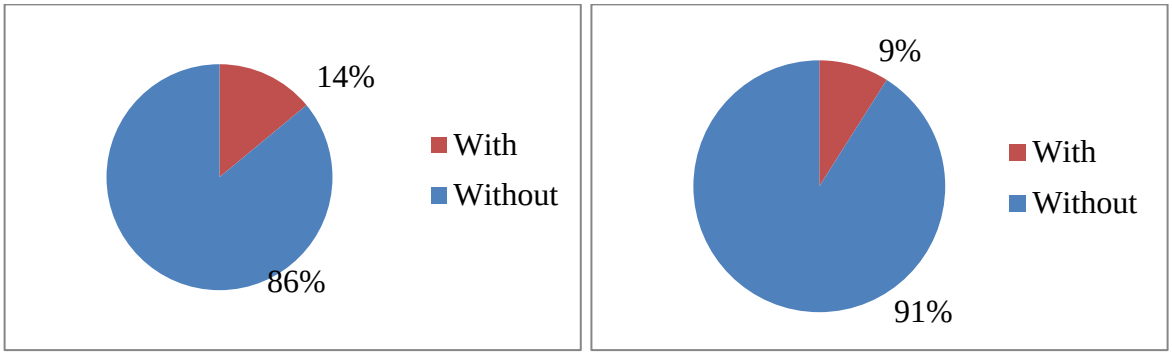

A) Medaram **B) Krishna Pushkaralu**

Figure 3.15 Child holding composition

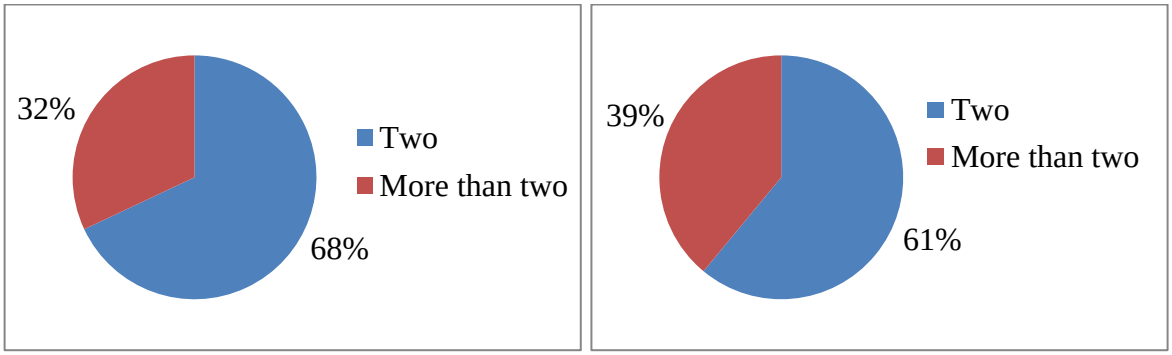

A) Medaram **B) Krishna Pushkaralu**

Figure 3.16 Group composition

3.3.7 Summary

This chapter discussed the methodology adopted for the current research that involved various stages to analyze crowd behavior based onmodeling and evacuation planning. The details of study areas and the collection of data at these sections were described. The extraction of data such as speed, density, flow and composition of crowd from video was done. The crowd characteristics and compositions of crowd were provided in this chapter. The data collected as reported in this chapter is very much useful in analyzing crowd behavior in microscopic and macroscopic ranges. From the data, crowd flow diagrams, MLR, ANN, ANFIS models were developed. The analysis of crowd will be discussed in detail in the next chapter.

4. MICROSCOPIC MODELING

4.1 General

In general, physical factors of individual people in the crowd adversely affect crowd flow and speed, especially in mass gatherings. Such gatherings act as severe threats for crowds because of high density in limited space, which ends up in adverse outcomes resulting in stampedes. The movement of an individual person in a crowd is influenced by physical factors. In the present chapter, characteristics like age, gender, group size, child holding, child carrying, people with luggage and without luggage are considered for crowd behaviour analysis. This study helps in proper dispersal of crowd in a planned manner to that of diversified directional flow that exist during crowd gathering events.

4.2 Results

The average crowd density, speed, and flow for both the locations are tabulated in Table 4.1. The average crowd density at L1 and L2 observed was 1.73 and 1.58 P/m^2 respectively. It is observed that L2 has lower density compared to L1.

Table 4.1 Crowd flow parameters for two locations

Location	Total frames	Average people on each frame	Average Density (p/m^2)	Average speed (m/s)	Average flow (p/min/m)
L1	4500	91	1.73	0.703	73
L2	4500	79	1.58	0.931	64

4.2.1 Density Classification

In this study, for density classification, pedestrian LOS from HCM (2010) was used. The density and number of persons were calculated using Pedestrian LOS table using classic traffic flow equation (Q = K×U). Density classification as per pedestrian LOS is tabulated in Table 4.2. Crowd density is classified into three categories such as low (<0.72), medium (0.72 – 1.64) and high (>1.64). Also, based on the number of persons, the crowd density is further classified into five categories such as very low (<0.20), low (0.20 – 0.45), moderate (0.45 – 0.72), high (0.72 – 1.64), very high (>1.64). The comparison was done for density values obtained from the present study with previous studies and is tabulated in Table 4.3 and 4.4. There are minor variations in the classification with respect to density in the present study and this has been adopted for further analysis. The average density observed at L1 is 1.73 P/m^2

which falls into level of service F. The speed is given as ≤ 0.76 and the observed speed is 0.703 m/sec. The flow for the level of service F was taken to be greater than 80 P/min/m, but the observed flow was 73 P/min/m. The lower flow values can be attributed to the fact that factors like age, gender, group size, CC, CH, people with luggage and without luggage affect the movement of people in the crowd. Further analysis was carried out at L1 to explore the effect of above mentioned factors on speed.

Table 4.2 Density classification as per pedestrian LOS, HCM (2010)

LOS	Speed	Flow rate	Density	People	Classification based on people	Classification based on density
A	≤ 1.32	≤ 16	0.20	10	Very low	Low
B	1.27–1.32	16 - 23	0.30	10-14	Low	
C	1.22 – 1.27	23 - 33	0.45	14-22		
D	1.14 – 1.22	33 - 49	0.72	22-35	moderate	
E	0.76 – 1.14	49 - 75	1.64	35-80	high	Medium
F	≤ 0.76	Var.	> 1.64	> 80	Very high	High

Table 4.3 Comparison of density classification based on people count with other related work

Density	Number of people			
	Marana et al. (1998)	Jiang et al. (2014)	Ramalan et al. (2006)	Present study
Very low	0-20	0-10	<7	0-10
Low	21-40	11-30	7-10	10-22
Moderate	41-60	31-60	11-16	22-35
High	61-80	61-100	17-26	35-80
Very high	>80	>100	>26	>80

Table 4.4 Comparison of density with other studies

Reference	Density (P/m^2)		
	Low	Medium	High
Meynberg et al. (2016)	0.2-0.5	0.5-1.5	> 1.5
Jacobs method	1.07	2.4	4.3
Bao et al. (2013)	< 0.6	0.6-2.0	>2.0
Present study	< 0.72	0.72-1.64	>1.64

4.2.2 Descriptive Analysis on Speed

A descriptive analysis has been done and tabulated to easily identify the parametric difference thoroughly. The statistical summary of average speeds of crowd for both the locations for different factors is tabulated in Table 4.5.

Table 4.5 Descriptive statistics of speed at both locations

Factor		Speed (m/s)			
		L1		L2	
		Mean	Std. Deviation	Mean	Std. Deviation
Gender	Male	0.81	0.21	1.01	0.28
	Female	0.70	0.25	1.16	0.29
Age	Child	0.82	0.25	1.06	0.30
	Young	0.80	0.23	1.16	0.29
	Middle	0.74	0.24	1.07	0.26
	Old	0.69	0.24	0.86	0.25
Luggage	With	0.76	0.25	1.07	0.32
	Without	0.80	0.18	1.09	0.29
Child carrying	Yes	0.74	0.14	0.85	0.29
	No	0.81	0.26	1.09	0.25
Child holding	Yes	0.76	0.16	0.91	0.26
	No	0.82	0.22	1.12	0.20
Group	Two	0.73	0.23	0.91	0.27
	≥ Two	0.66	0.15	0.83	0.19

In general, male persons show higher speeds than female and speed decreases with age. In general, people without luggage show higher speeds than people with luggage. In general, people carrying children report lower speeds than single persons. Also, child holding people show lower speeds than single persons. The group which contains two persons shows higher speeds than the group with more than three persons.

4.2.3 Speed comparison

Figure 4.1 and 4.2 represent the comparison of crowd speed with respect to gender, age, group size, CC, CH, and people with luggage and without luggage for both locations. The average speed of a younger male pedestrian without luggage was high compared to other pedestrians. The average speed of CH and CC of the male pedestrian was high compared to a female pedestrian. The speed of three or more persons in a group was low compared to single and paired persons.

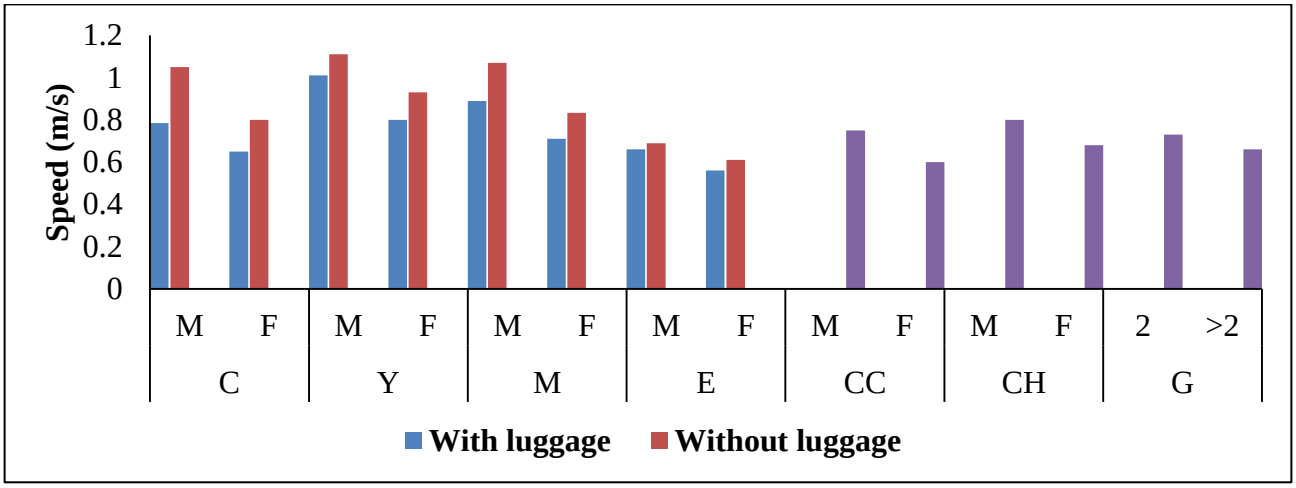

Figure 4.1 Speed of crowd movement at L1

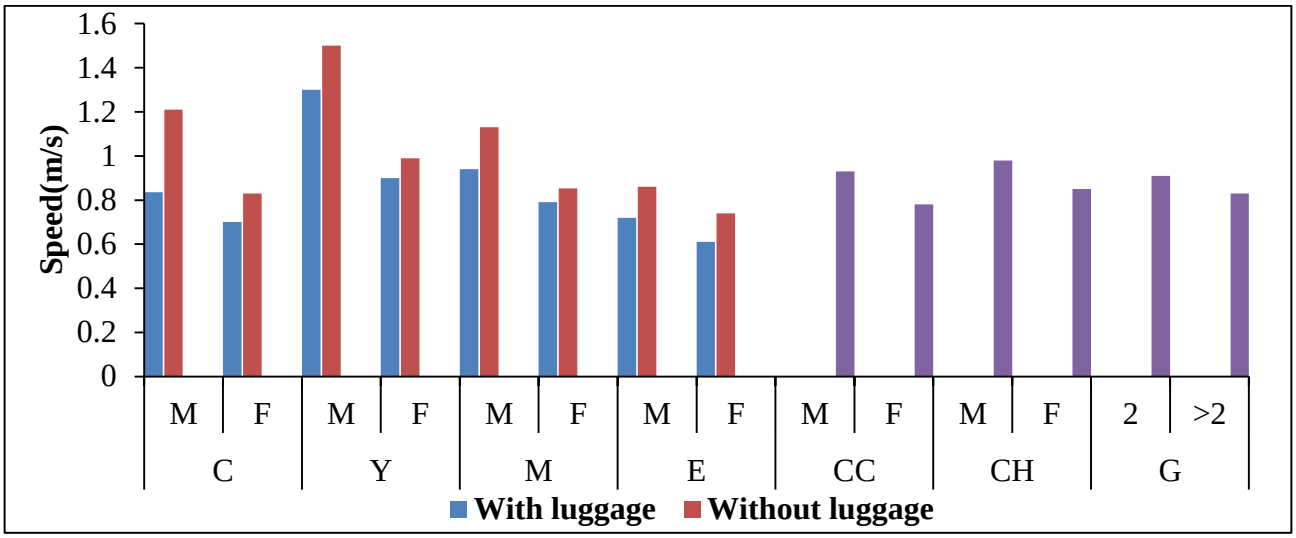

Figure 4.2 Speed of crowd movement at L2

4.2.4 Fundamental Diagrams

The relation between flow and density, density and speed, speed and flow, can be represented with the help of fundamental relationships. They are referred to as fundamental diagrams of traffic flow. These relationships help in planning, design and operations of facilities. When the movement of people is not constrained and freedom is available, they travel at a maximum speed (free flow speed). At free flow speed, flow rate and density will be close to zero. On saturated facilities, flow rate and speed are down to zero. People are queuing and there is a maximum density (jam density). The capacity of a facility is equal to the maximum flow rate. From Figure 4.3 (a), speed of the crowd was low at L1 compared to L2, because density was high at L1. From Figure 4.3 (b) and 4.3 (c), maximum flows for L1 and L2 were observed to be 135 p/min/m and 102 p/min/m respectively.

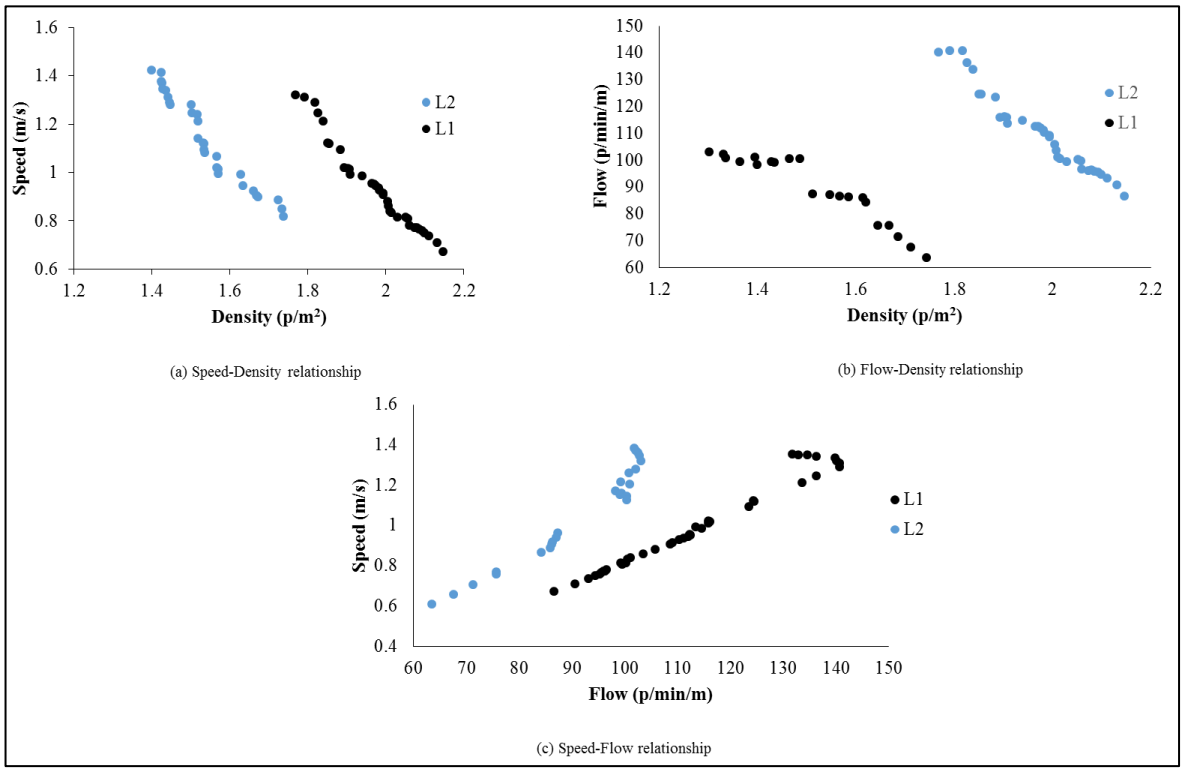

Figure 4.3 Speed, Density and Flow relationships for the two locations

The flow–density, speed–density, relationships of crowd and other previous studies (Fruin 1971; Older 1968; Sarkar 1993; Tanaboriboon et al. 1986; Virkler and Elayadath 1994) were shown in Figure 4.4.

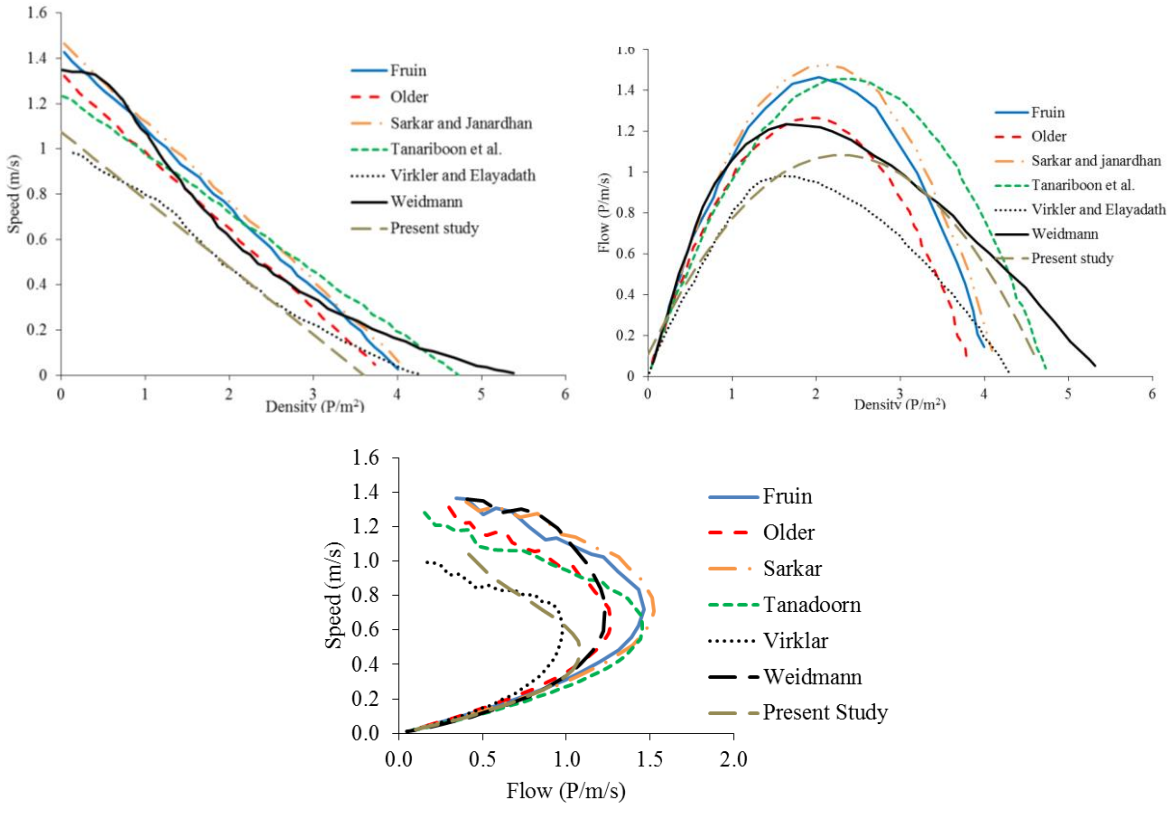

Figure 4.4 Speed-Desnity-Flow relationships with other studies

On saturated facilities, flow rate and speed are down to zero. People are queuing and there is a maximum density (jam density).The capacity of a facility is equal to the maximum flow rate. These relationships/diagrams will be helpful in understanding the phases of transformation from uncongested to congested flow.

4.2.5 Statistical Tests

For statistical analysis, ANOVA and Pearson correlation tests were performed using SPSS and variables considered for analyses were gender, age group, group size, CH, CC and person with luggage and without luggage factors. Gender was divided into two categories, and the values were assumed as 0 for male pedestrian and 1 for female pedestrian. Age was divided into four categories, and the values were considered 0 for child, 1 for the young, 2 for middle age, and 3 for the old. The values were assumed as 0 for people without luggage and 1 for people with luggage. CH was divided into two categories, and the values were considered as 0 for not holding children and 1 for holding children. CC was divided into two categories, and the values were assumed as 0 for not carrying children and 1 for carrying children. Group size was divided into three categories, 0 for single, 1 for pair and 2 for more than three persons. All tests were performed at 95% confidence level. From Table 4.6, it can be said that a persons gender, age, group size and luggage factors have significant effect on pedestrian walking speed. From Table 4.6, F value is greater than the Table value (3.842), and P value is less than 0.05 for all factors. Pearson correlation coefficient value ranges between -1 and + 1. Where -1 shows total negative correlation, 0 is non linear correlation and +1 shows total positive correlation. Pearson correlation coefficients were found to be negative linear correlation for gender, age, and luggage. A nonlinear correlation was observed for CC, Group and CH with respect to speed. For density, there was a significant effect on speed at L-1 as the p value was found to be < 0.05. The gender of a person had significant effect on the speed of the crowd. The speed of a male was 1.23 times more compared to female pedestrian speed. It was observed that younger pedestrians had the fastest speed compared to others. A person without luggage was 1.2 times faster than a person with luggage.

Table 4.6 Statistical tests for crowd movement

Factor	L1				L2				Remarks
	ANOVA		Pearson Coefficient		ANOVA		Pearson Coefficient		
	F	P	Coefficient	P	F	P	Coefficient	P	
Gender	191.11	0.00	-0.52	0.00	42.62	0.00	-0.25	0.00	Significant
Age	53.96	0.00	-0.32	0.00	39.47	0.00	-0.15	0.00	Significant
Luggage	68.19	0.00	-0.33	0.00	58.14	0.00	-0.20	0.00	Significant
CC	2.75	0.09	-0.07	0.09	3.14	0.19	-0.06	0.08	Not significant
CH	0.90	0.34	0.04	0.34	0.87	0.25	0.03	0.25	Not significant
Group	1.09	0.31	-0.03	0.54	1.56	0.61	-0.02	0.47	Not significant
Density	16.04	0.00	-0.16	0.02	18.74	0.00	-0.17	0.01	Significant

4.3 Modelling

For developing the model, the data extracted from L1 was used.

4.3.1 Multiple Linear Regression Analysis

The general form of the linear regression model suggested is:

$$B = A_1X_1 + A_2X_2 + \ldots. + A_kX_K + \varepsilon \quad (4.1)$$

Where B = crowd speed, X1= gender, X2 = age, X3 = luggage, X_4 = Density, A = Parameter, ε = constant.

For the location under current study, a regression analysis is applied to the crowd movement at L1 as tabulated in Table 4.7. Negative values of β are obtained which will significantly decrease the speed with every increase of the following parameters i.e. children, female, persons with luggage, and density. Pedestrian gender has more effect on speed of the crowd compared to others because the coefficient of gender is more compared to other factors. The observed speed and estimated speed values using MLR are plotted in Figure 4.4.

The regression expression is obtained as follows:

$$\text{Speed} = 1.171 - 0.242 \times \text{gender} - 0.070 \times \text{age} - 0.179 \times \text{luggage} - 0.150 \times \text{Density} \quad (4.2)$$

Table 4.7 Regression analysis for the crowd speed

Model	β	Standard Error	Significance
Constant	1.171	0.015	0.000
Gender	-0.242	0.012	0.000
Age	-0.070	0.006	0.000
Luggage	-0.179	0.014	0.000
Density	-0.150	0.022	0.000

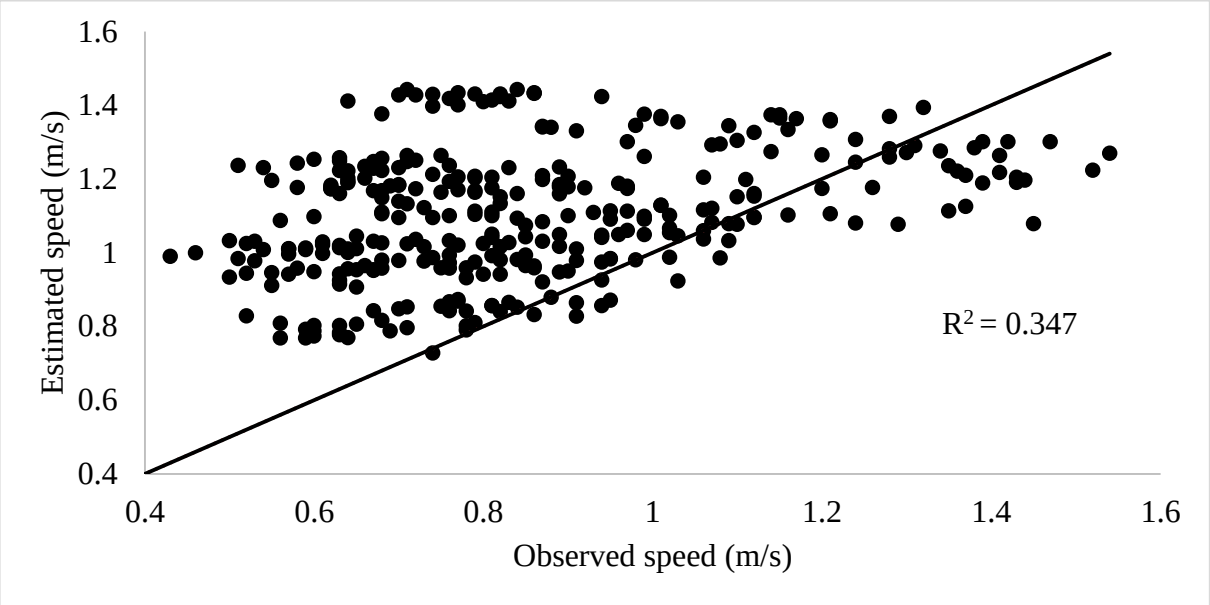

Figure 4.5 Comparison of speed between observed and MLR

From the Figure, it was observed that the predicted speed values were not close to the observed values. This is because speed and physical factors are not linearly correlated. The relationship between speed and physical factors may be non linear. To observe the non linearity, ANN model is developed.

4.3.2 ANN

In this study, ANN approach is adopted to develop a model using parameters affecting crowd speed. A neural network model consists of processing elements (neurons) and connections (links). The model based on neural network approach is efficient and practical as it facilitates its own implementation and learning based on real data. A network is referred to as a layered network where hidden units lie between input and output units. Architectural view of a typical neural network is shown in Figure 4.5. The input nodes provide information from the outside world to the network and are together referred to as the input layer. The input nodes do not perform any computation and they just pass the information to the hidden layers. The hidden

nodes as a group are called hidden layer and there is no direct connection with the outside world. Hidden nodes perform computations and transfer information from the input to output nodes. The output nodes are collectively referred to as the output layer. Output nodes are responsible for computations and transferring information from the network to the outside world. A two-layer feed forward network trained with Levenberg–Marquardt algorithm is used. Feed forward networks consist of a sequence of layers, and each following layer has a connection with the previous layer and the final layer produces the network's output.

For analysis of ANN models, 85 % of data were used for training and 15 % for validation. The sigmoid function was used for hidden neuron activation. Mainly, feed forward computation consists of simple run, product, and sigmoid evaluation. Levenberg–Marquardt back propagation (trainlm) algorithm was used as a network training function which is the fastest back propagation algorithm. Training may be defined as first stage of modeling in ANN. It can be classified in two groups as supervised and unsupervised. In supervised training, both the inputs and the outputs are provided. The network then processes the inputs and compares its resulting outputs against the desired outputs. Errors are then propagated back through the system, causing the system to adjust the weights which control the network. This process occurs over and over as the weights are continually tweaked. The other type of training is called unsupervised training. In unsupervised training, the network is provided with inputs but not desired outputs. The system itself must then decide what features it will use to group the input data. This is often referred to as self-organization or adaption. In the neural networks, one forward and one backward pass of all training samples is called epoch. Batch size is defined as the number of samples that are going to be propagated through the network. In this study, total samples were divided into 10 batches (batch size = 50). The number of iterations obtained to cover all the training samples is 10. The number of epochs obtained while training the data was 10. Network performance was measured according to the mean of squared error (MSE). In the network used, sigmoid transfer function was employed in the hidden layer and a linear transfer function in the output layer. Four ANN models were developed using NN tool in MATLAB. Performance of ANN models are given in Table 4.8. From Table 4.8, ANN 3 model gives better performance compared to other three ANN models in terms of R-value and MSE. Graphical representation of observed and ANN3 model crowd speed is shown in Figure 4.6. From Figure 4.6, it was observed that the predicted values were not close to the observed values.

Table 4.8 Performance of ANN models

Models	No of Neurons	R	MSE
ANN 1	5	0.8535	0.0206
ANN 2	10	0.8445	0.0198
ANN 3	15	0.8489	0.0183
ANN 4	20	0.8423	0.0194

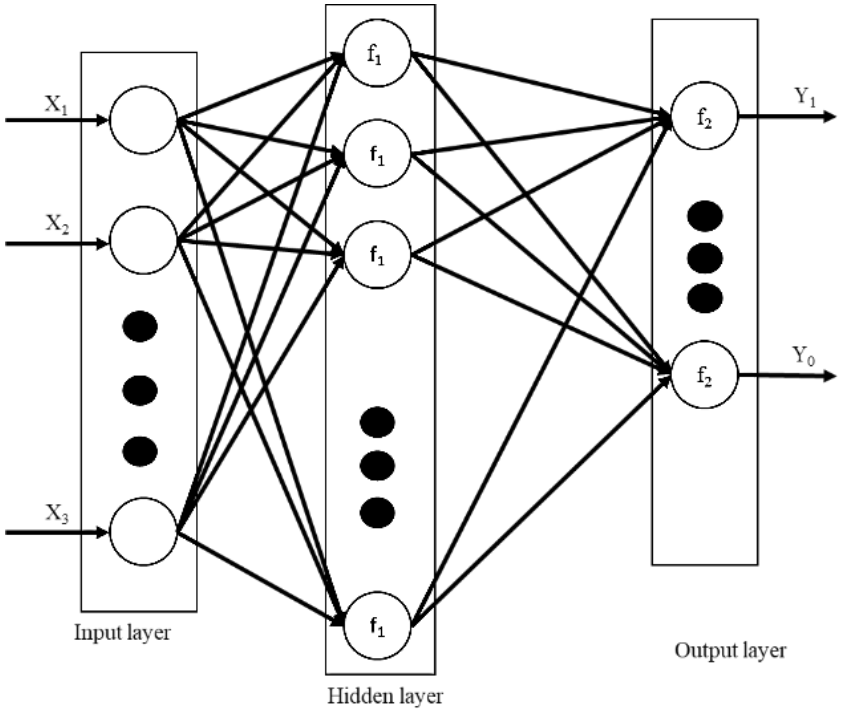

Figure 4.6 Architecture of Neural Network

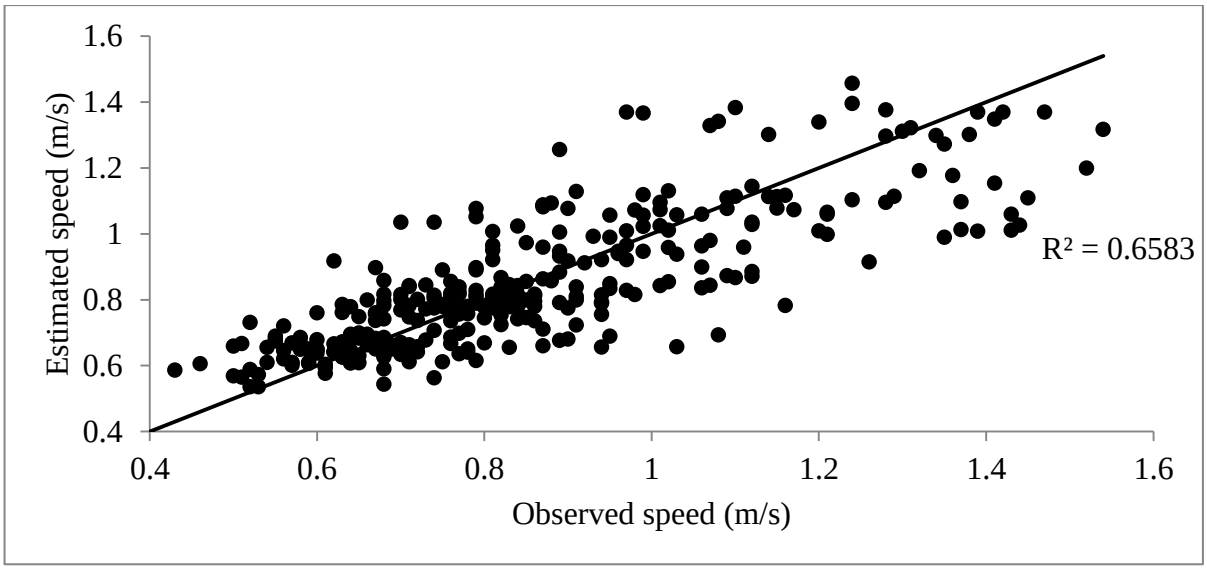

Figure 4.7 Comparison of observed and predicted (Estimated) speed

4.3.3 ANFIS

Jang (1992) developed an Adaptive Network-based Fuzzy Inference System (ANFIS) and used it in The Fuzzy Logic Toolbox of MATLAB software. Before constructing ANFIS model, select input and output variables and divide the data into training and checking data sets. Gender, age, density, and luggage variables are considered independent variables and speed is a dependent variable for this modelling. The data were divided randomly into a training data set (80%) and checking data set (20%). For building the ANFIS model, training dataset was assigned. The checking data set was used to avoid over fitting of the system to the training dataset.

ANFIS model construction involves two steps, fuzzification and training. The main aim of fuzzification is to establish an initial fuzzy inference system. ANFIS model structure is selected by determining the number, type, and shape of membership functions per input variable. The next step is training the parameters to minimize RMSE and adjusting the shape of the membership functions. ANFIS model is developed based on a hybrid algorithm. This algorithm consisted of back propagation for the parameters associated with the input membership functions and least squares estimation for the parameters associated with output membership functions.

ANFIS uses training and checking datasets simultaneously to avoid over fitting. Training of the ANFIS may be stopped by two measures. In the first measure, the learning process is stopped when the training data error remains within tolerance. In the second measure, the learning process stops when a maximum number of iterations (epochs) is achieved. In this study, ANFIS training is stopped if the error tolerance is near 0, or if the number of training iterations reaches 100, whichever comes first. The best ANFIS model is selected based on achieving a minimum RMSE for both training and checking data sets. The constructed fuzzy model with four inputs and 3 rules and one output is shown in Figure 4.7. The constructed ANFIS model is shown in Figure 4.8, and the 3 rules created were summarized in Table 4.9. Rules are created based on the results observed in Table 4.5. For example, the speed of younger males without luggage was found to be high of elderly female persons with luggage low and younger male persons with luggage medium. The model structure has a total of 12 nodes (3×4) for layer 1, three nodes for layer 2 and three nodes for layer 3, representing the following parameters of the linear function. Figure 4.9 shows the input membership functions of ANFIS model. The 3-D diagram of the training data is shown as target surface in Figure 4.10.

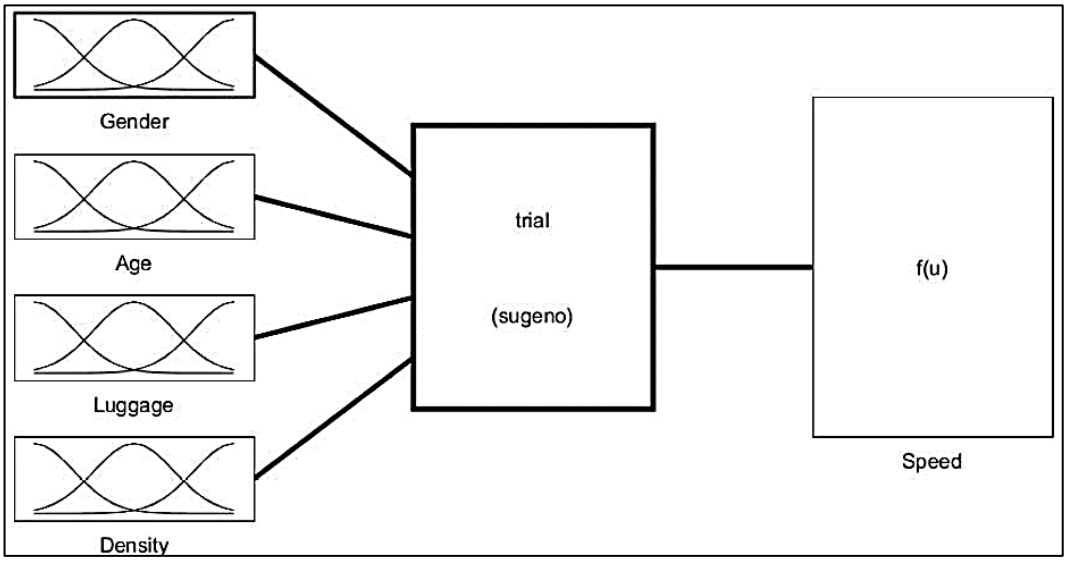

Figure 4.8 Fuzzy model construction

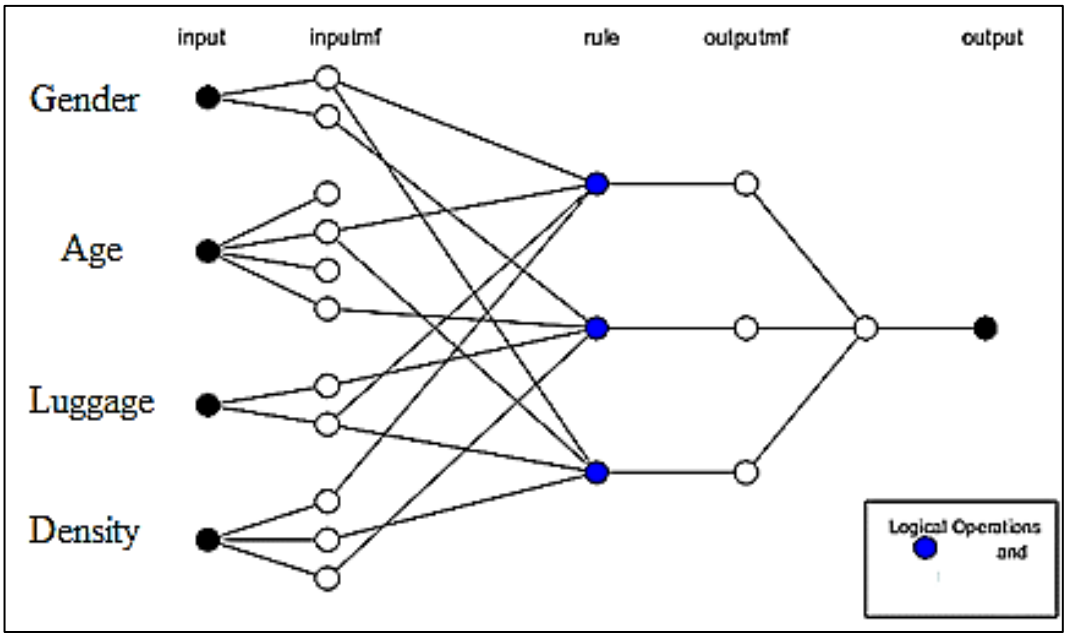

Figure 4.9 ANFIS model structure

Table 4.9 Constructed rules for ANFIS model

Rule No	Rules
1	If gender is male and age is young, and without luggage and density is low then speed is high
2	If gender is female and age is old, and with luggage, and density is high then speed is low
3	If gender is male and age is young, and with luggage, and density is medium then speed is medium

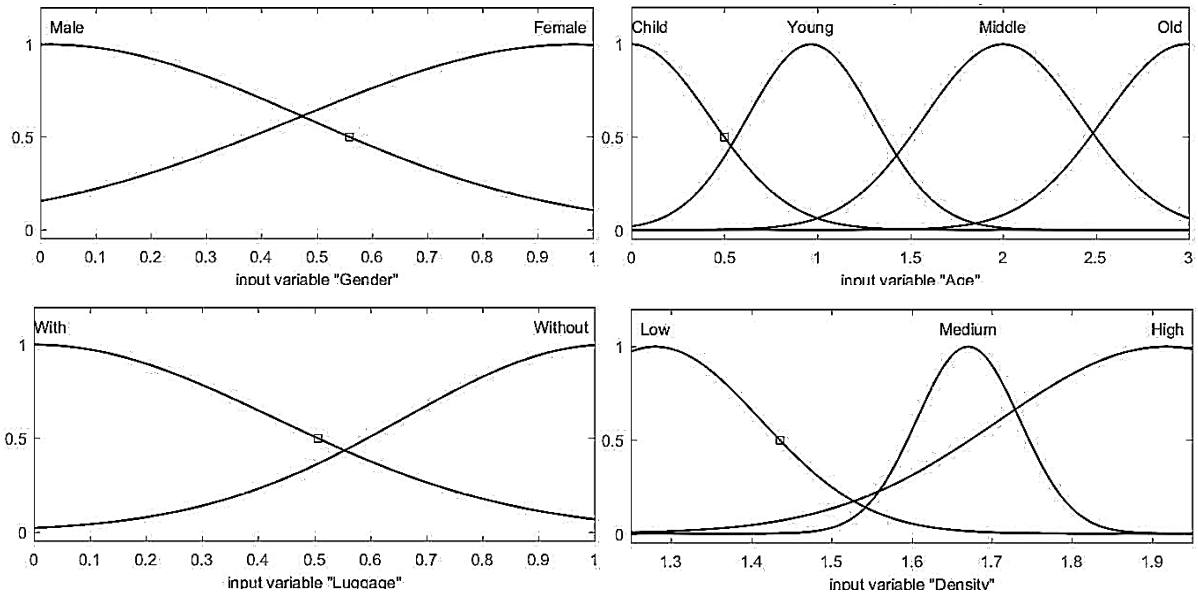

Figure 4.10 Input membership functions

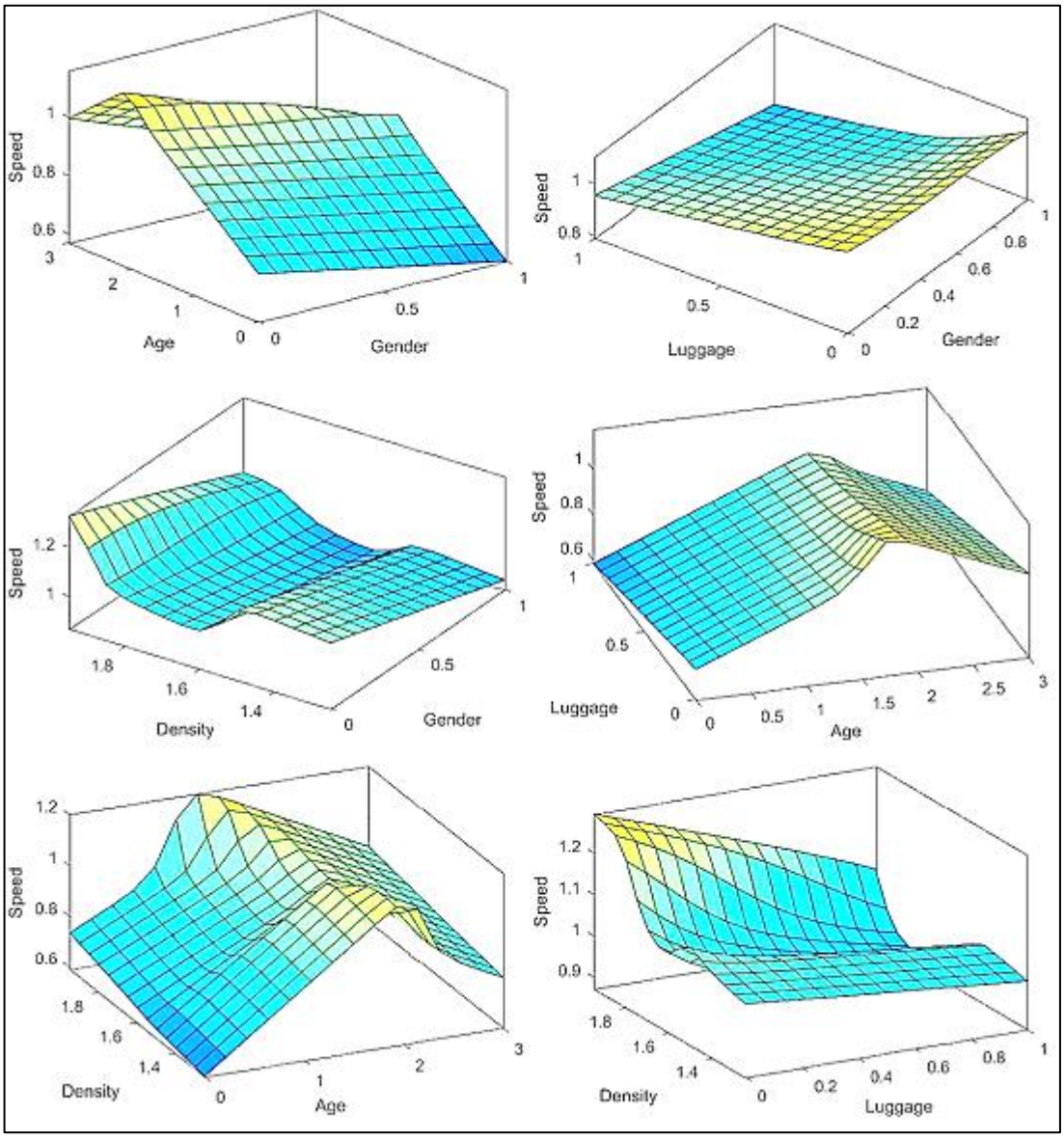

Figure 4.11 3D diagram of training data

The linguistic labels male and female are assigned for gender while child, young, middle age, and old are assigned for age. With and without labels are assigned for luggage and low, medium, and high labels assigned to Density. The estimated parameters of the output functions are demonstrated in Table 4.10. Figure 4.11 shows the observed, MLR, ANN, and ANFIS model speed data.

The estimated consequent parameters of Sugeno linear function are:

$$U_i = G \times p_i + A \times q_i + L \times r_i + K \times s_i + t_i \quad (4.3)$$

Table 4.10 Output parameter of Sugeno linear function

Membership	p_i	q_i	r_i	s_i	t_i
Low	0.264	-0.134	-0.241	-0.229	1.110
Medium	-0.193	0.270	0.550	0.129	0.620
High	-0.166	0.164	0.610	-1.753	2.724

Case -1 for low speed

$$U_i = 0.264\times G - 0.134\times A - 0.241\times L - 0.229\times K + 1.110 \quad (4.4)$$

Case -2 for medium speed

$$U_i = -0.193\times G + 0.270\times A + 0.550\times L + 0.129\times K + 0.620 \quad (4.5)$$

Case -3 for high speed

$$U_i = -0.166\times G + 0.164\times A + 0.610\times L - 1.753\times K + 2.724 \quad (4.6)$$

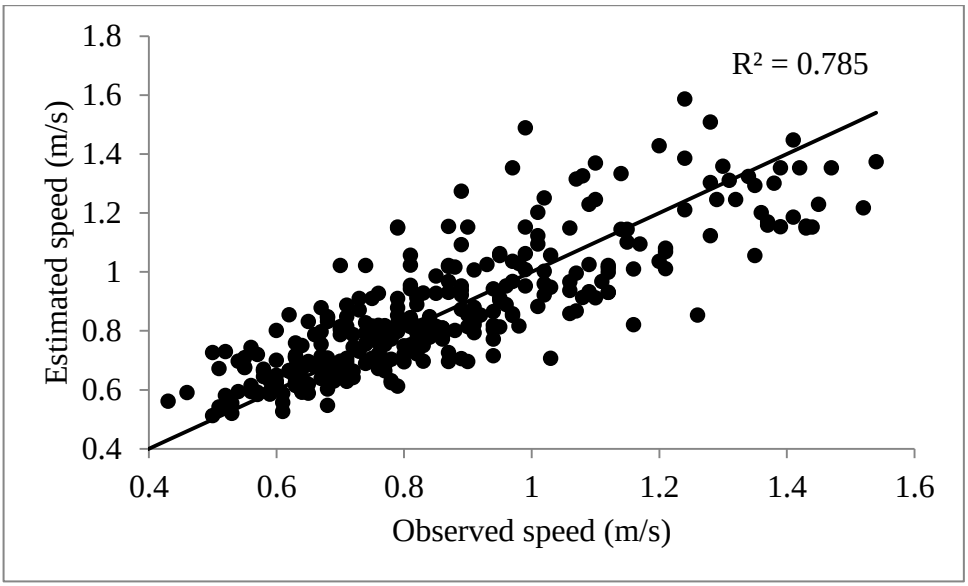

Figure 4.12 Comparison of observed speed with Estimated speed

4.4 Validation

Validation is an essential part of modelling which shows that the model is a realistic representation of the actual data. MAE (The Mean Absolute Error) and RMSE (Root Mean Square Error) are used to check the accuracy of model prediction. MAE states accuracy as an error whereas RMSE is used to measure the differences between the estimated value and the observed value. The model which has low MAE and RMSE value is considered to be the best prediction. MAE and RMSE values were calculated using equation (4.7) and (4.8).The RMSE and MAE values for the developed models are given in Table 4.11.

$$MAE = \frac{1}{n}\sum_{i=1}^{n}\left|\frac{O_i - E_i}{O_i}\right| \quad (4.7)$$

$$RMSE = \sqrt{\frac{\sum_{i=1}^{n}(E_i - O_i)^2}{N}} \quad (4.8)$$

Table 4.11 Accuracy measurements for models validation

Model	RMSE	MAE
MLR	0.343	0.391
ANN	0.137	0.101
ANFIS	0.130	0.098

It can be observed that, RMSE values are less than 0.5 and ANFIS model RMSE value is less compared to other models. Hence, it can be concluded that, ANFIS model is the best-fitted model for the data observed in the validation process.

4.5 Discussion

From Table 4.10, the variables such as gender, density, and luggage have a negative effect while age has a conflicting effect on the speed of the crowd. More details regarding the effect of each variable are explained in the following sections.

Gender:

Gender is found to decrease the speed of the crowd because of the number of women in the crowd leads to speed reduction. Generally, the speed of the female is lower compared to male, especially in religious gatherings because of the attire. The walking speed differences between men and women could be explained by the specific physical characteristics, which lead to larger step lengths and higher step frequencies for men (Buchmüller, Stefan; Weidmann, Ulrich, 2006). Generally at religious gatherings most of female devotees wear sarees, because

of this type of costume, the step length was less. Speed of female person was observed less compared to male persons because speed is directly proportional to step length (weidmann 1993).

Density:

Density is found to be an adverse effect on speed; at low crowd density, the speed of the crowd was high due to fewer interactions between persons and more space for overtaking. The speed was low at high crowd density because of more interactions between persons and low space for overtaking and because of the formation of dynamic lanes.

Luggage:

Luggage is also found have adverse effect on crowd speed. The speed of people with luggage is low compared to those without luggage. In religious gatherings, crowd density is high, and the number of people carrying luggage is more. The speed of a person is low when compared to a person with normal walking speed.

Age:

The relation between speed and age seems to be somewhat confusing. The results of the ANFIS model show that the effect of age on crowd speed varies. Children and old persons are negatively associated with crowd speed. As number of children and old people increases, the speed of the crowd decreases. On the other hand, younger and elder persons are positively associated with crowd speed. The speed of the crowd is high when the number of younger and elder persons are more.

4.6 Summary

The present study focuses on the individual behaviour of a person in a crowd. It was observed that the average crowd density was 1.73 p/m^2 and average speed of the crowd was 0.703 m/s respectively. From the statistical tests, it was concluded that, gender, age, density and luggage factors affect the pedestrian walking behaviour be significantly. MLR, ANN, ANFIS models were developed using the above mentioned factors. The developed model was validated using RMSE and MAE values. Based on R^2, RMSE and MAE values enabling ANFIS model was a better-fit model compared to other models. This study helps in proper dispersal of the crowd in a planned manner during crowd gathering events.

5. MACROSCOPIC MODELING

5.1 General

Crowd gatherings at religious occasions, fairs, and transport terminals and so on can create severe threats for the crowd due to high density of people in a certain space, with adverse outcomes such as stampedes. Analysis of stream flow parameters describes the relationships among the characteristics of crowd traffic streams. A regime model chosen based on crowd density has an impact on the predicted crowd characteristics at both the micro-level (individual behaviours in a crowd) and macro-level (overall crowd behaviour). Two-regime and three-regime models were used in this study to characterize crowd traffic in different regimes such as uncongested flow, transitional flow and congested flow. A model was developed based on the better fitness of predicted data to actually observed data.

5.2 Statistics of crowd characteristics

This section describes the characteristics of crowd (speed, density, and flow) at two locations (Location-1 is Krishna pushkaralu and Location-2 is Medaram). The statistical summary of the observed flow characteristics of a crowd at both locations is tabulated in Table 5.1.

Table 5.1 Descriptive statistics of flow characteristics of a crowd at both locations

Statistics of data	Speed (m/sec)		Density(P/m^2)		Flow (P/min/m)	
	Location-1	Location-2	Location-1	Location-2	Location-1	Location-2
Maximum	1.280	1.910	0.460	0.430	23.410	31.560
Minimum	0.280	0.340	0.140	0.100	3.530	5.380
Mean	0.757	1.104	0.303	0.262	13.525	17.017
Variance	0.046	0.089	0.004	0.004	15.877	31.440

It was observed that, the speed and flow of crowd was high at Location-2 (1.1 m/s & 17.0 p/min/m) as compared to that of Location-1 (0.75 m/s & 13.52 p/min/m). Density was low at Location-2 (0.26 p/m^2) as compared to that of Location-1(0.3 p/m^2).The standard deviation observed in the flow data is larger than that of speed and density data at both the locations. The standard deviations of all the crowd flow characteristics are greater at Location-2 than at Location-1.

5.3 Model development

For developing the model, the data extracted from Location-1 was used. Speed-density-flow relationships are known as traffic stream models. The relationship between crowd characteristics was developed using the field data. Flow parameters such as free flow speed (U_f), optimum speed (U_0), jam density (K_j), optimum density (K_0) and maximum capacity (Q_m) were estimated from the fundamental relationships. Free flow speed is defined as the speed at which density and flow are zero. Jam density occurs in no flow condition. Maximum capacity is defined as the maximum rate of flow or a maximum number of people to cross a point during a given time period. Density and speed at maximum capacity is defined as optimum density and optimum speed. Optimum speed and optimum density can be estimated from the macroscopic flow diagrams (MFD). In this study, a speed-density relationship is considered as a fundamental relationship because of simplicity of the model and better understanding. Flow-density and speed-flow are calibrated from a speed-density relationship. These relationships help in planning, design, and operations of facilities. These relationships/diagrams will be helpful in understanding the phases of transformation from uncongested to congested flow. The multi-regime (two and three regimes) nature of movement of people can be better understood by these relations and hence these are used in the analysis. In this section, crowd flow models are discussed for single-regime and multi-regime models.

MAPE (Mean Absolute Percentage Error) and RMSE (Root Mean Square Error) are used to check the accuracy of the model prediction. The model which is having less MAPE and RMSE values is considered to be the best prediction. MAPE and RMSE values were calculated using equations (5.1) and (5.2).

$$\text{MAPE (\%)} = \frac{1}{n}\sum_{i=1}^{n}\left|\frac{O_i - E_i}{O_i}\right| \times 100 \quad (5.1)$$

$$\text{RMSE} = \sqrt{\frac{\sum_{i=1}^{n}(E_i - O_i)^2}{n}} \quad (5.2)$$

5.3.1 Single regime models

To observe the characteristics of crowd, single-regime speed-density models were used as shown in equations (5.3) and (5.4). Using these mathematical crowd flow models, free flow speed (U_f), jam density (K_j), optimum speed (U_0), optimum density (K_0) and maximum capacity (Q_m) were determined.

Greenshields' Model (1935):

$$U = U_f - \left(\frac{U_f}{K_j}\right) k \quad (5.3)$$

Underwood Model (1961):

$$U = U_f e^{-\frac{k}{k_m}} \quad (5.4)$$

The flow parameters for the location estimated using speed-density relationships are listed in Table 5.2. MAPE and RMSE values of crowd characteristics were obtained from observed data and from speed-density, flow-density and speed-flow relationships were obtained as shown in Table 5.3. Figure 5.1 shows macroscopic flow diagrams of the crowd. For Model –I, minimum MAPE and RMSE values were found to be 2.981 and 0.028. It shows that Model-I will give the best fitness of prediction data for crowd movement. Under real conditions, it is not possible to model the entire traffic as a single-regime due to the existence of both uncongested and congested flow. Hence, a multi regime model concept is essential to represent different flow conditions.

Table 5.2 Single regime speed-density models

Model	**Model equation**	**R^2**	**Flow parameters**				
			U_f	**U_0**	**K_j**	**K_0**	**Q_m**
Model I (G)	U = 1.084-1.0637k	0.927	1.084	0.542	1.020	0.510	16.560
Model II (Un)	$U = 1.136*e^{-1.346k}$	0.928	1.136	0.418	∞	0.743	18.630

(G = Greenshields, Un = Underwood)

Table 5.3 Model equations for flow parameters and accuracy measurements

Model	**Model equation**	**MAPE**	**RMSE**
Model I	U=1.084-1.0637k	2.981	0.028
	$Q=1.084k-1.0637k^2$	2.981	0.402
	Q=(1.084-u)u/1.0637	9.755	1.255
Model II	$U= 1.136*e^{-1.346k}$	2.983	0.028
	$Q=1.136k*e^{-1.346k}$	2.983	0.439
	Q=(u/1.346)(ln(1.136/u)	9.763	1.267

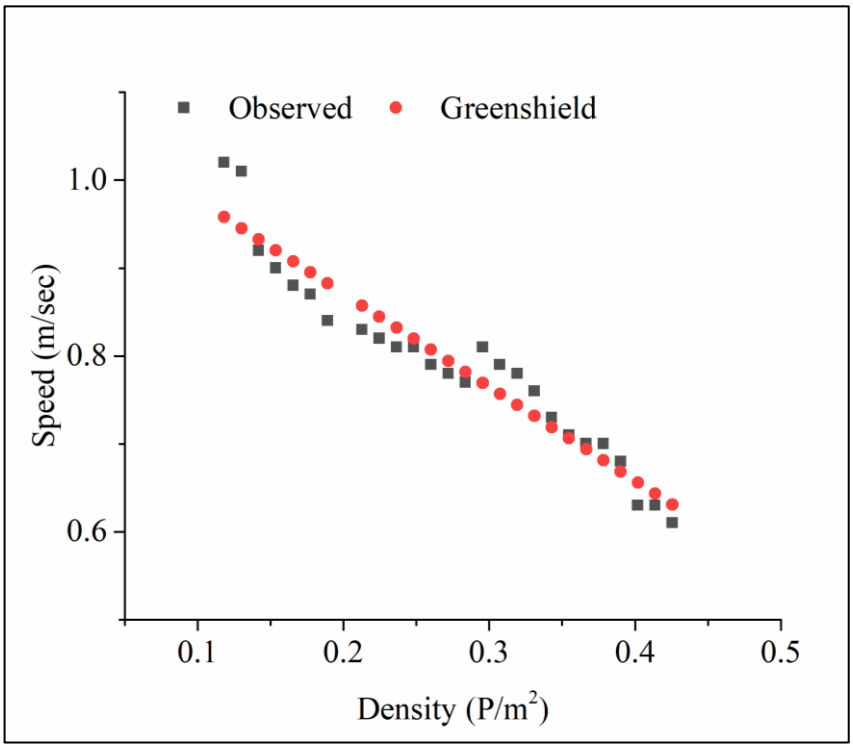

Figure 5.1 Best fitting single-regime model

5.3.2 Two regime models

In multi-regime models, a two-regime model was first attempted by Edie (Edie, 1961) which includes uncongested flow regime and congested flow regime. In two-regime model, speed-density relationship is developed for two regimes by introducing a break-point to distinguish the two different regimes. This break-point is identified by K-mean clustering analysis using SPSS software. The final selections of breakpoints were determined using a visual approach. The flow parameters for the location estimated using speed-density relationships are listed in Table 5.4. MAPE and RMSE values of crowd characteristics were obtained from observed data and that from speed-density, flow-density and speed-flow relationships were derived as shown in Table 5.5. Figure 5.2 shows the best fitted speed-density models in two regime modeling. The minimum MAPE and RMSE values for crowd characteristics (speed, density, and flow) estimated using Model –III are 1.678 and 0.0193 respectively which gives the best fitness of the predicted data.

Table 5.4 Speed-density models for two regime model

A	Model Name	Model equation	Critical values					R^2
			U_f	U_0	K_j	K_0	Q_m	
L L	Model I	U = 1.1315-1.3473K (K<=0.28) U = 1.2643-1.5349K (K>0.28)	1.132	0.632	0.824	0.411	15.620	0.876 0.979
L E	Model II	U = 1.1315-1.3473K (K<=0.28) $U = 1.5499*e^{-2.173K}$(K>0.28)	1.132	0.570	∞	0.460	15.740	0.876 0.974
E L	Model III	$U = 1.1674*e^{-1.535K}$(K<=0.28) U = 1.2643-1.5349K (K>0.28)	1.167	0.632	0.824	0.411	15.620	0.900 0.979
E E	Model IV	$U = 1.1674*e^{-1.535K}$(K<=0.28) $U = 1.5499*e^{-2.173K}$(K>0.28)	1.132	0.570	∞	0.460	15.740	0.900 0.974

(A = Relationship, L = Linear, E = Exponential)

Table 5.5 Accuracy measurements for model performance and evaluation

Model	Relation	MAPE	RMSE
Model I	Speed – Density	1.829	0.020
	Flow – Density	1.829	0.239
	Speed - Flow	6.123	0.839
Model II	Speed – Density	1.880	0.020
	Flow – Density	1.880	0.244
	Speed - Flow	6.199	0.842
Model III	Speed – Density	1.678	0.019
	Flow – Density	1.678	0.223
	Speed - Flow	5.445	0.743
Model IV	Speed – Density	1.728	0.019
	Flow – Density	1.728	0.228
	Speed - Flow	5.5209	0.747

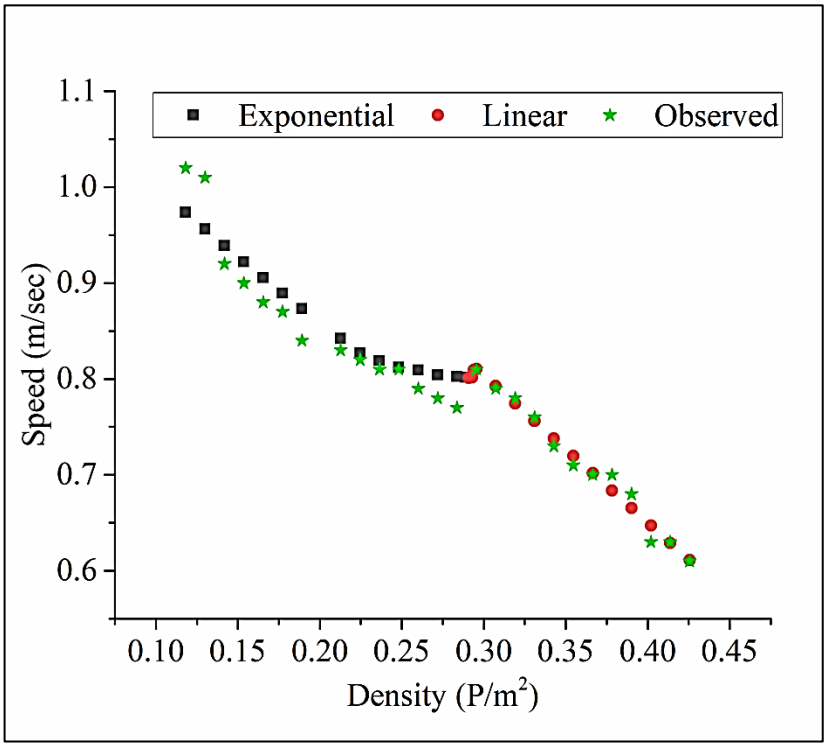

Figure 5.2 Best fitting two-regime model

5.3.3 Three regime models

Three-regime models were introduced by Drake and May (Drake and May 1967; May 1990) considering uncongested flow, transitional flow, and congested flow regimes. In three-regime model, speed-density relationship is developed for three regimes by introducing a break-point to distinguish three different regimes. This break-point is identified by K-mean clustering analysis using SPSS software. The final selections of breakpoints were determined using a visual approach. The flow parameters for the location were estimated using speed-density relationships and are listed in Table 5.6. MAPE and RMSE values of crowd characteristics were obtained from observed data and from speed-density, flow-density and speed-flow relationships as shown in Table 5.7. It was observed that, Model II provides a better prediction because of lower MAPE and RMSE values among all the four models. RMSE and MAPE values less means field and and predicted data were very close. It means that, Underwood model (exponential) is fit to filed data in three regime model. Figure 5.3 shows the best-fitted model in three-regimes.

Table 5.6 Speed-density model for three regime model

A	Model Name	Model equation	Critical values					R^2
			U_f	U_0	K_j	K_0	Q_m	
L L L	Model I	U = 1.3193-2.5979K (K<=0.20) U = 0.9507-0.5921K (0.20<K<0.31) U = 1.2715-1.5532K (K>=0.31)	1.320	0.640	0.820	0.410	15.610	0.910 0.773 0.955
E E E	Model II	$U = 1.4104*e^{-2.795K}$ (K<=0.20) $U = 0.9656*e^{0.741K}$ (0.20<K<0.31) $U = 1.5979*e^{-2.251K}$ (K>=0.31)	1.410	0.590	∞	0.440	15.670	0.921 0.785 0.968
E E L	Model III	$U = 1.4104*e^{-2.795K}$ (K<=0.20) $U = 0.9656*e^{-0.741K}$ (0.20<K<0.31) U = 1.2715-1.5532K (K>=0.31)	1.410	0.640	0.820	0.410	15.610	0.921 0.785 0.955
E L E	Model IV	$U = 1.4104*e^{-2.795K}$ (K<=0.20) U = 0.9507-0.5921K (0.20<K<0.31) $U = 1.5979*e^{-2.251K}$ (K>=0.31)	1.410	0.590	∞	0.440	15.670	0.921 0.773 0.968

Table 5.7 Accuracy measurements for model performance and evaluation

Model	Relation	MAPE	RMSE
Model I	Speed – Density	1.280	0.013
	Flow – Density	1.280	0.193
	Speed - Flow	3.407	0.532
Model II	Speed – Density	1.218	0.012
	Flow – Density	1.218	0.193
	Speed - Flow	3.281	0.532
Model III	Speed – Density	1.233	0.012
	Flow – Density	1.233	0.190
	Speed - Flow	3.306	0.530
Model IV	Speed – Density	1.222	0.012
	Flow – Density	1.222	0.193
	Speed - Flow	3.282	0.528

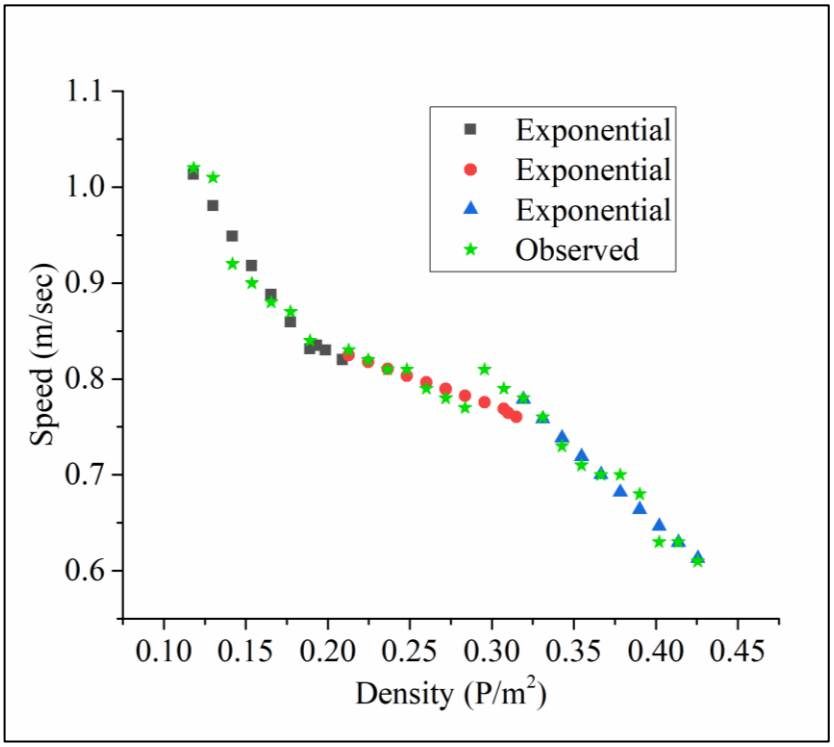

Figure 5.3 Best fitting three-regime model

5.3.4 Comparison between single regime and multi regime models

Firstly, comparing the characteristics obtained from two single-regime models, free flow speed varies from 1.084 m/sec to 1.136 m/sec and optimum speed varies from 0.418 m/sec to 0.542 m/sec. Using R^2, MAPE, and RMSE values Underwood model was found to be the best fit. Secondly, for two-regime models, the estimated free flow speed varies from 1.132 m/sec to 1.167 m/sec, optimum speed varies from 0.57 m/sec to 0.632 m/sec. It was observed that, Model-III was the best fit from R^2, MAPE, and RMSE values. Thirdly, for three-regime models free flow speed varies from 1.320 to 1.410 m/sec, optimum speed varies from 0.59 m/sec to 0.64 m/sec. Using R^2, MAPE, and RMSE values, Model-II was found to be the best fit. It can be observed that MAPE and RMSE values of multi-regime models ((1.678, 0.019), (1.218, 0.012)) are lower than that of single-regime model (2.981, 0.028). Therefore multi-regime model can predict better than single-regime model. In multi-regime models, MAPE and RMSE values of three-regime model (1.218, 0.012) are lower than that of two-regime model (1.678, 0.019). Therefore three-regime model can predict better than two-regime model.

5.4 Validation

Validation is an important part of modelling which shows that the predicted model is a realistic representation of the actual system. Coefficient of determination, Coefficient of correlation, RMSE and MAPE are used for validating the predicted model. The field values

from Location-2 were applied for the best fit three-regime model (Model -II) to validate the performance of the model. Figure 5.4 and 5.5 represent the scattered plots of expected and observed speed and flow values for Location-2. MAPE, RMSE, and R^2 values of speed and flow are tabulated and presented in Table 5.8. It can be observed that MAPE values are lower than 5% and RMSE values are less than 0.5. Hence, it can be concluded that three regime model (model II as per Table 5) is best fitted model for the observed data. Hence, the predicted model is validated.

Table 5.8 Accuracy measurements for model validation

Parameters	MAPE	RMSE	R^2 value
Speed	2.766	0.315	0.644
Flow	2.766	0.284	0.929

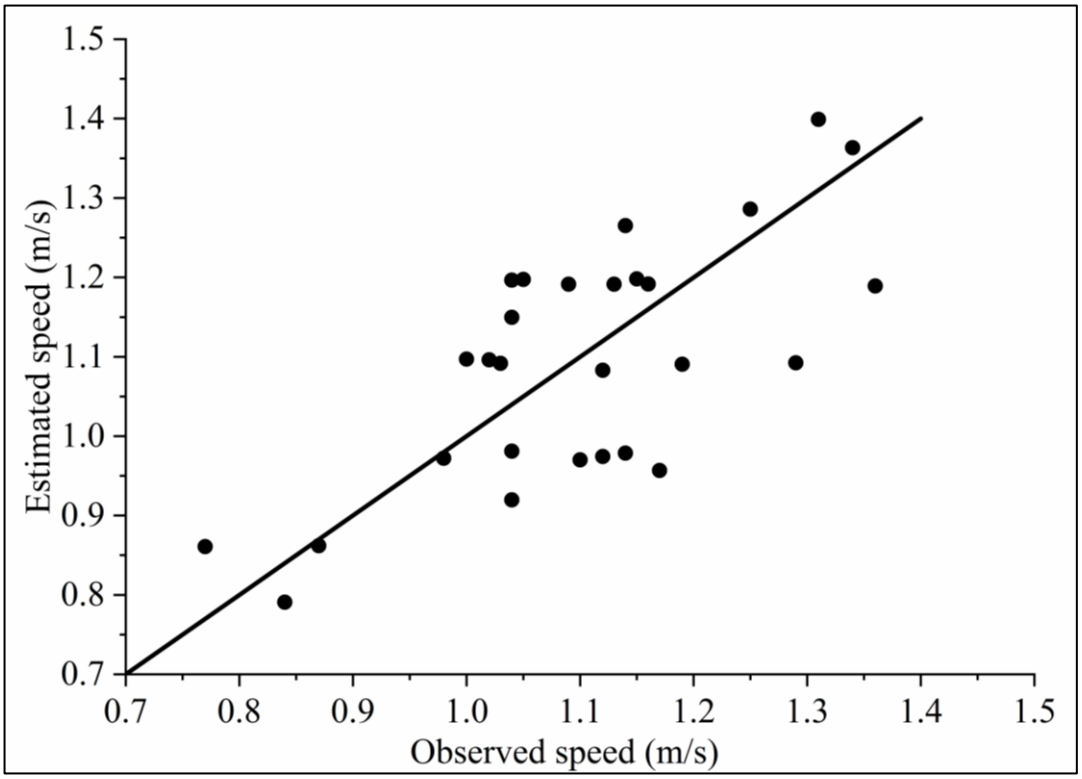

Figure 5.4 Comparision of observed and estimated speeds

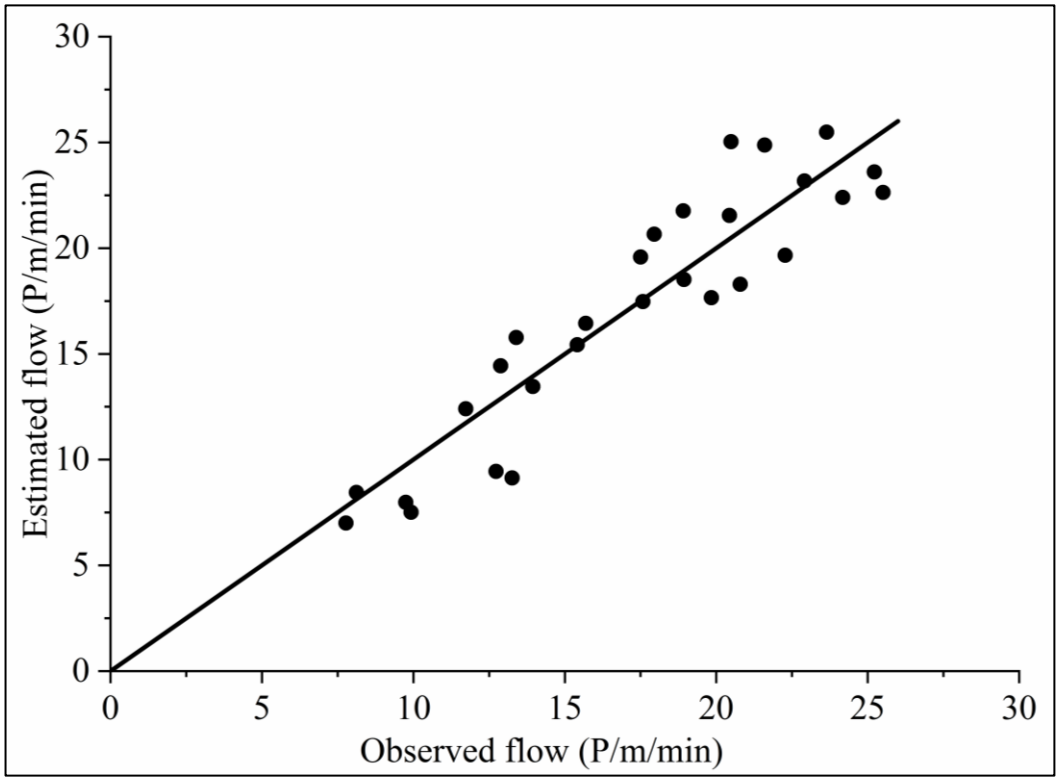

Figure 5.5 Comparision of observed and estimated flows

5.5 Summary

This chapter focused on the estimation of crowd characteristics (speed, density and flow) and the relationships among stream flow parameters. In the single-regime concept, the Greenshields model (linear) and Underwood model (exponential) were tested for their fits with observed data. Other stream flow models were developed using the classic equation (Equation Q = K×U). In the case of the single-regime models, critical points of free flow speed and capacity in the actual field scenario were not represented effectively and thus estimations for uncongested flow, transitional flow and congested flow regimes were modeled separately. Multi-regime models estimate flow parameters more precisely and realistically. This study evaluated four different models for multi-regime modelling. K-means clustering was used to calculate the breakpoints for multi-regime modelling. In the multi-regime models, the speed–density relation was modelled using four categories of models and flow–density and speed–flow relations were then established. Of the two-regime models considered, the exponential–linear model III was found to give the best fit. Of the three-regime models, model II was found to be the best fit. Statistical analysis revealed that the MAPE value varied from 2·981 to 2·983 for the single-regime speed–density model. For two-regime and three-regime models, MAPE values were in the range 1·678–1·880 and 1·218–1·280, respectively. It was thus concluded that, three-regime models give better predictions than single-regime and two-regime models.

This study showed that the multi-regime stream flow modeling concept can be applied to crowd modelling and represent real-life scenarios. Multi-regime models comprising the transition between various flow conditions are thus useful for crowd density estimations of future scenarios, which will be helpful in crowd management and facility planning for the smooth flow of large congregations.

6. CAPACITY OF BOTTLENECKS

6.1 General

The present chapter focuses on analysing the effect of composition and bottleneck width on crowd behaviour. The inclusion of buffer space on the crowd dispersion is analysed. The relationship between total times versus bottleneck width, flow versus bottleneck width and specific flow versus bottleneck width was established.

6.2 Capacity of corridors

From the experimental study conducted at NIT Warangal, total time, time gaps, flows, specific flows and densities were parameters extracted from data. Various relations such as time gap versus bottleneck width, total time versus bottleneck width, flow versus bottleneck width and specific flow versus bottleneck width, density plots and dynamic layer formations were studied.

6.2.1 Time gaps

Time gap is defined as the time distances between successive persons. The following tables 6.1 to 6.4 show the descriptive statistics of time gaps for various widths.

Table 6.1 Descriptive statistics of time gaps for N = 30 (with buffer space)

Width(cm)	Mean	Standard Deviation	Minimum	Median	Maximum
80	0.69445	0.20923	0.456	0.671	1.372
100	0.59641	0.2219	0.245	0.58	1.045
120	0.56393	0.19581	0.255	0.497	0.899
140	0.52097	0.24771	0.245	0.432	1.412
160	0.5147	0.20526	0.239	0.383	1.28

Table 6.2 Descriptive statistics of time gaps for N = 30 (without buffer space)

Width(cm)	Mean	Standard Deviation	Minimum	Median	Maximum
80	0.79352	0.3468	0.226	0.713	1.448
100	0.7739	0.31995	0.306	0.621	1.515
120	0.6958	0.21443	0.333	0.588	1.092
140	0.66734	0.32135	0.307	0.561	1.405
160	0.61224	0.30603	0.22	0.508	1.463

Table 6.3 Descriptive statistics of time gaps for N = 50 (with buffer space)

Width(cm)	Mean	Standard Deviation	Minimum	Median	Maximum
80	0.67186	0.1862	0.361	0.653	1.02
100	0.65304	0.21186	0.311	0.64	1.106
120	0.64339	0.23059	0.101	0.588	1.031
140	0.62443	0.23437	0.271	0.58	1.177
160	0.60713	0.19479	0.256	0.55	1.0183

Table 6.4 Descriptive statistics of time gaps for N = 50 (without buffer space)

Width(cm)	Mean	Standard Deviation	Minimum	Median	Maximum
80	0.59449	0.18827	0.3	0.588	0.999
100	0.57708	0.19758	0.209	0.574	1.022
120	0.57033	0.22043	0.253	0.562	1.069
140	0.56803	0.25041	0.023	0.561	1.0401
160	0.56056	0.22098	0.253	0.56	1.0273

The variation of time gaps for different bottleneck widths are shown in Figures 6.1 to 6.4. From the figures, it was observed that the average time gap is decreasing as the width of exit is increasing for both cases with and without buffer space. It means that speeds and flows are increasing as the width increases.

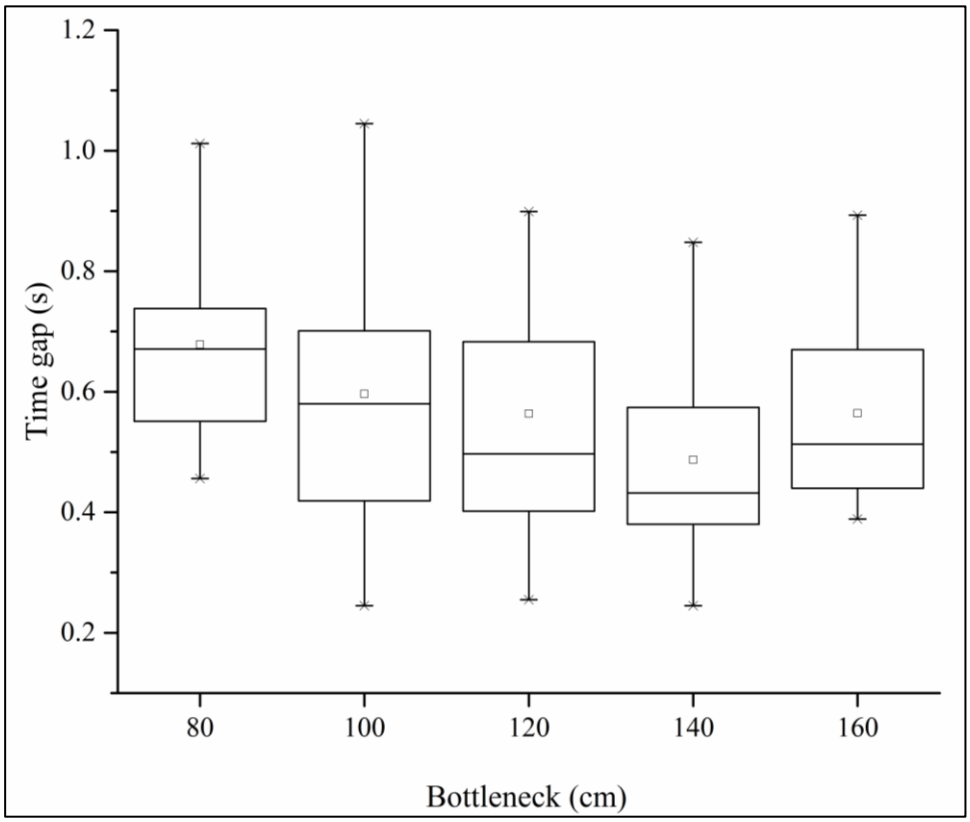

Figure 6.1 Time gap versus bottleneck width for with buffer case (N = 30)

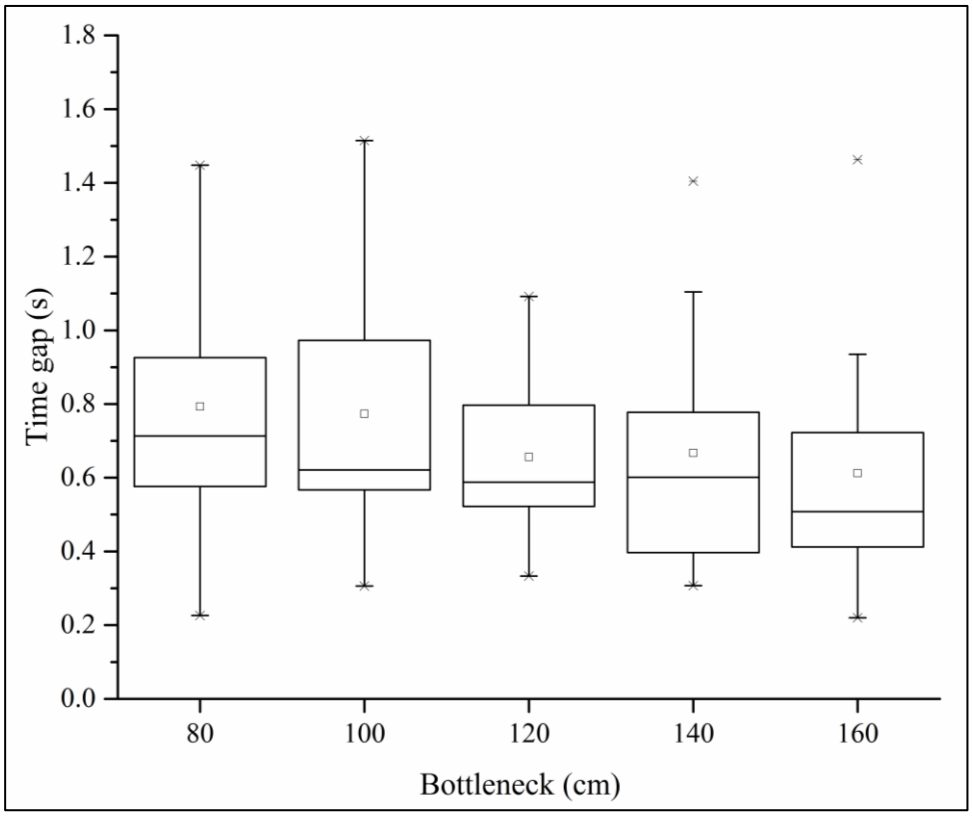

Figure 6.2 Time gap versus bottleneck width for without buffer case (N = 30)

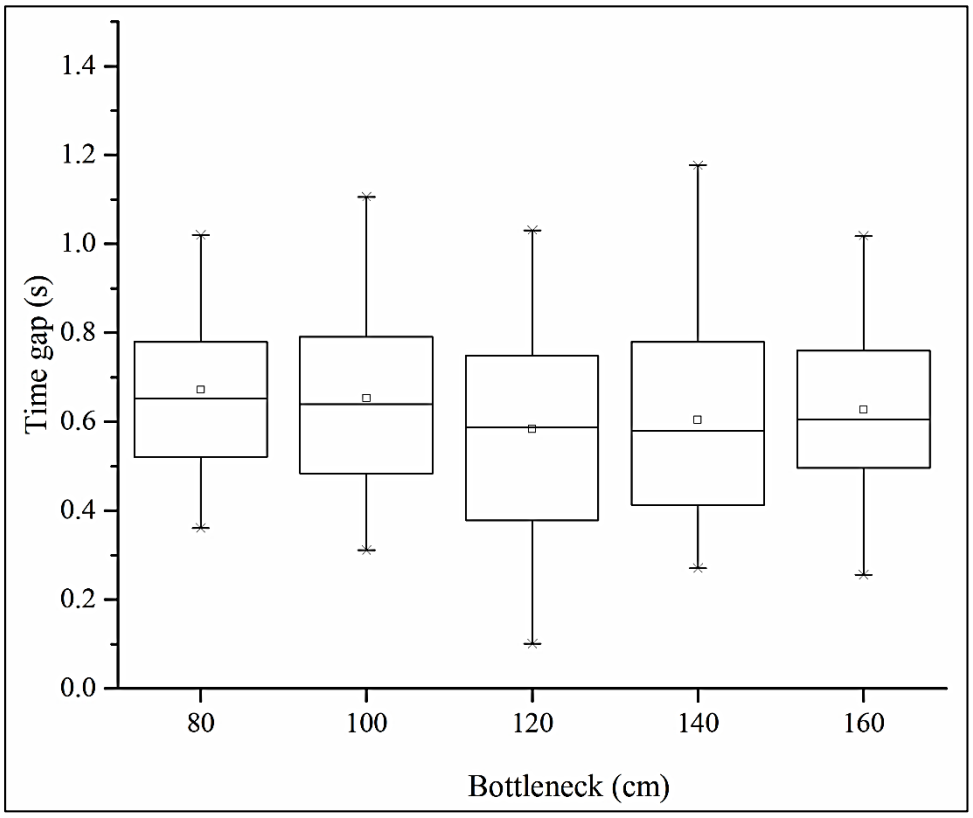

Figure 6.3 Time gap versus bottleneck width for with buffer case (N = 50)

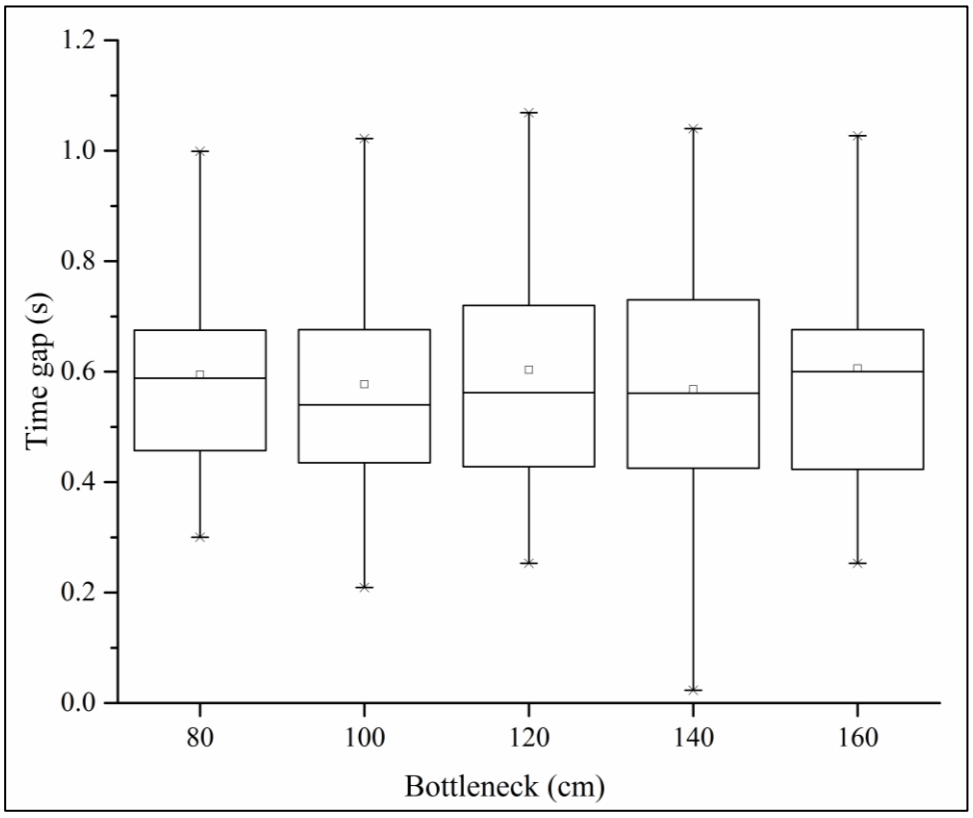

Figure 6.4 Time gap versus bottleneck width for without buffer case (N = 50)

The variation of time gaps with time is shown in Figures 6.5 to Figure 6.14. From these figures, it can be noticed that as the width of bottleneck increases the total time to cross the

exit is decreasing. It can also be observed that the time gap variations are independent of buffer space availability.

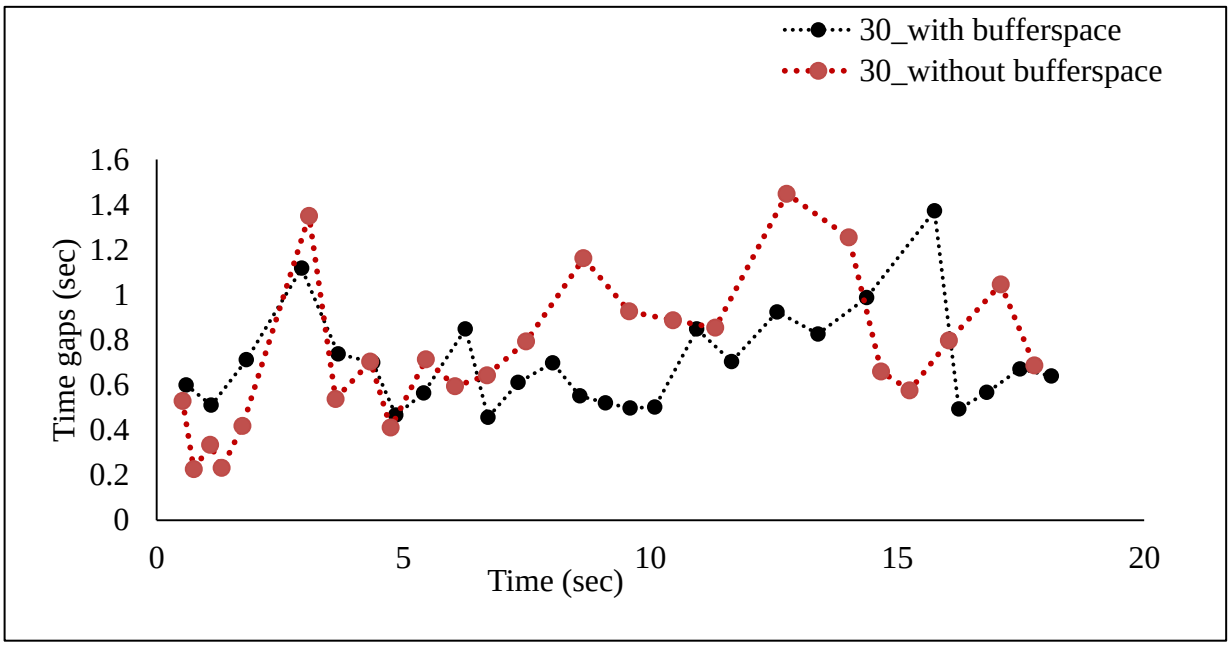

Figure 6.5 Time gap versus time for N= 30 and B = 80 cm

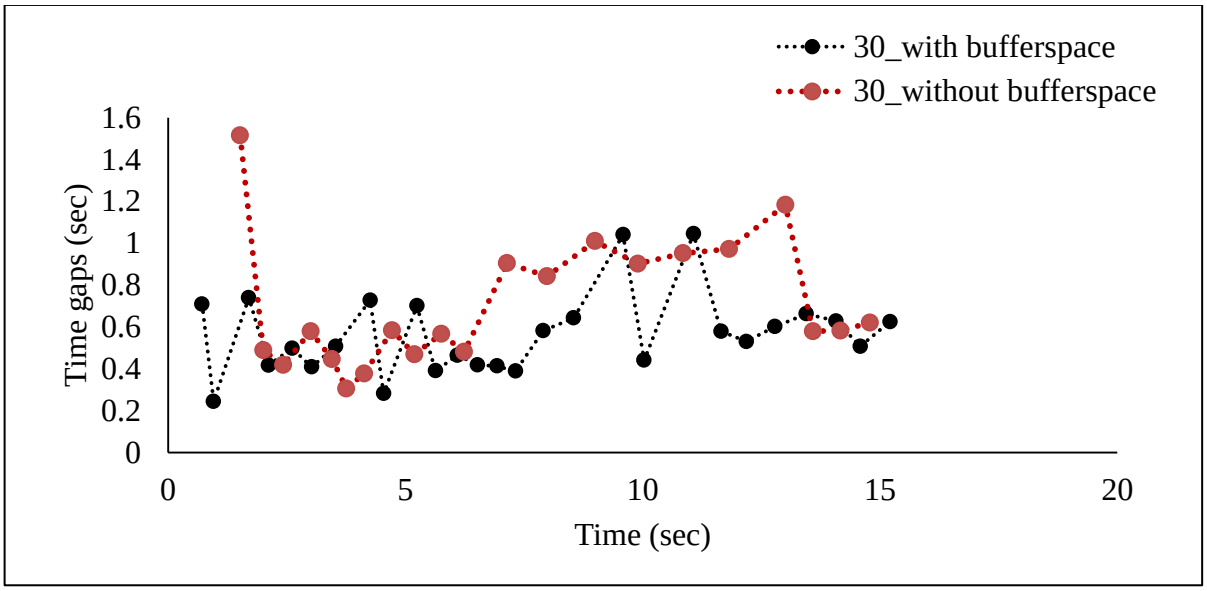

Figure 6.6 Time gap versus time for N = 30 and B = 100 cm

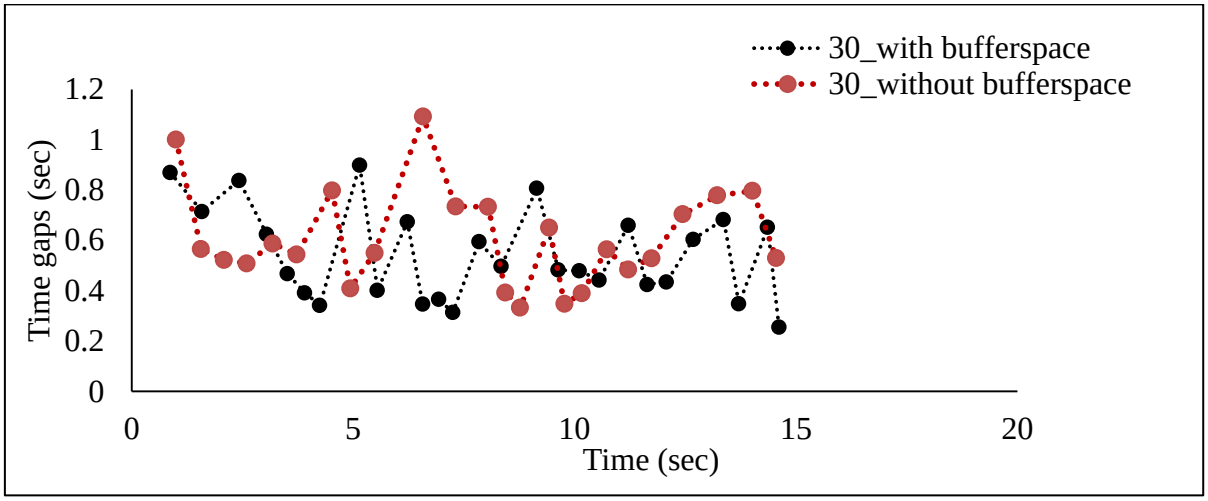

Figure 6.7 Time gap versus time for N = 30 and B = 120 cm

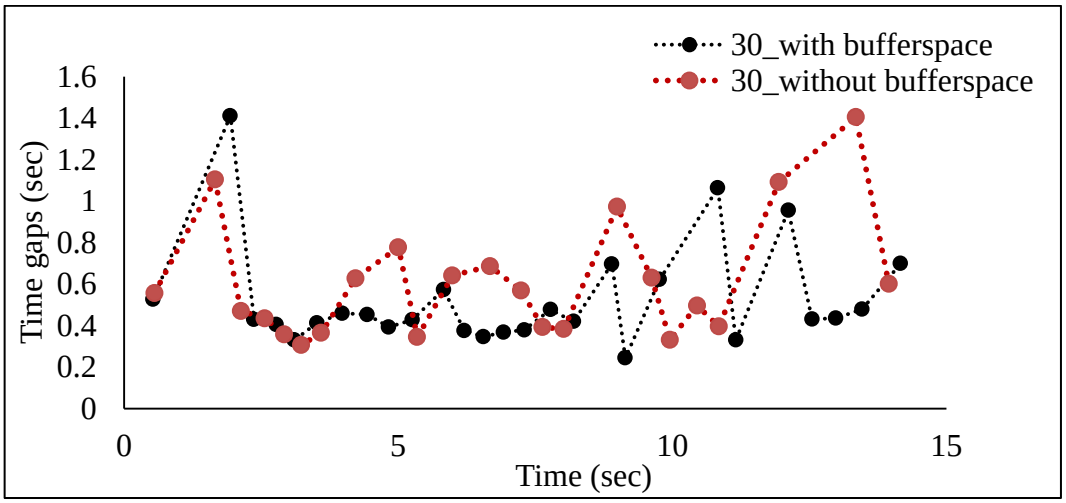

Figure 6.8 Time gap versus time for N = 30 and B = 140 cm

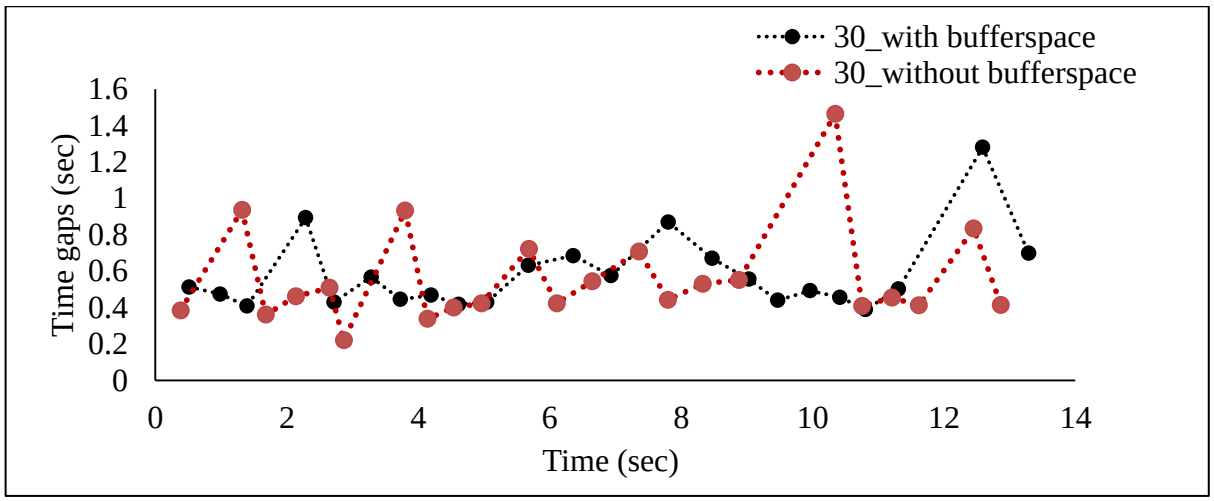

Figure 6.9 Time gap versus time for N = 30 and B = 160 cm

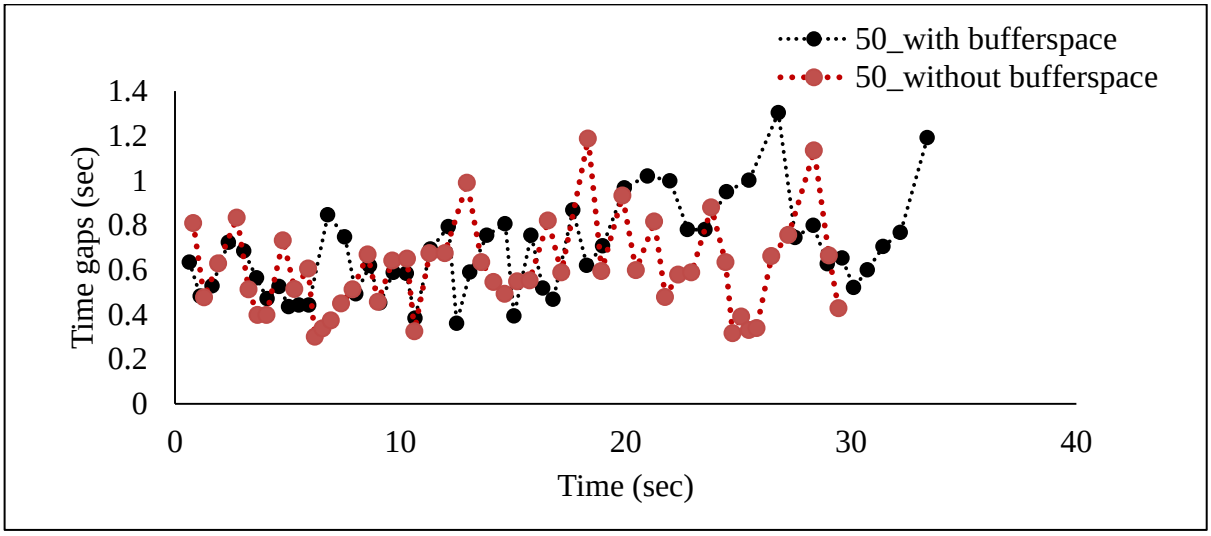

Figure 6.10 Time gap versus time for N = 50 and B = 80 cm

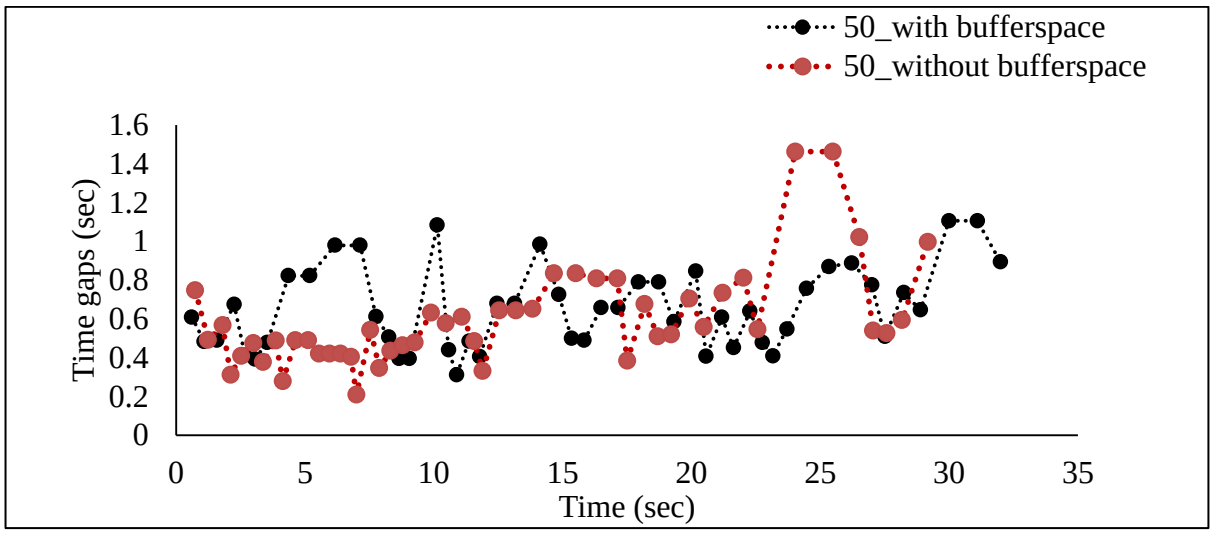

Figure 6.11 Time gap versus time for N = 50 and B = 100 cm

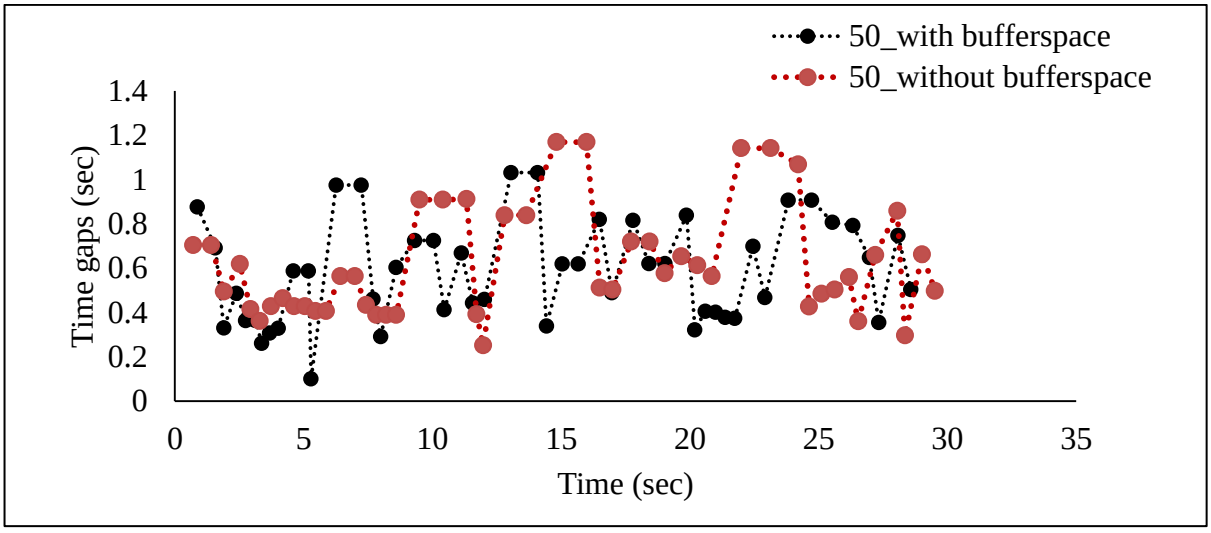

Figure 6.12 Time gap versus time for N = 50 and B = 120 cm

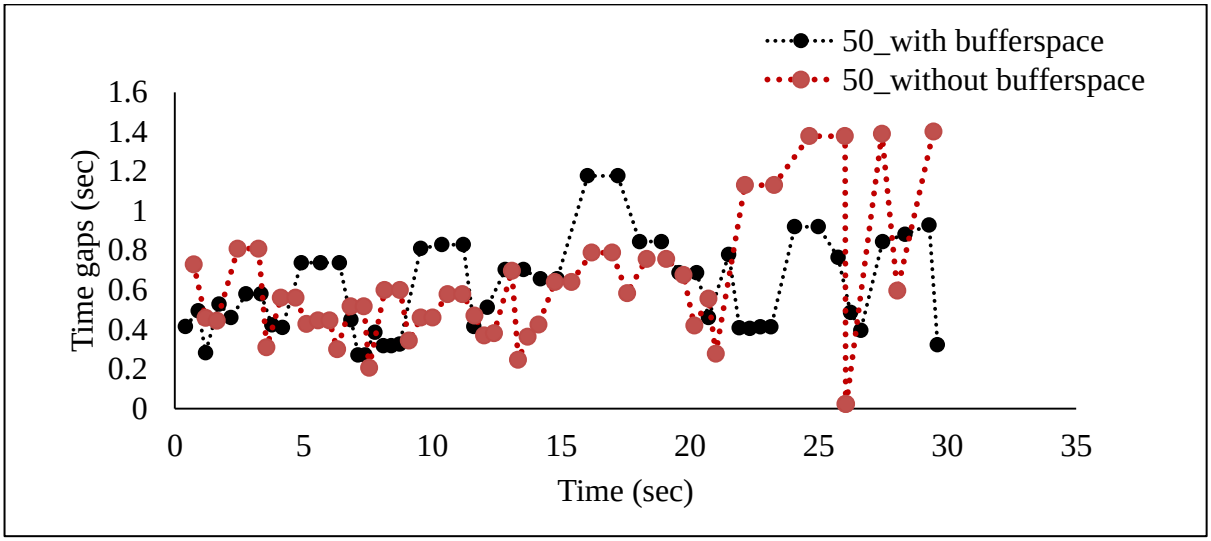

Figure 6.13 Time gap versus time for N=50 and B=140 cm

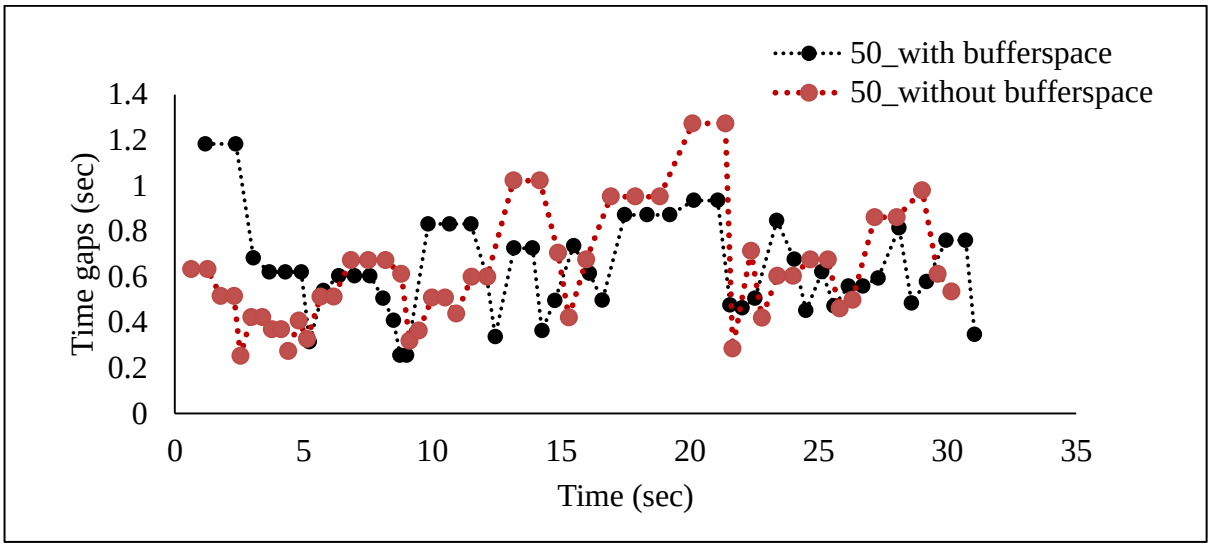

Figure 6.14 Time gap versus time for N = 50 and B = 160 cm

6.2.2 Total time

The time duration from the first person crossing the reference line to the last person crossing the reference line is called total time. If there are ‘n' persons, the total time is the sum of ‘n-1’ time gaps. Figures 6.15 and 6.16 show the variation of total time with respect to bottleneck width. It was observed that the total time decreased as the bottleneck width increases for both the compositions involving both cases with and without buffer space. The buffer space effect in the reduction of total time is more in case of 50 persons than in case of 30 persons.

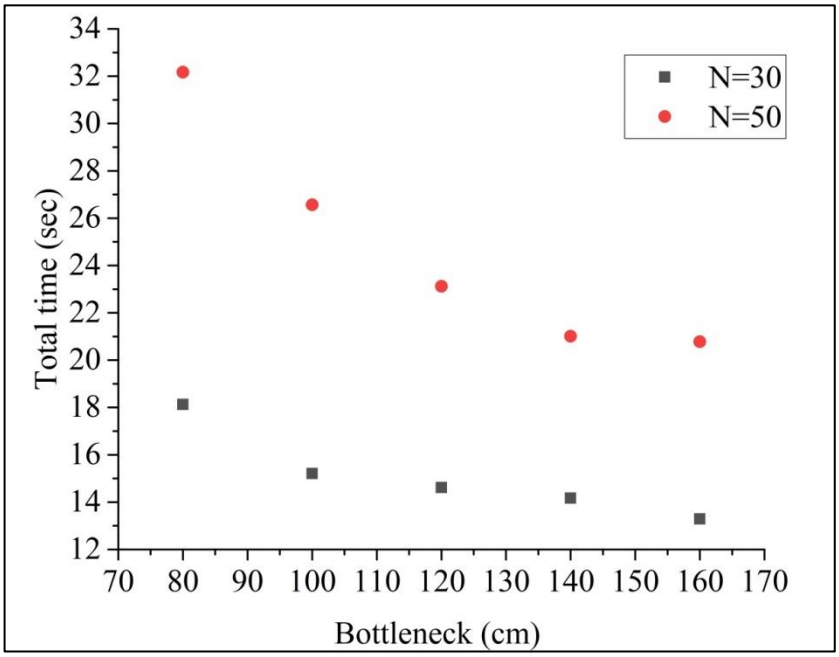

Figure 6.15 Total time versus bottleneck width for with buffer case

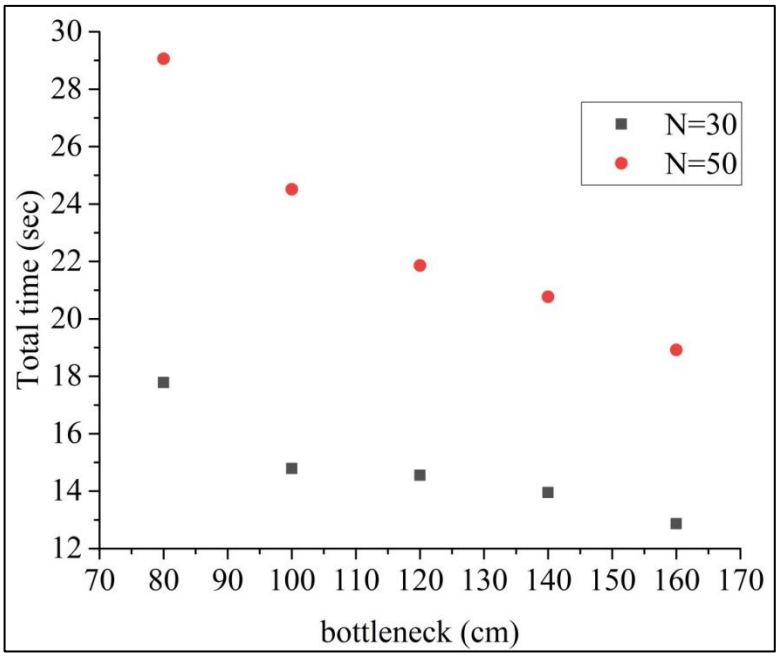

Figure 6.16 Total time versus bottleneck width for without buffer case

6.2.3 Flow

Flow is the ratio of the total number of persons walking through a bottleneck to the total time required to cross exit line. Figures 6.17 and 6.18 show the variation of the flow versus bottleneck widths. From these figures, it was observed that, flow increased as the width of the bottleneck increases and this increase in flow is due to the formation of the dynamic layer, as some of the researchers recorded in their studies. When the crowd entered the bottleneck, formation of layers occurs inside the bottleneck as width increases due to zipper effect. The

zipper effect is a self-organization phenomenon leading to an optimization of the available space and velocity inside the bottleneck.

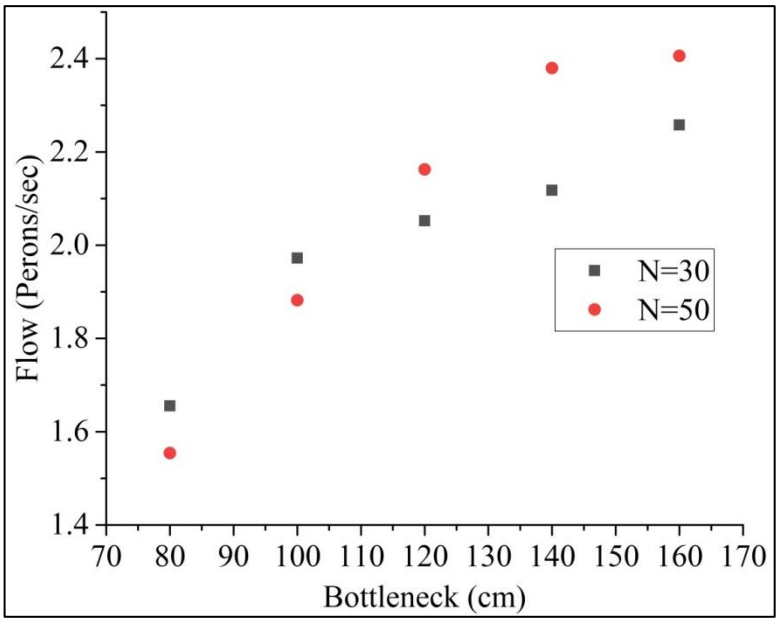

Figure 6.17 Flow versus bottleneck width for with buffer case

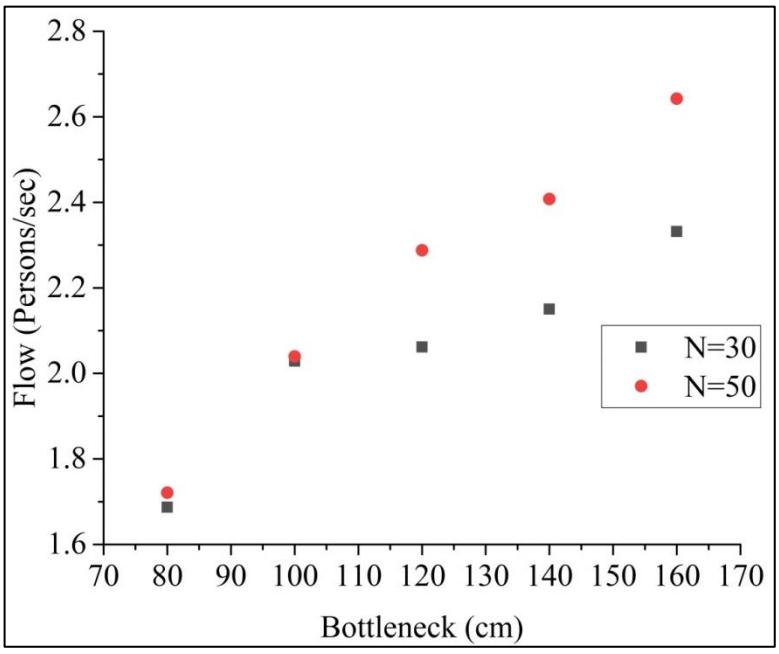

Figure 6.18 Flow versus bottleneck width for without buffer case

6.2.4 Specific flow

Specific flow is the ratio of flow to bottleneck width. The variation of specific flow versus bottleneck width has been shown in Figure 6.19 and 6.20. It has been observed that specific flow is decreasing as the width of the bottleneck increases and specific flows are more without buffer space as compared to with buffer space.

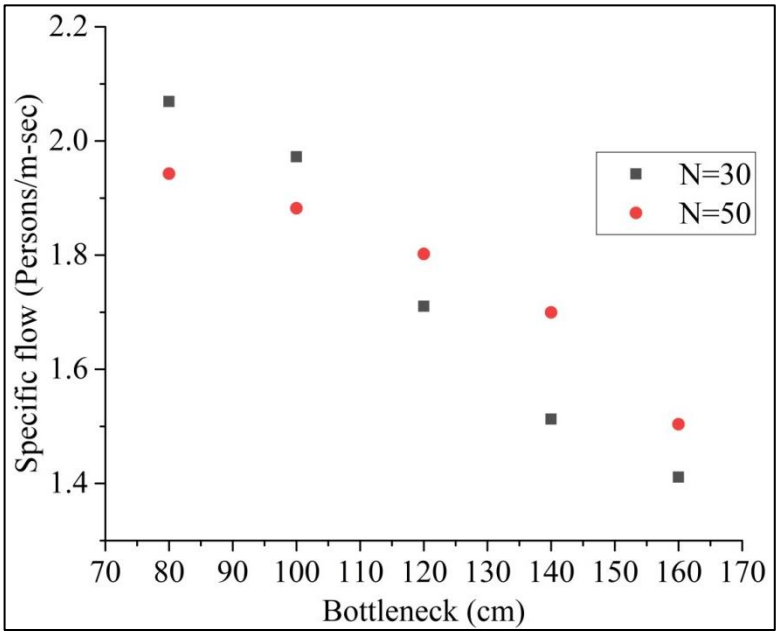

Figure 6.19 Specific flow versus bottleneck width for with buffer case

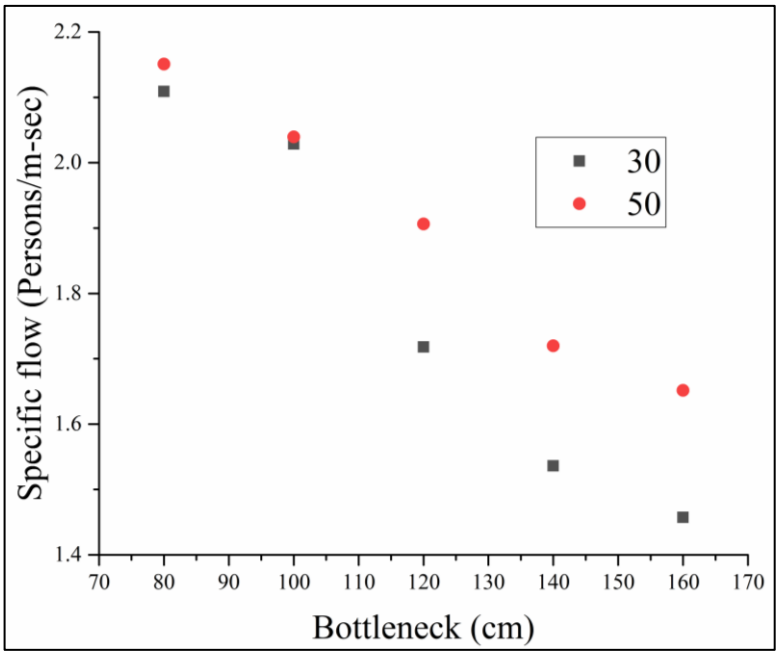

Figure 6.20 Specific flow versus bottleneck width for without buffer case

6.2.5 Trajectories

Trajectories of different persons for different widths for both cases with and without buffer space have been shown in Figures 6.21 to 6.30. This is plotted in order to know the route choice of each individual throughout the evacuation period in the study area. It can be identified that, lateral occupancy pedestrians are more in the case of without buffer space as compared to with buffer space for both the compositions(i.e., for (N = 30 & 50). Observations have shown a phenomenon called arching, which appears when a crowd with a highly desired

velocity tries to pass through a door in little time, the door gets clogged, and the crowd gets arc-shaped.

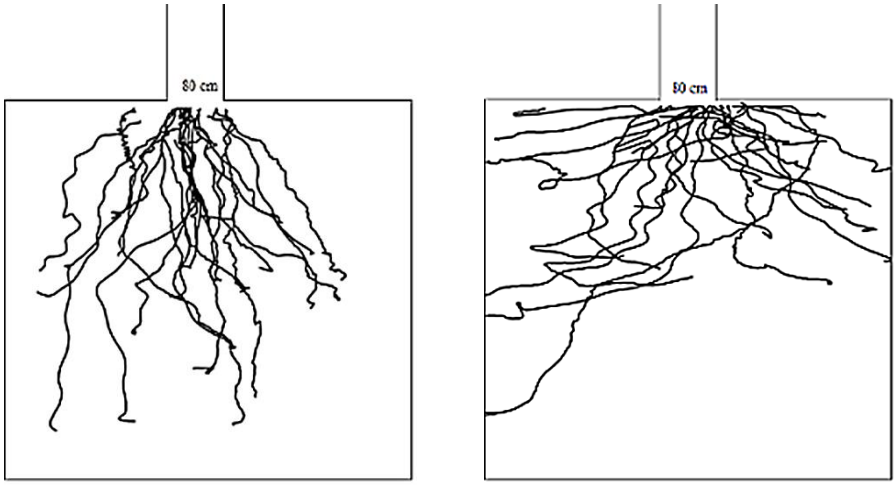

(A) With buffer space (B) Without buffer space

Figure 6.21 Trajectories of persons with N = 30 and width (B) = 80 cm

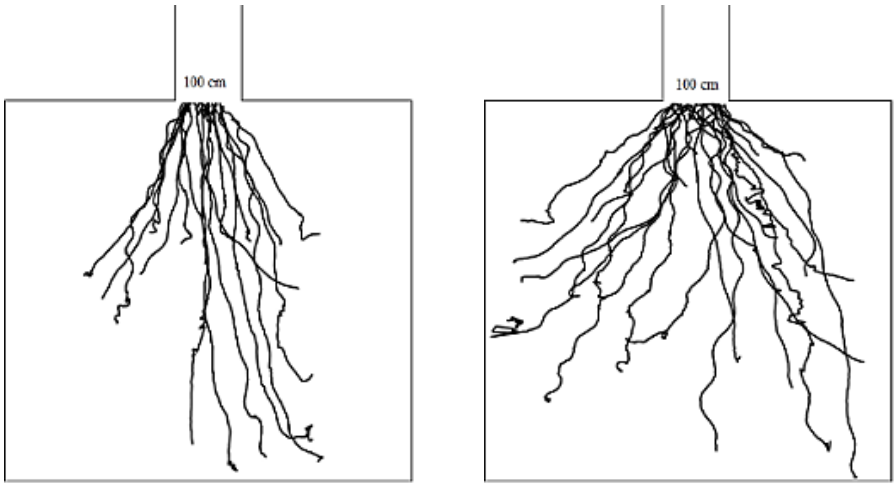

(A) With buffer space (B) Without buffer space

Figure 6.22 Trajectories of persons with N = 30 and width (B) = 100 cm

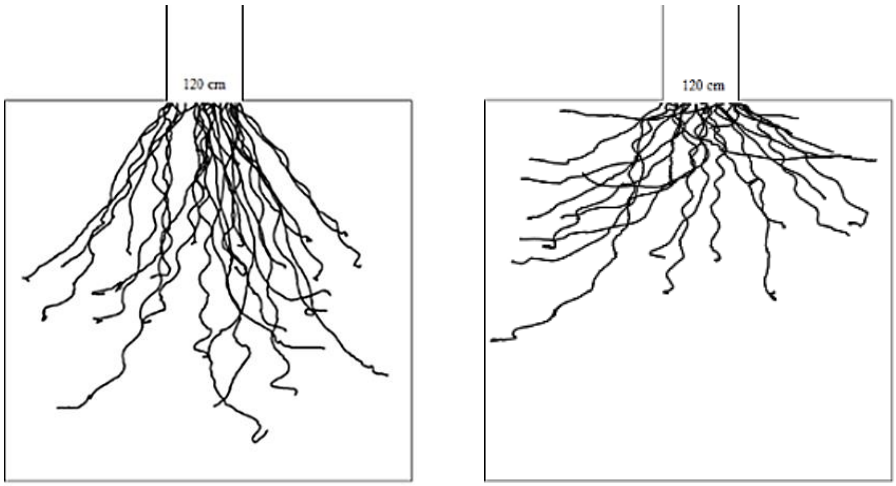

(A) With buffer space (B) Without buffer space

Figure 6.23 Trajectories of persons with N = 30 and width (B) = 120 cm

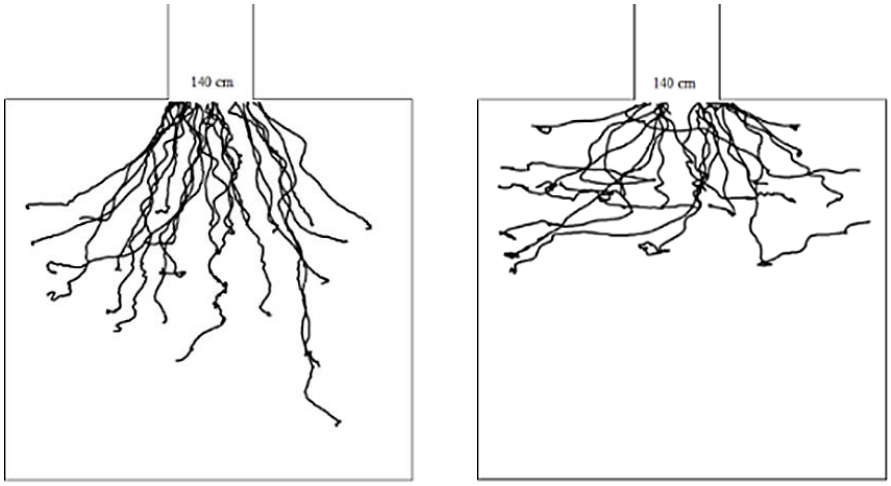

(A) With buffer space (B) Without buffer space

Figure 6.24 Trajectories of persons with N = 30 and width (B) = 140 cm

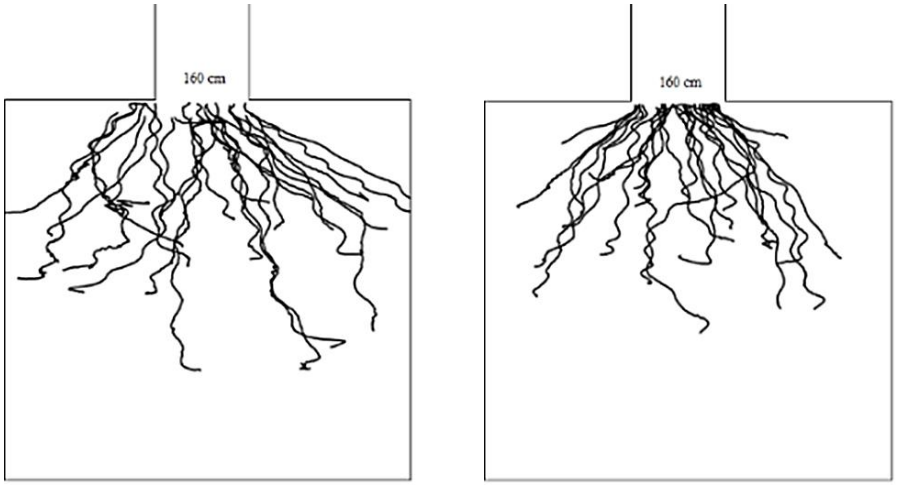

(A) With buffer space (B) Without buffer space

Figure 6.25 Trajectories of persons with N = 30 and width (B) = 160 cm

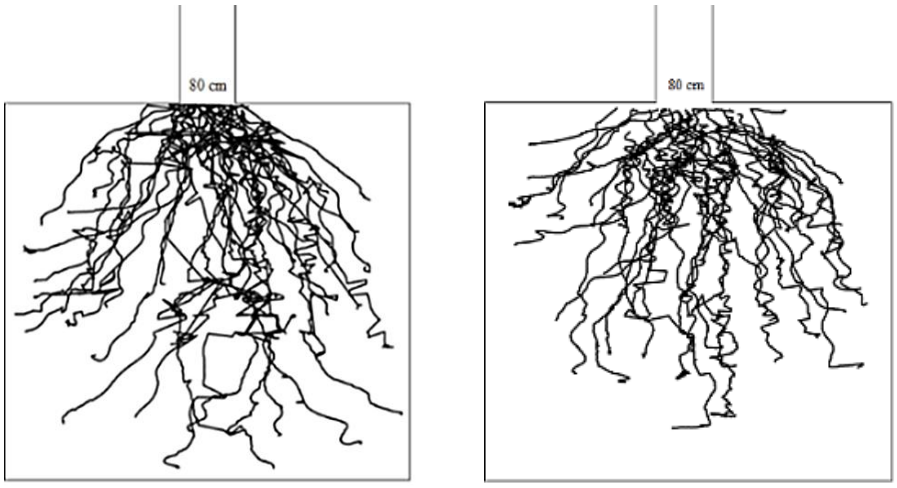

(A) With buffer space (B) Without buffer space

Figure 6.26 Trajectories of persons with N = 50 and width (B) = 80 cm

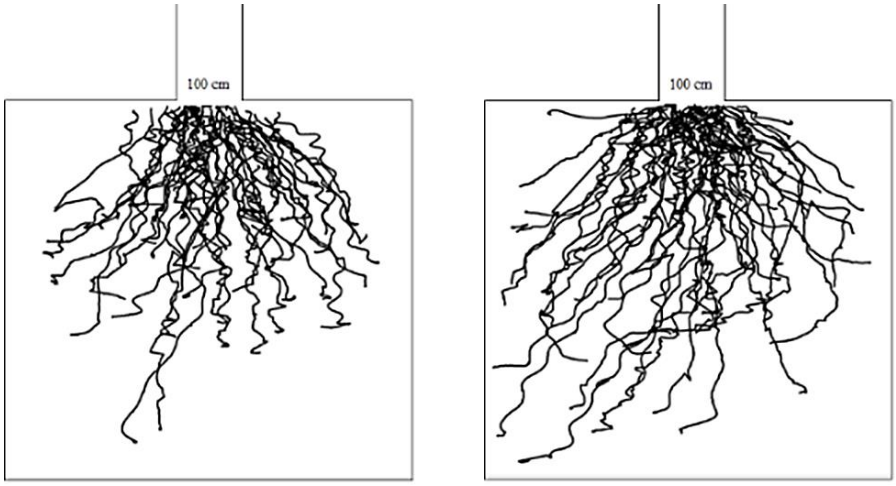

(A) With buffer space (B) Without buffer space

Figure 6.27 Trajectories of persons with N = 50 and width (B) = 100 cm

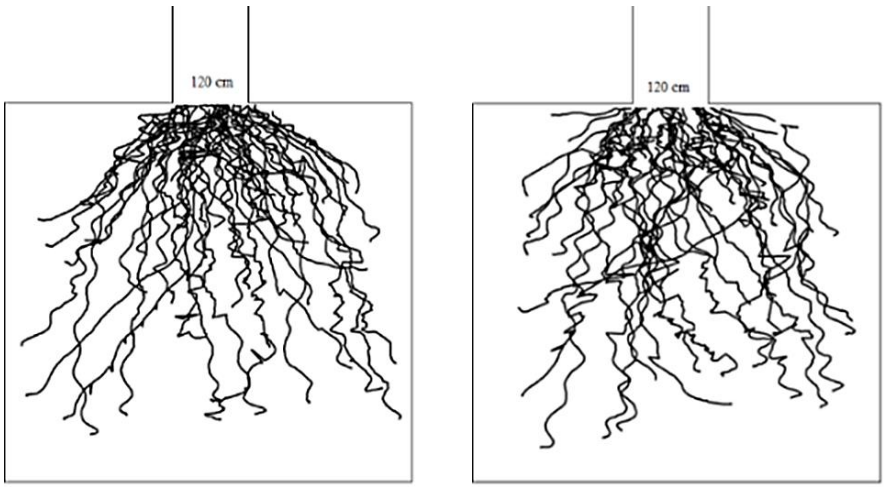

(A) With buffer space (B) Without buffer space

Figure 6.28 Trajectories of persons with N = 50 and width (B) = 120 cm

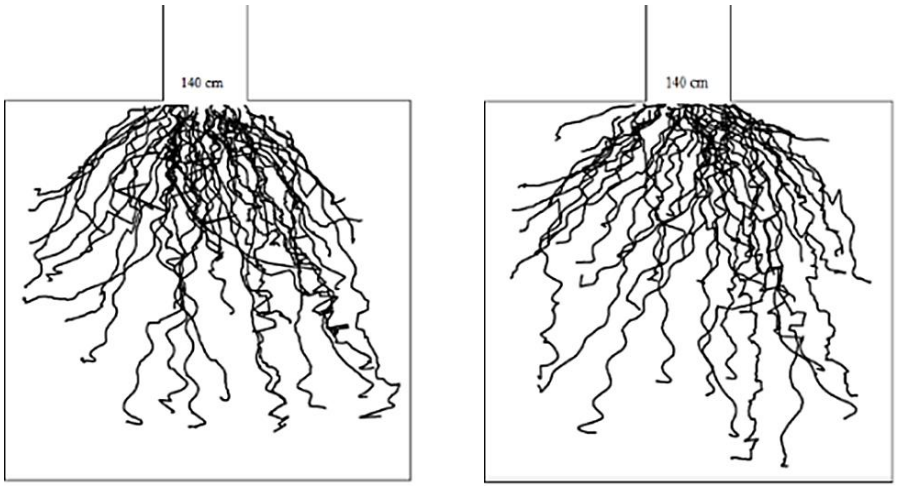

(A) With buffer space (B) Without buffer space

Figure 6.29 Trajectories of persons with N = 50 and width (B) = 140 cm

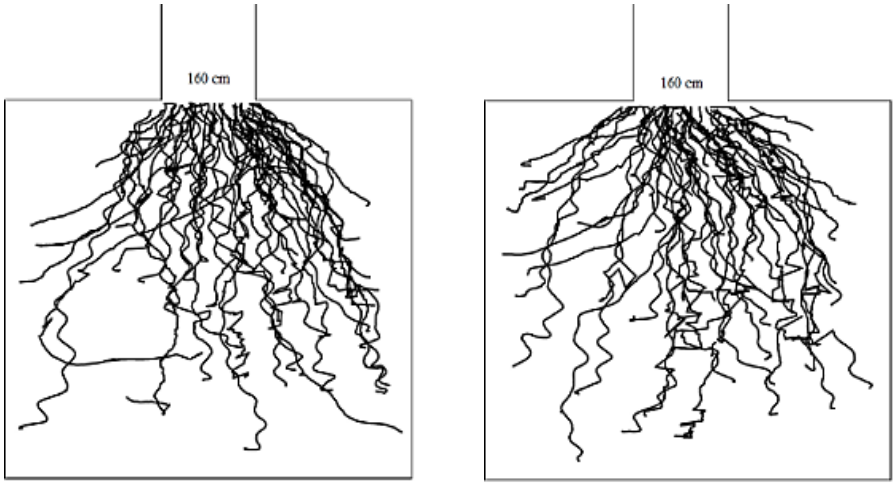

A) With buffer space (B) Without buffer space

Figure 6.30 Trajectories of persons with N = 50 and width (B) = 160 cm

6.2.6 Density analysis

The variation of density over the entire area for different bottleneck widths considered with and without buffer space are shown in Figures 6.31 to 6.40. It can be observed that, densities are decreasing as the width of the bottleneck increases. Density values have increased if the number of people was fifty as compared to thirty for the same width of bottleneck. High densities (i.e., p = 3 to 2.65 pedestrians/meter^2 for 30 people and p = 3.8 to 2.98 pedestrians/meter^2 for 50 people) were observed near the bottleneck opening and this happens when the incoming flow (through a surface in front of the bottleneck) exceeds the capacity of the bottleneck hence jamming occurs in front of the bottleneck.

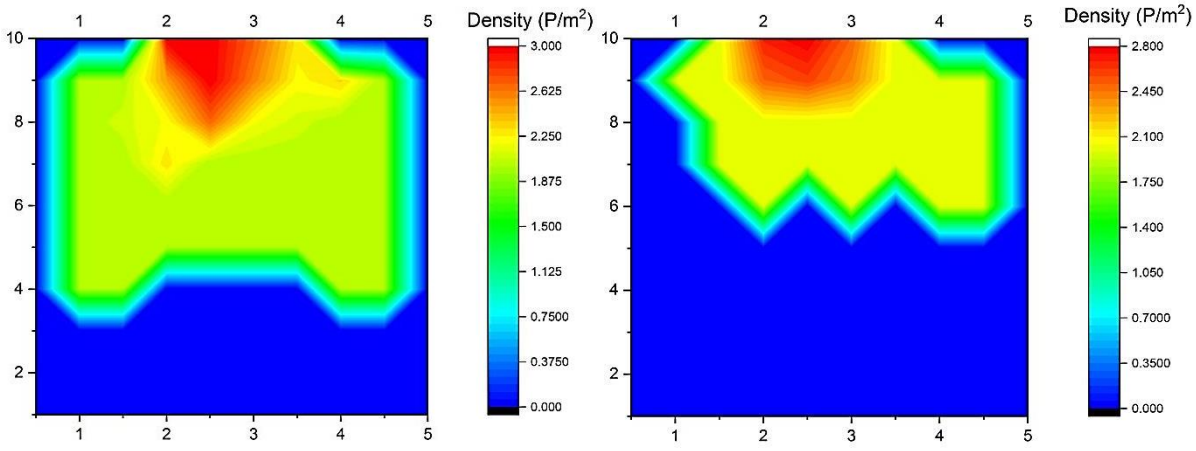

(A) With buffer space (B) Without buffer space

Figure 6.31 Density variation for Number of persons (N) = 30 and width (B) = 80 cm

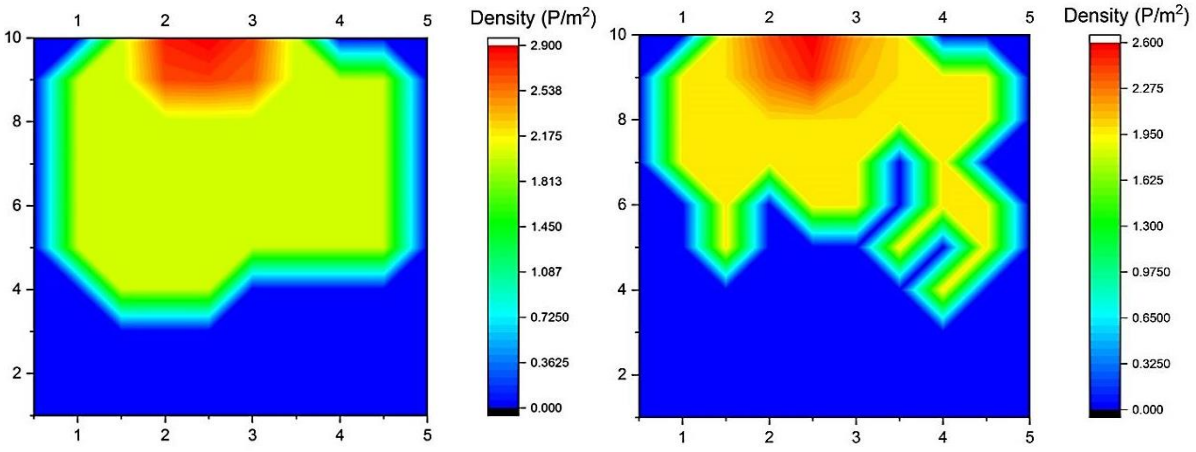

(A) With buffer space (B) Without buffer space

Figure 6.32 Density variation for Number of persons (N) = 30 and width (B) = 100 cm

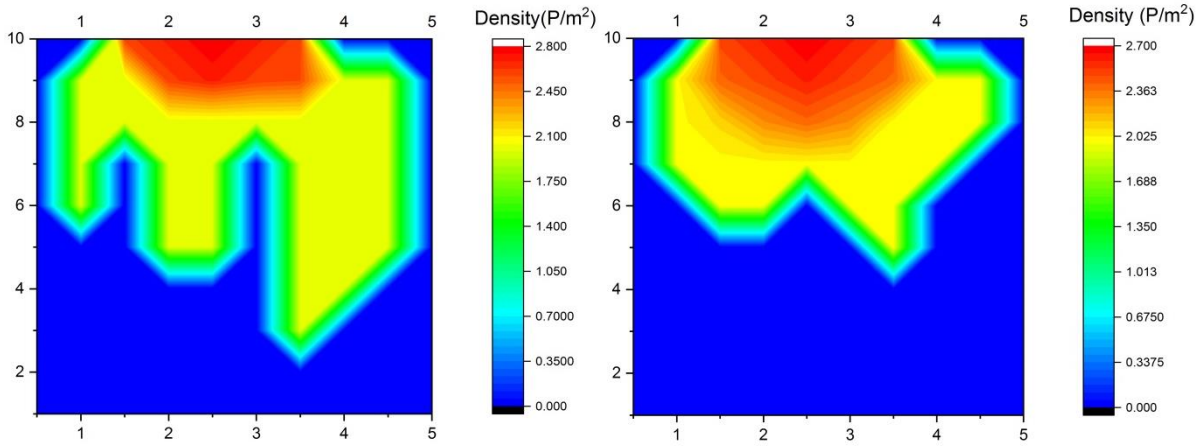

(A) With buffer space (B) Without buffer space

Figure 6.33 Density variation for Number of persons (N) = 30 and width (B) = 120 cm

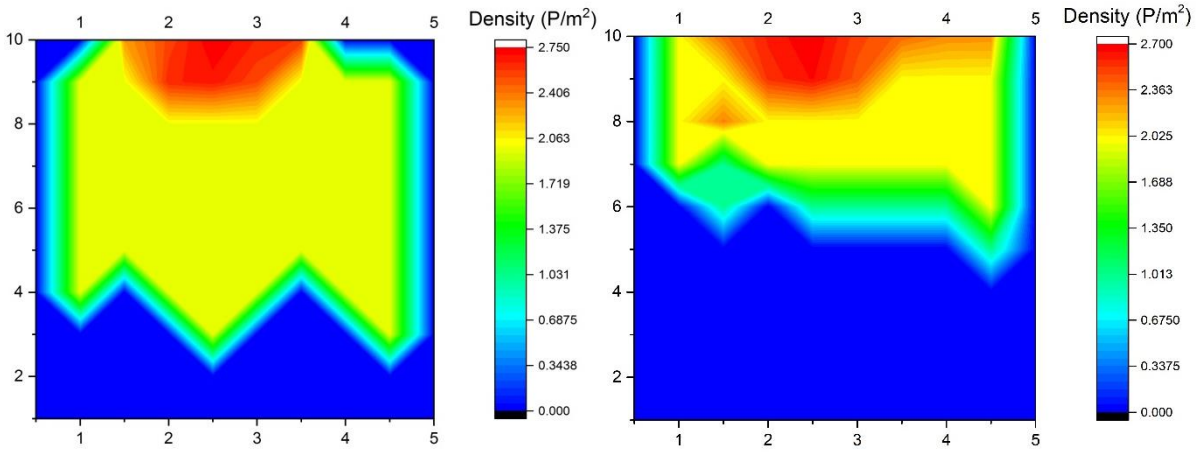

(A) With buffer space (B) Without buffer space

Figure 6.34 Density variation for Number of persons (N) = 30 and width (B) = 140 cm

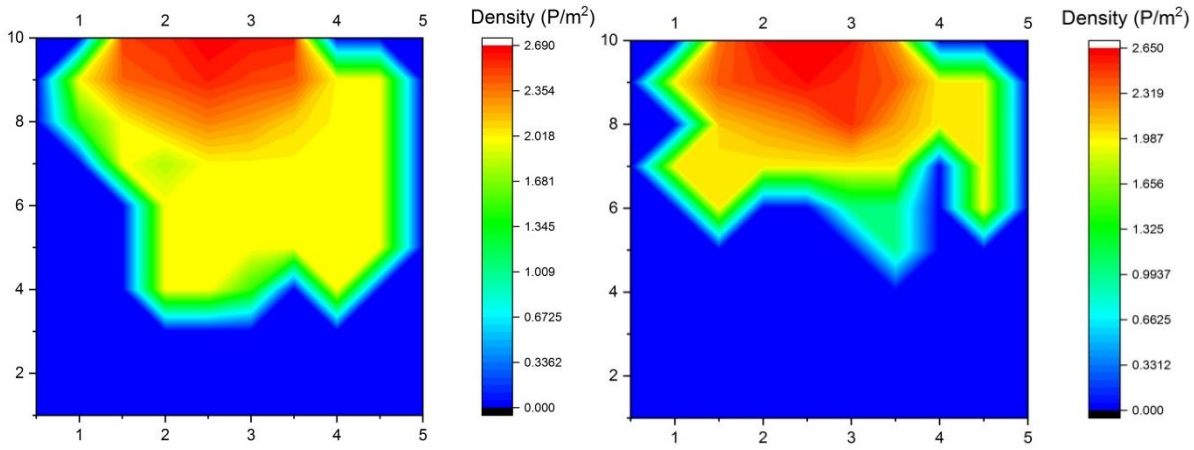

(A) With buffer space (B) Without buffer space

Figure 6.35 Density variation for Number of persons (N) = 30 and width (B) = 160 cm

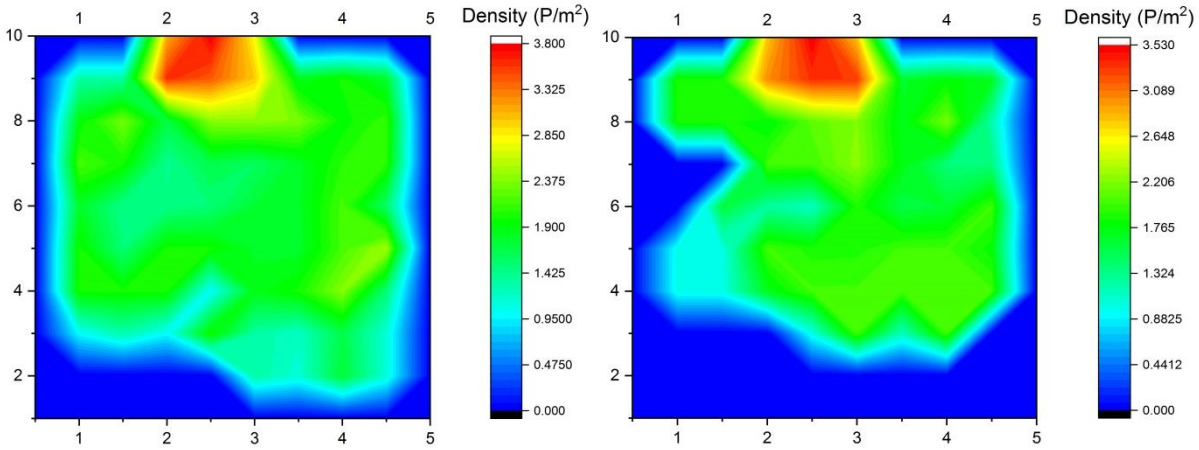

(A) With buffer space (B) Without buffer space

Figure 6.36 Density variation for Number of persons (N) = 50 and width (B) = 80 cm

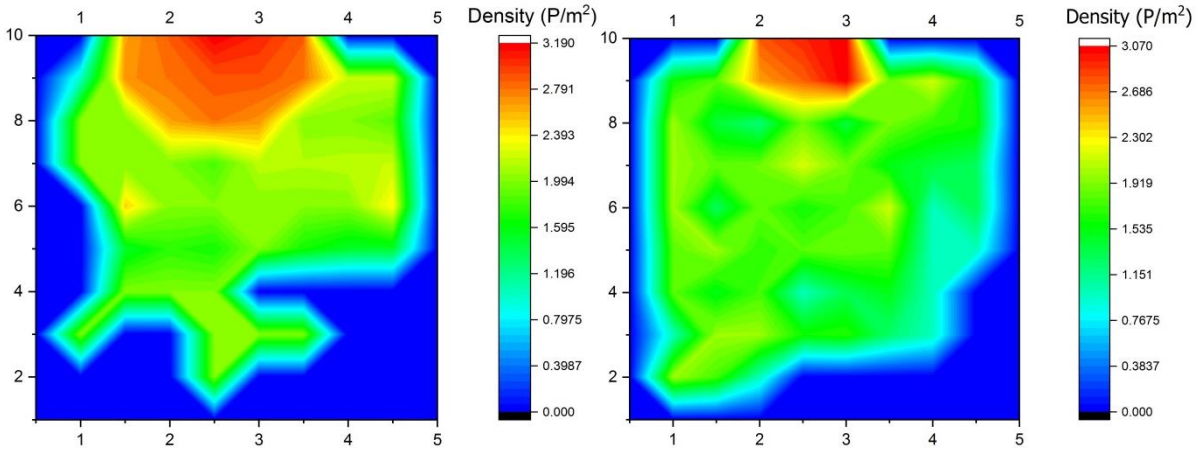

(A) With buffer space (B) Without buffer space

Figure 6.37 Density variation for Number of persons (N) = 50 and width (B) = 100 cm

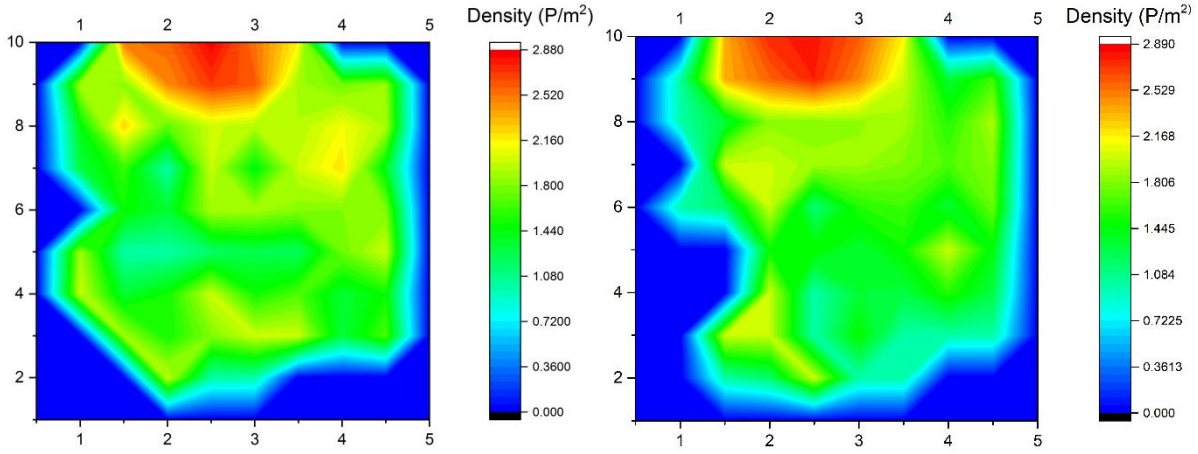

(A) With buffer space (B) Without buffer space

Figure 6.38 Density variation for Number of persons (N) = 50 and width (B) = 120 cm

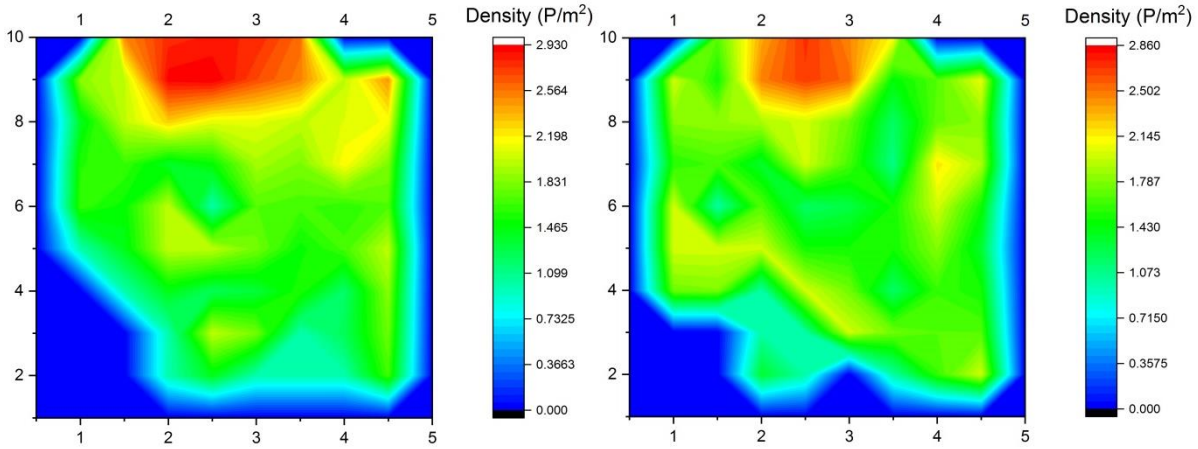

(A) With buffer space (B) Without buffer space

Figure 6.39 Density variation for Number of persons (N) = 50 and width (B) = 140 cm

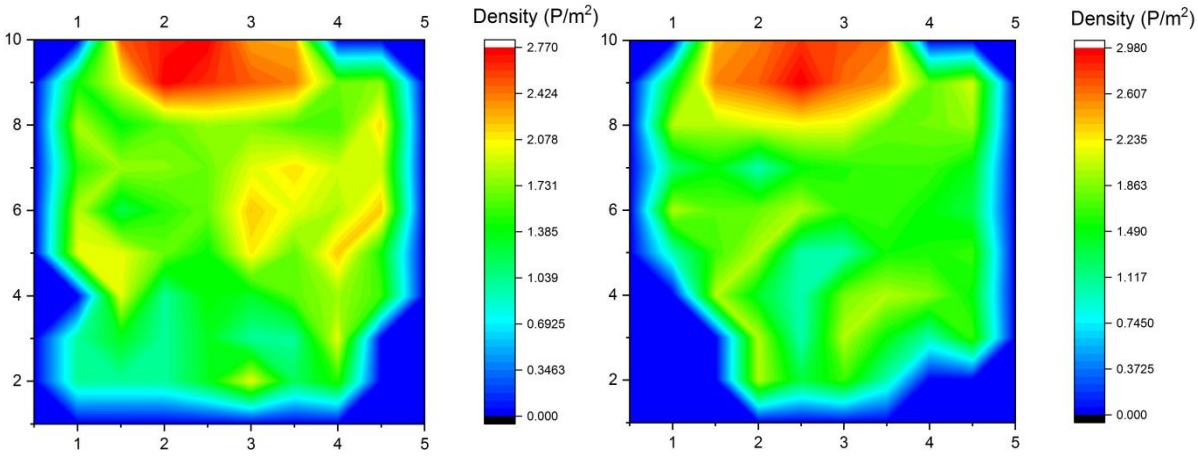

(A) With buffer space (B) Without buffer space

Figure 6.40 Density variation for Number of persons (N) = 50 and width (B) = 160 cm

6.2.7 Dynamic layer formation

Figure 6.41 shows the formation of lanes as the width of the bottleneck increases. From the figure, it can be observed that the flow of crowd increases as the width of bottleneck increases and this increase is in a stepwise manner, not a linear increase. When the crowd entered the bottleneck, formation of lanes occurs inside the bottleneck as width increases due to zipper effect. For the width of 80 cm, formation of lanes is absent. As the width increases from 80 cm to 100 cm, two lanes were formed and these lanes were continued and laterally expanded up to the width of 140 cm. For the width of 160 cm, it can be clearly observed that, three lanes were formed. It can also be observed that, the distance between the lanes does not depend on the bottleneck width (B).

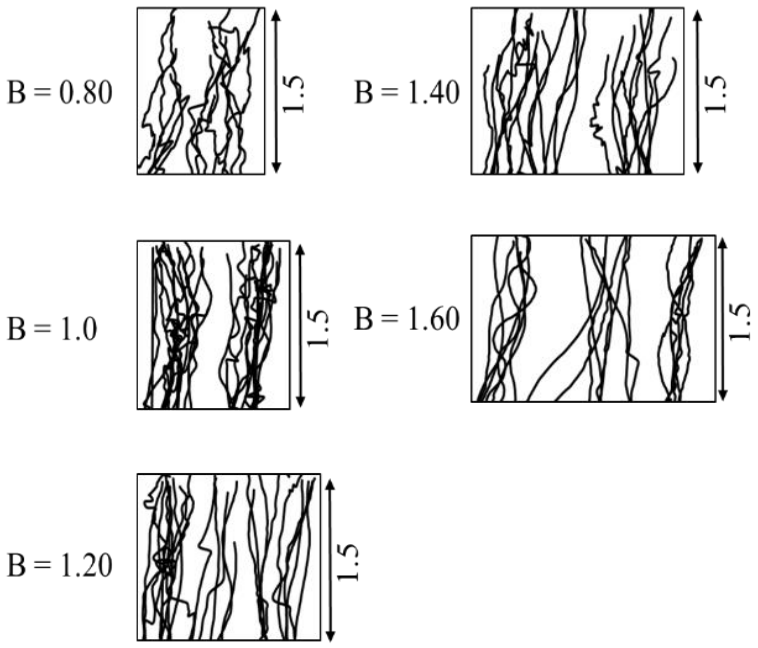

Figure 6.41 Formation of dynamic layers for different widths

6.2.8 Headway distribution and Capacity estimation

The elapsed time between the arrival of pairs of pedestrians is called time headway. The shape of time headway distribution varies considerably as the pedestrian flow rate increased. For example, under very low flow conditions, there is very little interaction between the pedestrians and the time headways appear to be somewhat random. As the flow of pedestrians increases, there are increasing interactions between pedestrians. In simple terms some headway appears to be random, while other headways follow one another. Generally, headways are classified into three types: random headway, intermediate headway, composite headway.

6.2.8.1 Random headway

The negative exponential distribution and displaced negative exponential distributions are mathematical distributions that represent the distribution of random intervals such as time headways. For time headways to be truly random, two conditions must be met. First, any point in time is as likely to have a pedestrian arriving as any other point in time. Second, the arrival of one pedestrian at a point in time does not affect the arrival of any other pedestrian. The probability density functions $P(x)$ of negative exponential and displaced negative exponential distribution are given by equations 6.1 and 6.2 respectively.

$$P(x) = \frac{1}{\beta} e^{-\frac{x}{\beta}} \tag{6.1}$$

$$P(x) = \frac{1}{\beta} e^{-\frac{x-\alpha}{\beta}} \tag{6.2}$$

6.2.8.2 Intermediate headway

The intermediate headway lies between two boundary conditions. That is, some pedestrians are travelling independent of one another, while other pedestrians are interacting. The Gamma and displaced Gamma or Pearson type III distribution is the mathematical distribution that represents the distribution of intermediate headways. The probability density functions of Gamma and Pearson type III distributions are given by the following equations.

$$P(x) = \frac{1}{\beta\Gamma(k)} \left(\frac{x}{\beta}\right)^{k-1} e^{-\frac{x}{\beta}} \tag{6.3}$$

$$P(x) = \frac{1}{\beta\Gamma(k)} \left(\frac{x-\alpha}{\beta}\right)^{k-1} e^{-\frac{x-\alpha}{\beta}} \tag{6.4}$$

Where, $\alpha, \beta \; and \; k$ are the parameters.

6.2.8.3 Composite headway model

Buckely (1968) proposed a semi random model for the pedestrian headways. According to Buckley's semi random model, headways are divided into two categories, one is free headways and other is constrained headways. Free headways are head ways of pedestrians experiencing no hindrance from pedestrians ahead, and who are thus able to walk at their free speed. Constrained headways are headways of pedestrians following pedestrians in front that, because no direct overtaking opportunity exists, force constrained walking. The headway will fluctuate around a desired minimum headway (the so-called empty zone). Different pedestrians will adopt different empty-zone size causes because these interpersonal variations are, among other things, subjective in what is perceived as comfortable, differences in walking purpose, but also differences in kinematics (i.e., step size and frequency).

Additionally, no pedestrian is able to maintain the same empty zone all the time, and thus the headway of a constrained pedestrian will fluctuate around a desired minimum headway. Let g(t) and h(t), respectively, denote the probability density functions of the empty zone and the free headway, and let φ denote the fraction of constrained pedestrians. The composite headway model of Buckley infers that the probability density function f (t) of the composite headway T equals

$$f(t) = \varphi g(t) + (1-\varphi)h(t) \tag{6.5}$$

Where, $g(t) = \frac{1}{\sqrt{2\pi\sigma^2}} e^{-\frac{(x-\theta)^2}{2\sigma^2}}$ (6.6)

$$h(t) = e^{\theta\lambda - 0.5\sigma^2\lambda^2}\ \lambda e^{-\lambda x} \int_{-\infty}^{x} \frac{1}{\sqrt{2\pi\sigma^2}} e^{-\frac{(t-\theta)^2}{2\sigma^2}}\, dt \tag{6.7}$$

Where, φ is the fraction of constrained headways and λ denotes the free headway arrival rate. In the present study, five types of distributions were taken to cover the random, intermediate, composite headways. The probability density functions, population moments of these distributions are presented in Table 6.5.

In table below μ_1', μ_2', μ_3' and μ_4' are the population moments, which are obtained by using the following equations.

$$\mu_1' = \frac{\sum fd}{N} * I \tag{6.8}$$

$$\mu_2' = \frac{\sum fd^2}{N} * I^2 \tag{6.9}$$

$$\mu_3' = \frac{\sum fd^2}{N} * I^3 \tag{6.10}$$

$$\mu_4' = \frac{\sum fd^2}{N} * I^4 \tag{6.11}$$

Where f is the frequency, d is the deviation, N is the total number of samples and I denote the width of the class interval. The time headways for different widths considering with and without buffer space are extracted, and five summaries (i.e., minimum, maximum, range, and class interval, mean) have been calculated, and observed frequencies were obtained using frequency function in MS Excel. To get the predicted frequencies, population moments were calculated using the formulas mentioned earlier and different parameters were estimated. The Tables 6.6 to 6.9 show the population moments and parameter values for different types of distributions considered in the study

Table 6.5 Headway distribution table

Distribution type	Probability density function	Population moments
Negative exponential	$\frac{1}{\beta} e^{-\frac{x}{\beta}}$	$\mu_1' = \beta$
Displaced negative exponential	$\frac{1}{\beta} e^{-\frac{x-\alpha}{\beta}}$	$\mu_1' = \alpha + \beta$ $\mu_2' = \alpha^2 + 2\alpha\beta + 2\beta^2$
Gamma	$\frac{1}{\beta\Gamma(k)} \left(\frac{x}{\beta}\right)^{k-1} e^{-\frac{x}{\beta}}$	$\mu_1' = \beta k$ $\mu_2' = \beta^2 k(k+1)$
Pearson type III	$\frac{1}{\beta\Gamma(k)} \left(\frac{x-\alpha}{\beta}\right)^{k-1} e^{-\frac{x-\alpha}{\beta}}$	$\mu_1' = \alpha + \beta k$ $\mu_2' = \alpha^2 + 2\alpha\beta k + \beta^2 k(k+1)$ $\mu_3' = \alpha^3 + 3\alpha^2\beta k + 3\alpha\beta^2 k(k+1) + \beta^3 k(k+1)(k+2)$
Semi random Note: $\epsilon = (\theta - \sigma^2\lambda)$	$\frac{\phi}{\sqrt{2\pi\sigma^2}} e^{-\frac{(x-\theta)^2}{2\sigma^2}} +$ $(1-\phi) e^{\theta\lambda - 0.5\sigma^2\lambda^2}$ $\lambda e^{-\lambda x} \int_{-\infty}^{x} \frac{1}{\sqrt{2\pi\sigma^2}} e^{-\frac{(t-\theta)^2}{2\sigma^2}} dt$	$\mu_1' = \phi\theta + (1-\phi)(\epsilon + \frac{1}{\lambda})$ $\mu_2' = \phi(\theta^2 + \lambda^2) + (1-\phi)(\varepsilon^2 + \sigma^2 + \frac{2\epsilon}{\lambda} + \frac{2}{\lambda^2})$ $\mu_3' = \phi(\theta^3 + 3\sigma^2\theta) + (1-\phi)(\varepsilon^3 + 3\sigma^2\epsilon + \frac{3}{\lambda}\varepsilon^2 + \frac{3}{\lambda}\sigma^2 + \frac{6}{\lambda^2}\varepsilon + \frac{6}{\lambda^3})$ $\mu_4' = \phi(\theta^4 + 6\theta^2\sigma^2 + 3\sigma^4) + (1-\phi)(\varepsilon^4 + 6\varepsilon^2\sigma^2 + 3\sigma^4 + \frac{4}{\lambda}(\varepsilon^3 + 3\sigma^2\epsilon) + \frac{12}{\lambda^2}(\varepsilon^2 + \sigma^2) + \frac{24}{\epsilon}\lambda^3 + \frac{24}{\lambda^4})$

Table 6.6 Population moments for different widths with number of persons (N) = 30

Width (meter)	μ_1'		μ_2'		μ_3'		μ_4'	
	With buffer space	Without buffer space	With buffer space	Without buffer space	With buffer space	Without buffer space	With buffer space	Without buffer space
0.8	0.9	0.27	2.43	2.47	7.50	2.87	29.23	14.87
1.0	1.83	1.27	6.23	4.07	24.43	14.07	106.63	56.87
1.2	1.73	0.63	6.07	2.83	22.53	6.63	91.67	26.03
1.4	0.13	0.93	1.67	3.53	5.13	12.53	24.47	53.93
1.6	0.27	1.33	1.80	3.67	5.07	12.93	23.40	53.27

Table 6.7 Population moments for different widths with number of persons (N) = 50

Width (meter)	μ_1'		μ_2'		μ_3'		μ_4'	
	With buffer space	Without buffer space	With buffer space	Without buffer space	With buffer space	Without buffer space	With buffer space	Without buffer space
0.8	0.42	0.120	2.42	2.52	5.58	4.44	25.22	25.08
1.0	2.02	0.620	7.38	2.10	31.66	6.98	152.10	30.18
1.2	1.6	1.00	5.16	4.32	17.44	15.52	67.56	69.36
1.4	1.76	0.360	6.16	2.28	24.08	5.76	106.00	25.08
1.6	1.00	0.58	3.32	2.98	9.52	8.14	38.60	36.82

Table 6.8 Parameter estimations of different types of distributions with number of persons (N) = 30

Width (meter)	Distribution type									
	Negative exponential		Displaced Negative exponential		Gamma		Pearson type III		Semi random	
	Parameters									
	With buffer space	Without buffer space	With buffer space	Without buffer space	With buffer space	Without buffer space	With buffer space	Without buffer space	With buffer space	Without buffer space
0.8	$\beta = 0.9$	$\beta = 0.27$	$\alpha = -0.37$, $\beta = 1.27$	$\alpha = -1.27$, $\beta = 1.54$	$\beta = 1.8$, $k = 0.5$	$\beta = 8.87$, $k = 0.03$	$\alpha = -1.28$, $\beta = 0.739$, $k = 3$	$\alpha = -12.37$, $\beta = 0.189$, $k = 67$	$\phi = 0.102$, $\theta = 3.779$, $\sigma = -0.8$, $\lambda = 5.3$	$\phi = 0.173$, $\theta = 0.08$, $\sigma = -1.70$, $\lambda = 0.80$
1.0	$\beta = 0.18$	$\beta = 1.27$	$\alpha = 0.132$, $\beta = 1.697$	$\alpha = -0.297$, $\beta = 1.567$	$\beta = 1.574$, $k = 1.16$	$\beta = 1.934$, $k = 0.656$	$\alpha = -4.852$, $\beta = 0.431$, $k = 16$	$\alpha = -3.269$, $\beta = 0.541$, $k = 8$	$\phi = 1$, $\theta = 1.83$, $\sigma = -1.697$, $\lambda = 0$	$\phi = 1$, $\theta = 1.269$ $\sigma = 1.567$, $\lambda = 0$
1.2	$\beta = 1.73$	$\beta = 0.63$	$\alpha = -0.024$, $\beta = 1.754$	$\alpha = -0.929$, $\beta = 1.559$	$\beta = 1.778$, $k = 0.972$	$\beta = 3.862$, $k = 0.163$	$\alpha = -11.97$, $\beta = 0.224$, $k = 61$	$\alpha = -6.01$, $\beta = 0.36$, $k = 18$	$\phi = 0.587$, $\theta = 0.437$, $\sigma = 0.827$, $\lambda = -4.867$	$\phi = 1$, $\theta = 0.629$, $\sigma = 1.559$, $\lambda = 0$
1.4	$\beta = 0.13$	$\beta = 0.93$	$\alpha = -1.557$, $\beta = 1.285$	$\alpha = -0.702$, $\beta = 1.63$	$\beta = 12.71$, $k = 0.01$	$\beta = 2.86$, $k = 0.324$	$\alpha = -1.089$, $\beta = 1.355$, $k = 1$	$\alpha = -2.38$, $\beta = 0.804$ $k = 4$	$\phi = 1$, $\theta = 0.13$, $\sigma = 1.285$, $\lambda = 0$	$\phi = 0.1847$, $\theta = 3.843$, $\sigma = 0.843$, $\lambda = 5.286$
1.6	$\beta = 0.27$	$\beta = 1.33$	$\alpha = -1.044$, $\beta = 1.31$	$\alpha = -0.048$, $\beta = 1.378$	$\beta = 6.39$, $k = 0.04$	$\beta = 1.42$, $k = 0.93$	$\alpha = -1.36$, $\beta = 1.05$, $k = 1.5$	$\alpha = -1.08$, $\beta = 0.78$, $k = 3$	$\phi = 1$, $\theta = 0.269$, $\sigma = 1.314$, $\lambda = 0$	$\phi = 0.1483$, $\theta = 4.087$, $\sigma = -0.744$, $\lambda = 6.14$

Table 6.9 Parameter estimations of different types of distributions with number of persons (N) = 50

Width (meter)	Distribution type									
	Negative exponential		Displaced Negative exponential		Gamma		Pearson type III		Semi random	
	Parameters									
	With buffer space	Without buffer space	With buffer space	Without buffer space	With buffer space	Without buffer space	With buffer space	Without buffer space	With buffer space	Without buffer space
0.8	$\beta = 0.42$	$\beta = 0.12$	$\alpha = -1.077$, $\beta = 0.49$	$\alpha = -1.462$, $\beta = 1.582$	$\beta = 5.34$, $k = 0.078$	$\beta = 20.88$, $k = 0.005$	$\alpha = -3.33$, $\beta = 0.597$, $k = 6$	$\alpha = -3.43$, $\beta = 0.705$, $k = 5$	$\phi = 0.132$, $\theta = 3.183$, $\sigma = -1.36$, $\lambda = 3.455$	$\phi = 0.526$, $\theta = 3.147$, $\sigma = -1.99$, $\lambda = 0.835$
1.0	$\beta = 2.02$	$\beta = 0.62$	$\alpha = 0.203$, $\beta = 1.816$	$\alpha = -0.689$, $\beta = 1.309$	$\beta = 1.633$, $k = 1.236$	$\beta = 2.76$, $k = 0.224$	$\alpha = -4.34$, $\beta = 0.518$, $k = 12$	$\alpha = -1.03$, $\beta = 1.03$, $k = 1.5$	$\phi = 1$, $\theta = 2.02$, $\sigma = -1.816$, $\lambda = 0$	$\phi = 0.726$, $\theta = 2.513$ $\sigma = 1.867$, $\lambda = 0.4704$
1.2	$\beta = 1.6$	$\beta = 1$	$\alpha = -0.012$, $\beta = 1.612$	$\alpha = -0.822$, $\beta = 1.822$	$\beta = 1.625$, $k = 0.9846$	$\beta = 3.32$, $k = 0.301$	$\alpha = -14.04$, $\beta = 0.166$, $k = 94$	$\alpha = -3.83$, $\beta = 0.686$, $k = 7$	$\phi = 0.584$, $\theta = 0.538$, $\sigma = 0.9806$, $\lambda = -3.008$	$\phi = 0.4$, $\theta = 2.578$, $\sigma = 2.185$, $\lambda = 0.79$
1.4	$\beta = 1.76$	$\beta = 0.36$	$\alpha = 0.01$, $\beta = 1.749$	$\alpha = -1.106$, $\beta = 1.466$	$\beta = 1.74$, $k = 1.011$	$\beta = 5.973$, $k = 0.06$	$\alpha = -5.868$, $\beta = 0.401$ $k = 19$	$\alpha = -2.36$, $\beta = 0.788$ $k = 3.5$	$\phi = 0.3033$, $\theta = 3.9487$, $\sigma = -0.962$, $\lambda = 3.6873$	$\phi = 0.581$, $\theta = 2.796$, $\sigma = 1.917$, $\lambda = 0.8595$
1.6	$\beta = 1$	$\beta = 0.58$	$\alpha = -0.523$, $\beta = 1.523$	$\alpha = -1.045$, $\beta = 1.625$	$\beta = 2.32$, $k = 0.431$	$\beta = 4.55$, $k = 0.127$	$\alpha = -5.9$, $\beta = 0.336$, $k = 20$	$\alpha = -3.59$, $\beta = 0.63$, $k = 6.5$	$\phi = 0.124$, $\theta = 3.35$, $\sigma = 1.169$, $\lambda = 2.281$	$\phi = 0.16$, $\theta = 3.38$, $\sigma = 1.03$, $\lambda = 3.413$

The probability density functions for different types of distributions were estimated with the help of obtained values of parameters. Predicted frequencies were obtained by multiplying probability density function values with sample size. Figures 6.42 to 6.51 show the headway versus frequency for different type of distributions. Five types of distributions mentioned above have been compared with the observed data and tested with the goodness of fit (χ^2 test). It was found that, among the five types of distributions, semi-random distribution is observed to be the best fit for the observed data. The percentage of constrained headways (ϕ)observed in case of 50 persons is more than that of 30 persons. This implies that free flow decreases with increase in density for a study area.

6.2.8.4 Headway distributions (Number of persons N = 30)

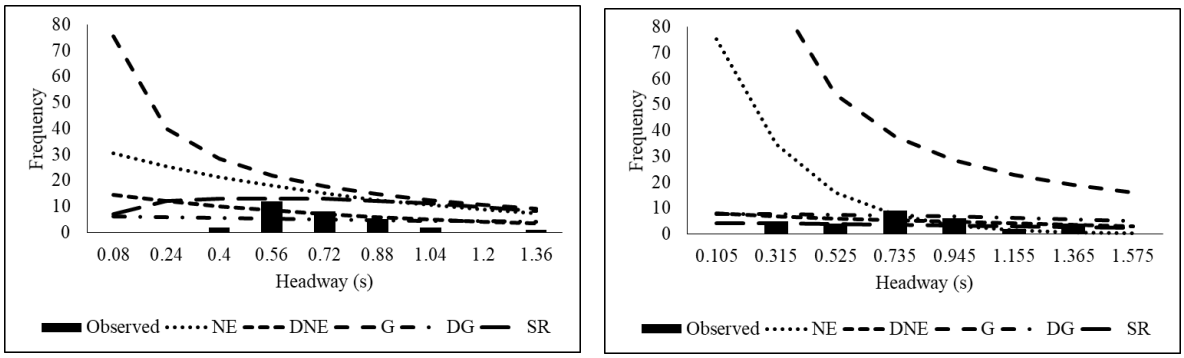

(A) With buffer space (B) Without buffer space

Figure 6.42 Frequency versus Headway for width (B) = 80 cm

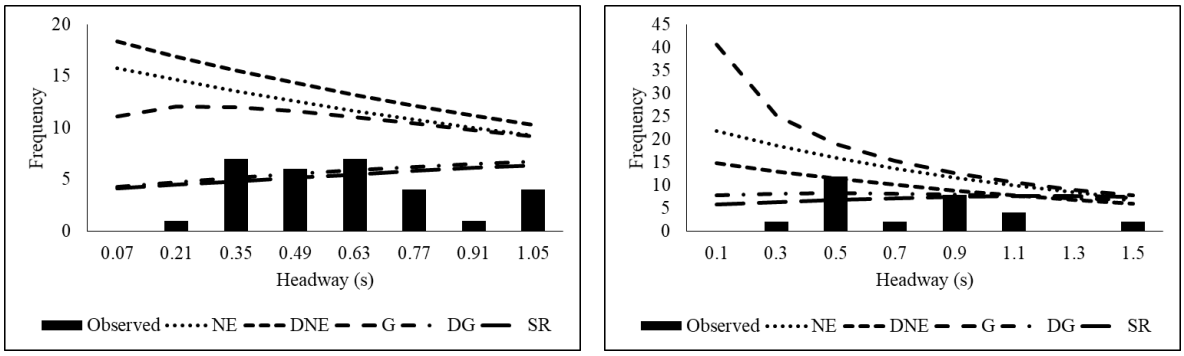

(A) With buffer space (B) Without buffer space

Figure 6.43 Frequency versus Headway for width (B) = 100 cm

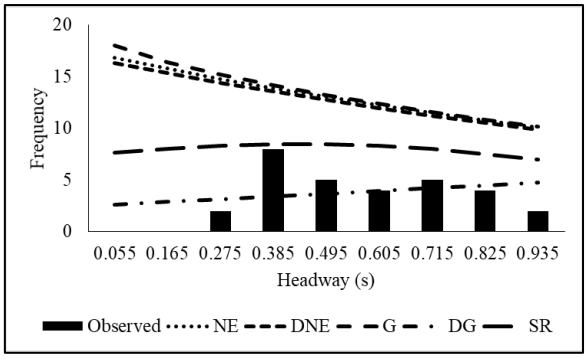

(A) With buffer space

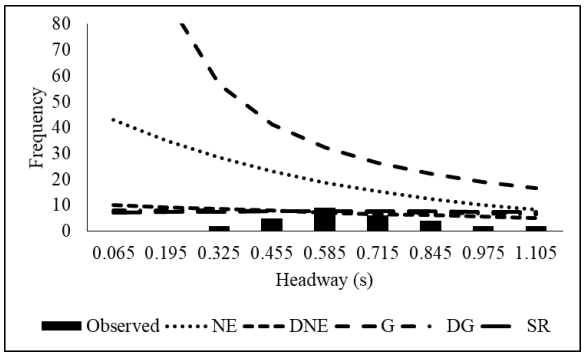

(B) Without buffer space

Figure 6.44 Frequency versus Headway for width (B) = 120 cm

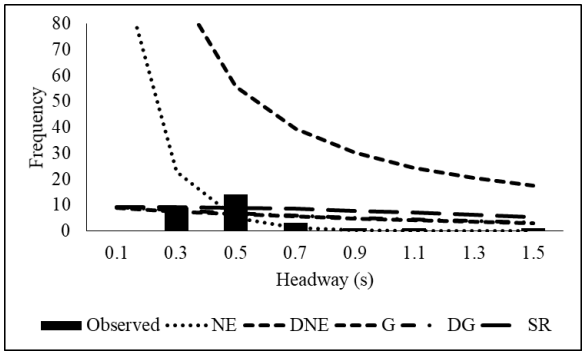

(A) With buffer space

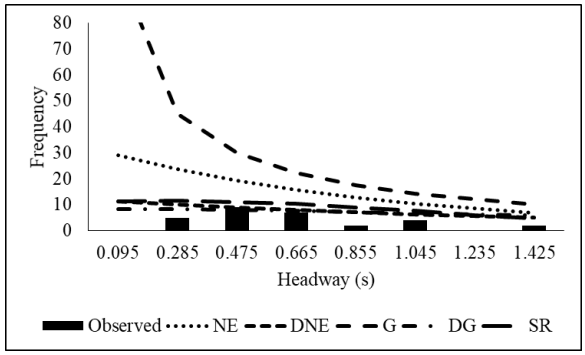

(B) Without buffer space

Figure 6.45 Frequency versus Headway for width (B) = 140 cm

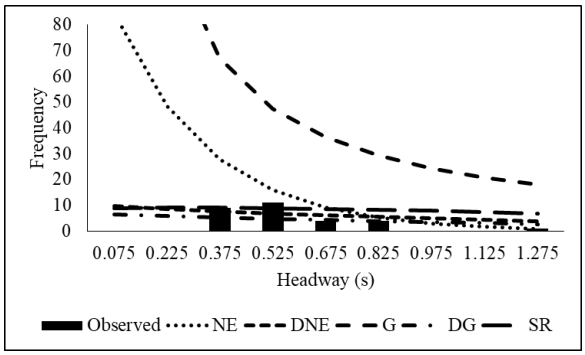

(A) With buffer space

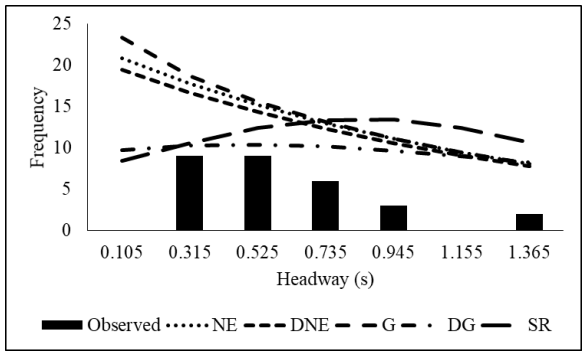

(B) Without buffer space

Figure 6.46 Frequency versus Headway for width (B) = 160 cm

6.2.8.5 Headway distributions (Number of persons N = 50)

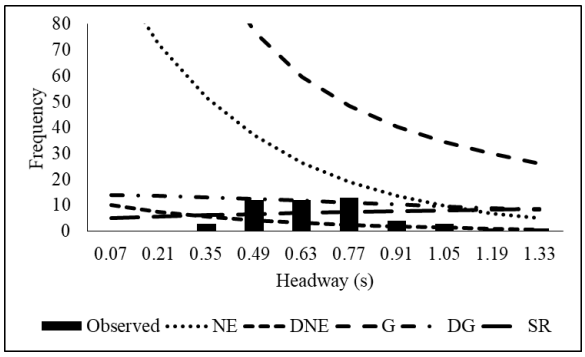

(A) With buffer space

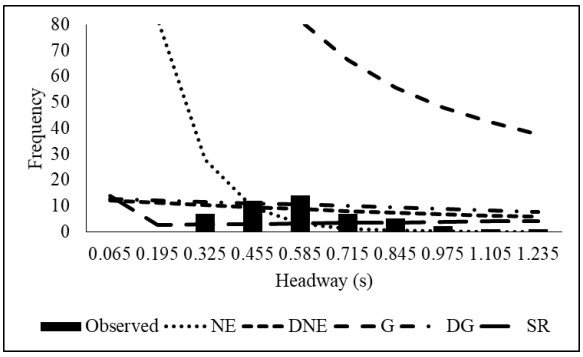

(B) Without buffer space

Figure 6.47 Frequency versus Headway for width (B) = 80 cm

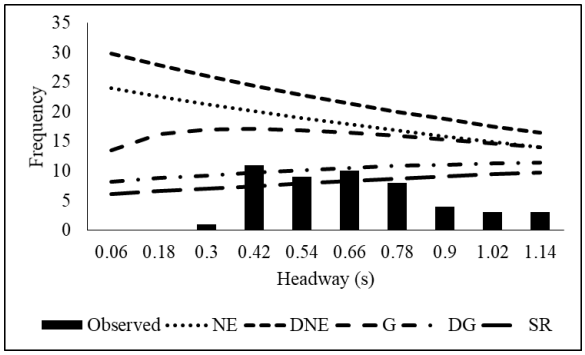

(A) With buffer space

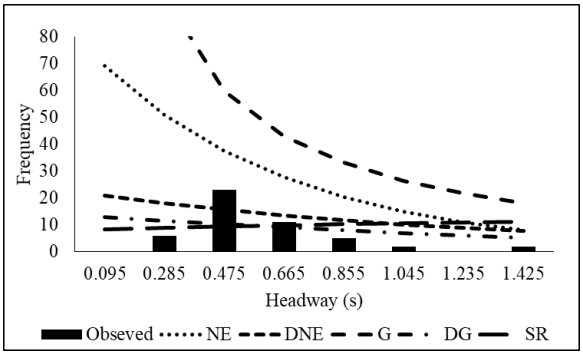

(B) Without buffer space

Figure 6.48 Frequency versus Headway for width (B) = 100 cm

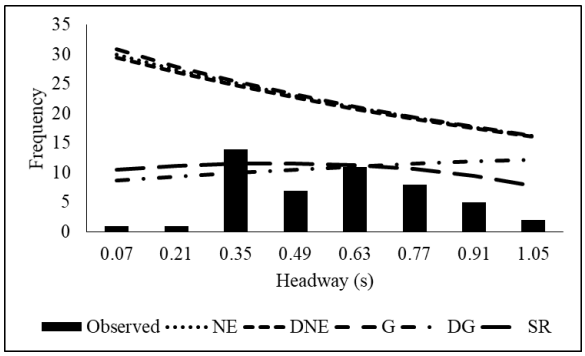

(A) With buffer space

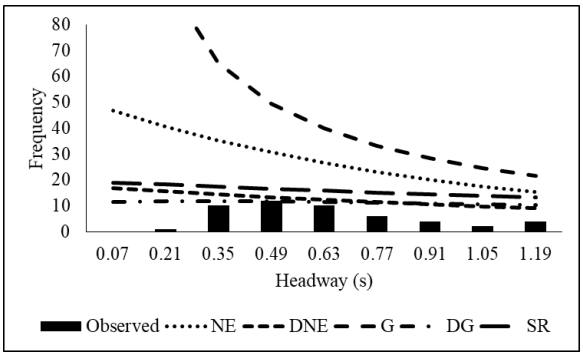

(B) Without buffer space

Figure 6.49 Frequency versus Headway for width (B) = 120 cm

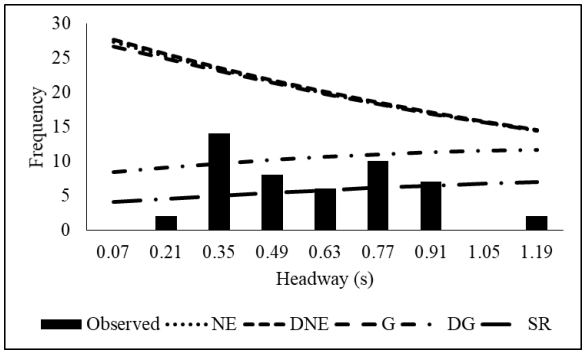

(A) With buffer space

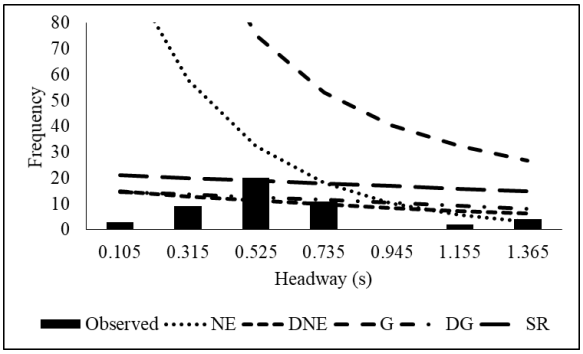

(B) Without buffer space

Figure 6.50 Frequency versus Headway for width (B) = 140 cm

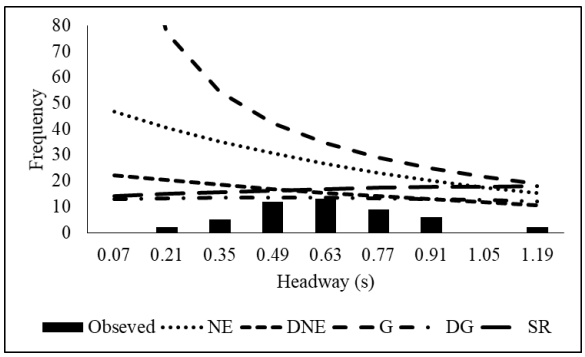

(A) With buffer space

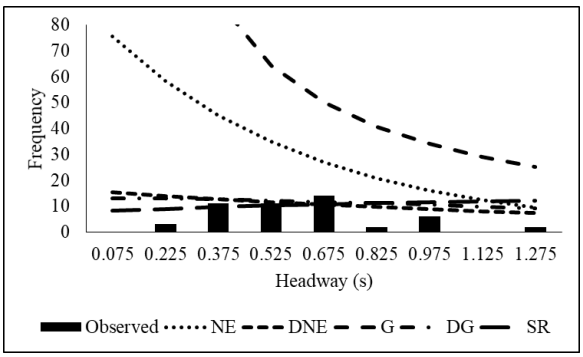

(B) Without buffer space

Figure 6.51 Frequency versus Headway for width (B) = 160 cm

6.2.9 Capacity estimation

In order to estimate the capacity of bottleneck, Buckley model is used. The probability density function of Buckley model is given in equation (6.12).

$$f(t) = \phi\, g(t) + (1-\phi)\, h(t) \quad (6.12)$$

Where g(t) denote probability density function of empty zone, h(t) denote probability density function of free headway, and ϕ denote the fraction of con strained pedestrians.

The capacities of dynamic layers can be found using empty zone i.e., by assuming saturated condition. The C (in Pedestrians/metre/second) equals the inverse of the mean empty zone.

$$C = \frac{1}{E(T)} \quad (6.13)$$

Where, E (T) is the mean of the empty zone. Capacity per lane C_1 (in pedestrians/second/lane) can be calculated by the following equation.

$$C_1 = \frac{1}{2aE(T)} \quad (6.14)$$

Where 2a denotes the average layer width and here the average layer width is equal to 50 cm because the minimum effective width of a bottleneck must encompass at least one layer

hence it must be greater than or equal to the expected maximum shoulder width of a pedestrian (i.e., 50 cm). The following Tables 6.10 and 6.11 show the capacity variations for different sets of bottleneck widths. From these tables, it can be observed that the capacity of bottleneck increases as the width of the bottleneck increases and this increase in capacity is because of the dynamic layer formations due to zipper effect. It can also be observed that, capacity with buffer space is more compared to that without buffer space.

Table 6.10 Capacity estimation for various bottleneck widths for N = 30

Bottleneck width (meters)	Mean empty zone		Capacity (Pedestrian/meter/second)		Capacity (Pedestrian/lane/second)	
	With buffer space	Without buffer space	With buffer space	Without buffer space	With buffer space	Without buffer space
0.8	0.70	0.79	1.43	1.27	2.86	2.53
1.0	0.61	0.77	1.64	1.30	3.28	2.60
1.2	0.57	0.65	1.75	1.54	3.51	3.08
1.4	0.52	0.64	1.92	1.59	3.85	3.17
1.6	0.51	0.61	1.96	1.64	3.92	3.28

Table 6.11 Capacity estimation for various bottleneck widths for N = 50

Bottleneck width (meters)	Mean empty zone		Capacity (Pedestrian/meter/second)		Capacity (Pedestrian/lane/second)	
	With buffer space	Without buffer space	With buffer space	Without buffer space	With buffer space	Without buffer space
0.8	0.68	0.71	1.47	1.42	2.94	2.84
1.0	0.60	0.65	1.67	1.54	3.33	3.08
1.2	0.58	0.62	1.72	1.61	3.45	3.23
1.4	0.57	0.60	1.75	1.67	3.51	3.33
1.6	0.52	0.56	1.75	1.79	3.85	3.57

6.2.9.1 Comparison of capacities with other studies

The obtained capacities are compared with capacities obtained from different experimental studies done related to pedestrian flows at bottlenecks. Figure 6.52 shows the experimental setup of different studies performed with respect to bottlenecks. In Kretz's experiment, the bottleneck was centered and there was no free space between evacuees and bottleneck. In Nagai experiment, bottleneck was located on the left side of the corridor and there was no free space between evacuees and bottleneck. In Muir experiment, bottleneck was formed due to the movement of evacuees in an airplane, where even the corridor is very small and the bottleneck is formed by the galley units in front of the main embarkation point.

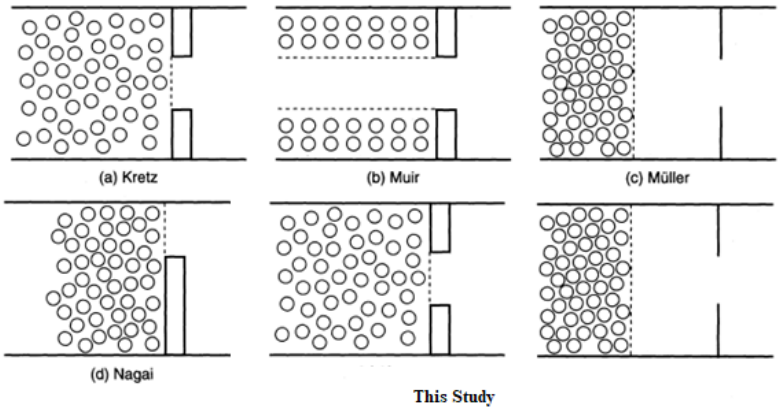

Figure 6.52 Experimental setups

The obtained capacities were compared with capacities from different experimental studies carried out with respect to pedestrian flows at bottlenecks. The Table 6.12 compares the capacities of the present study with previous literature. For the comparison, Kretz and Muller studies were considered because of similarity with this study. Capacities obtained in this study were lower than that of capacities obtained from Kretz and Muller. The reason behind the reduction in capacities was that Kretz and Muller didn't consider the formation of dynamic layers hence the effective utilization of width concept was absent resulting in larger capacities.

Table 6.12 Comparison of capacities of present study with other studies

Width (meter)	Capacity (C)										
	Estimation				Measurement						
	SFPE	PM	WM	HG	Kretz	Nagai	Muller	Present study			
								N = 30		N = 50	
0.8	1.04	1.28	0.98		1.43	2.58		1.43	1.27	1.47	1.42
1.0	1.30	1.60	1.23	0.78	1.85			1.64	1.30	1.67	1.54
1.2	1.56	1.92	1.47	0.78	2.15	3.27	2.75	1.75	1.54	1.72	1.61
1.4	1.95	2.40	1.84	1.56			3.59	1.92	1.59	1.75	1.67
1.6	2.08	2.56	1.96	1.56		3.86		1.96	1.64	1.92	1.79

6.3 Capacity of doors

From the experimental study, total time, time gaps and densities are extracted. Various relations such as time gap versus door width, total times versus door width, flow versus door width were studied. The average time gap of different door widths for different population and with and without buffer space is tabulated in Table 6.13. From the table, it was observed that the average time gap decreased as the width of exit increased. The average time gap observed was more in case of high population (N = 50) compared to low population (N = 30) for single doors. In the case of double doors, it was observed that, evacuees were choosing congested door rather than uncongested due to herding behavior. It was observed that the average time gap values were more in without buffer zone case compared to with buffer zone for both single and double doors.

Table 6.13 Extracted parameters for single and double doors with different population

Doors	N	Door width (cm)	With buffer			Without buffer		
			Avg. time gap (s)	Total time (s)	Flow (p/m/s)	Avg. time gap (s)	Total time (s)	Flow (p/m/s)
Single	30	80	0.584	16.08	1.865	0.634	15.915	1.885
		100	0.573	15.484	1.937	0.627	15.285	1.962
		120	0.569	14.275	2.101	0.618	13.126	2.285
		140	0.549	13.672	2.194	0.609	11.924	2.515

		160	0.496		12.407	2.417	0.596	11.342	2.645
	50	80	0.621		29.836	1.675	0.642	28.02	1.784
		100	0.598		25.118	1.990	0.638	22.297	2.242
		120	0.571		24.162	2.169	0.623	21.192	2.359
		140	0.562		22.115	2.260	0.612	19.296	2.591
		160	0.514		20.232	2.471	0.603	18.871	2.649
Double door	30	100	Door-1	0.749	11.53	1.38	0.803	9.65	1.29
			Door-2	0.577	9.49	1.47	0.683	8.88	1.69
	50	100	Door-1	0.809	16.76	1.78	0.832	16.07	1.74
			Door-2	0.698	10.39	1.92	0.722	10.17	2.16

6.3.1 Total time

The time duration from the first person crossing the reference line to the last person crossing the reference line is called total time. Figure 6.53 shows the variation of total time with door width. It was observed that, the total time decreased as the door width increases for both the compositions with both the cases with and without buffer space. The buffer space effect in the reduction of total time is more in case of 50 persons than in case of 30 persons. Figure 6.54 shows the total time comparison for two doors (door 1 and door 2). From the figure, it was observed that, more number of people chose the congested door (door 1) compared to uncongested door (door 2) due to herding behaviour. Figure 6.55 shows the total time comparison for single door and double doors. From the Figure, it was observed that, people were taking less time to evacuate in the case of double doors compared to single door.

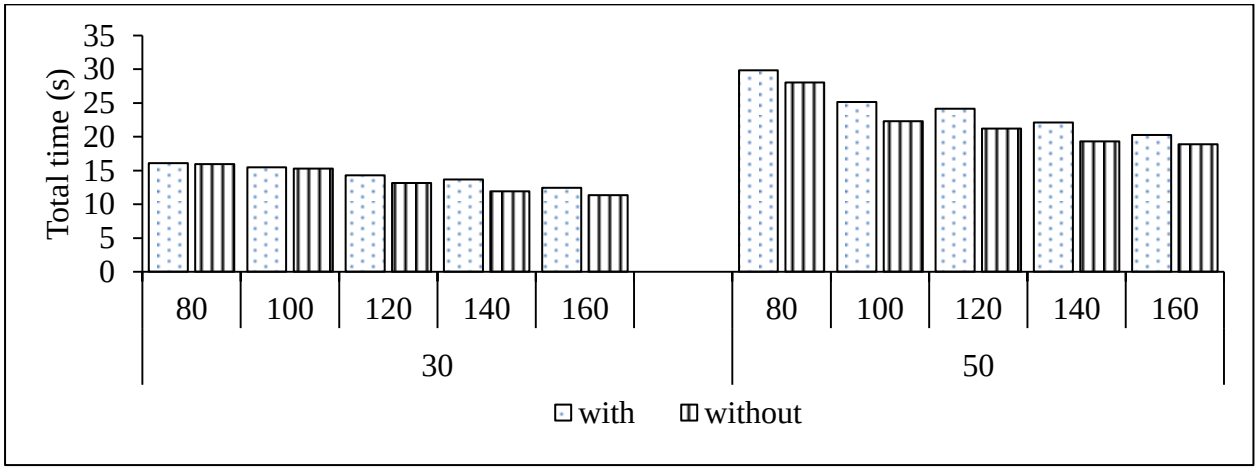

Figure 6.53 Total time vs door widths for different n values (30 and 50)

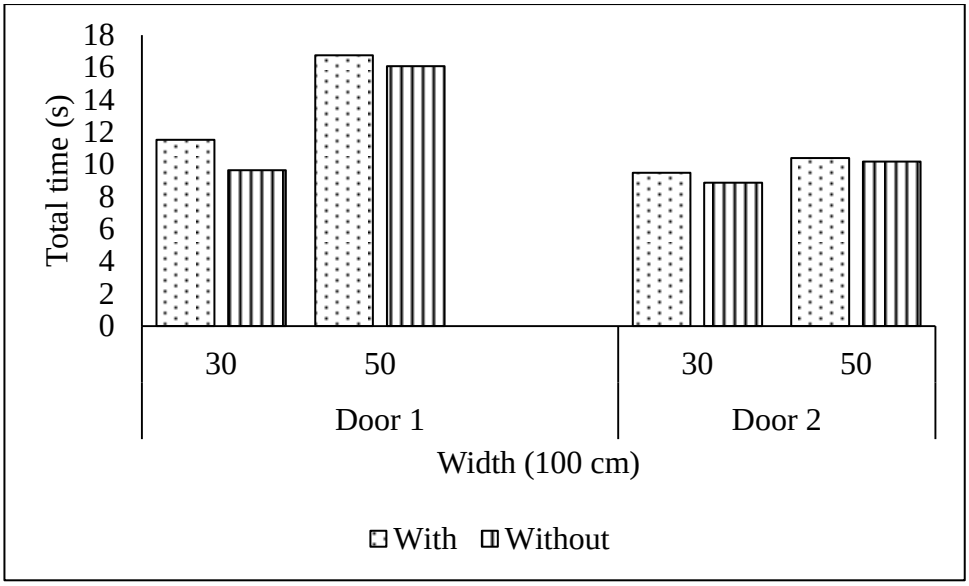

Figure 6.54 Total time comparison for two doors in double door condition

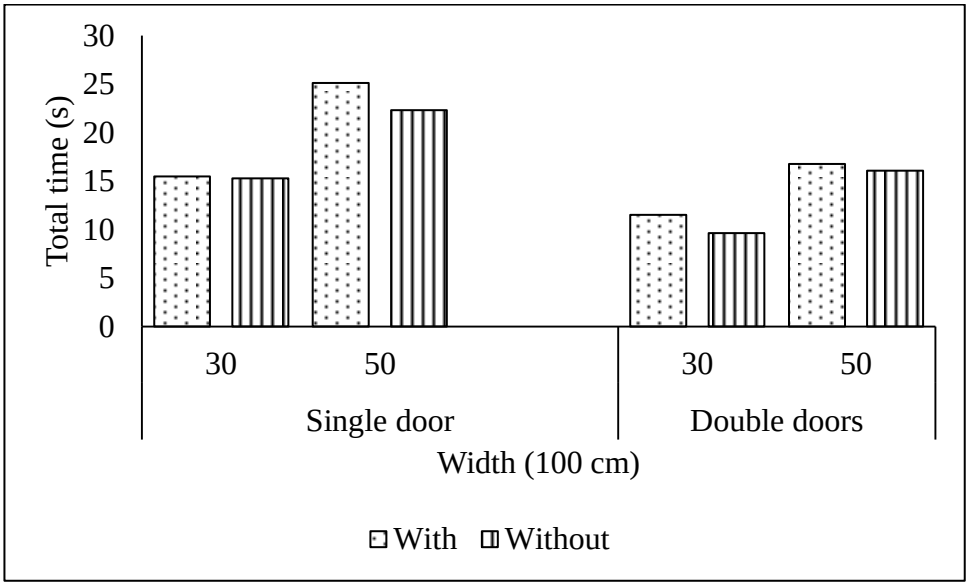

Figure 6.55 Total time vs door type (single and double)

6.3.2 Flow (Q)

The number of persons passing a reference point (exit or door) per unit time is called flow. From Table 6.13, it was observed that, flow increased as the width of the door increased in both the compositions and in both the cases, i.e. with and without buffer space in single and double doors. From Table 6.13, the flow of door-1 was observed to be low compared with door-2 because more number of evacuees chosen door-1 rather than door-2 due to herding behaviour.

6.3.2 Trajectories

Trajectories of different persons for single and double doors for both cases with and without buffer space are shown in Figure 6.56 to 6.59. It can be identified that, lateral occupancy persons are more in the case of without buffer space as compared to those with buffer space for both compositions (N = 30 & 50). Arching phenomena was observed due to clogging of doors in front of the exit door. This appears when a crowd tries to pass through a door in less time with high velocity or gives a chance to oncoming evacuees to pass through the door. From Figures 6.58 and 6.59, it was observed that, more number of people was chosen door-1 due to herding behaviour.

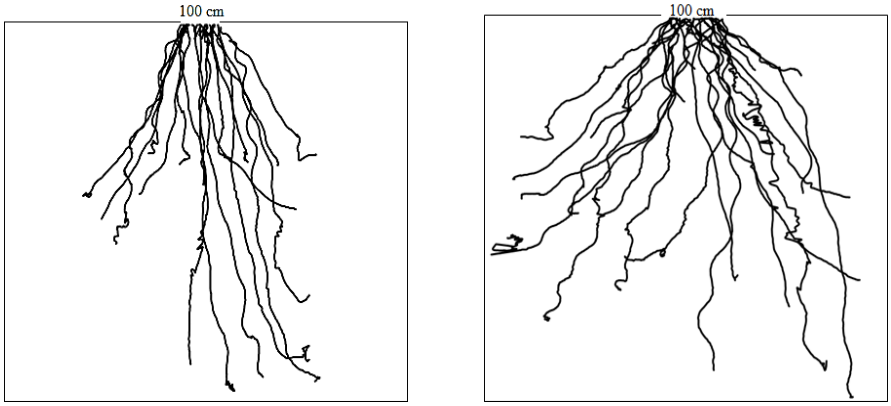

(A) With buffer space (B) Without buffer space

Figure 6.56 Trajectories of persons with N = 30 and width (B) = 100 cm of a single door

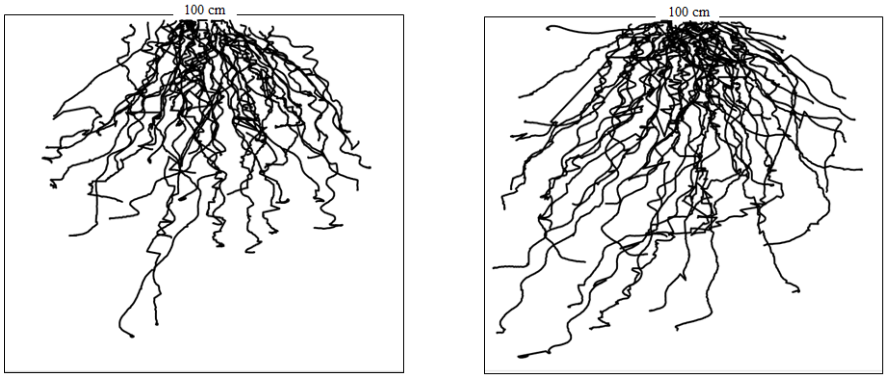

(A) With buffer space (B) Without buffer space

Figure 6.57 Trajectories of persons with N = 50 and width (B) = 100 cm of a single door

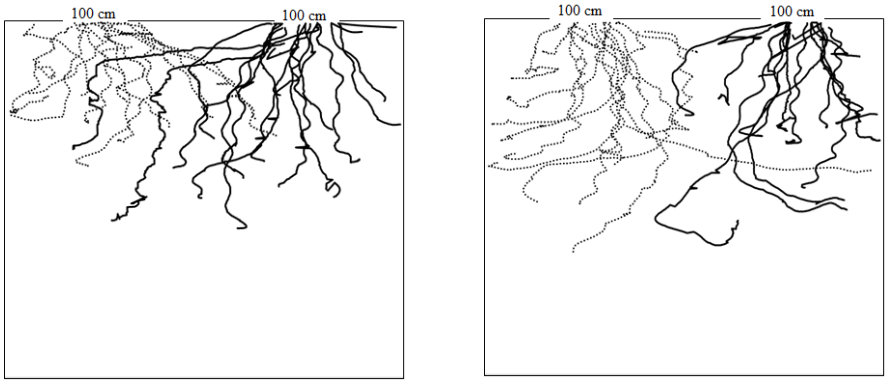

(A) With buffer space (B) Without buffer space

Figure 6.58 Trajectories of persons with N = 50 and width (B) = 100 cm of a double door

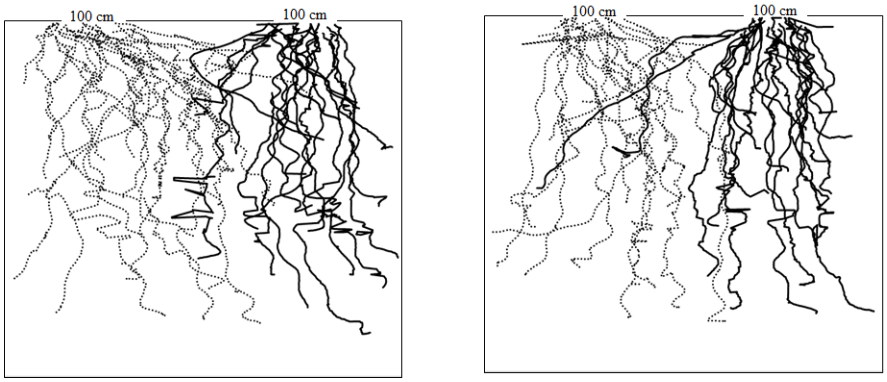

(A) With buffer space (B) Without buffer space

Figure 6.59 Trajectories of persons with N = 50 and width (B) = 100 cm of a double door

6.3.4 Density

The variation of density over the entire area for different door widths considering with and without buffer space has been shown in Figures 6.60 to 6.63. Density values increase as the number of people increases for both the cases with and without buffer space conditions. High densities were observed near the exits openings when the incoming flow exceeds the capacity of the door.

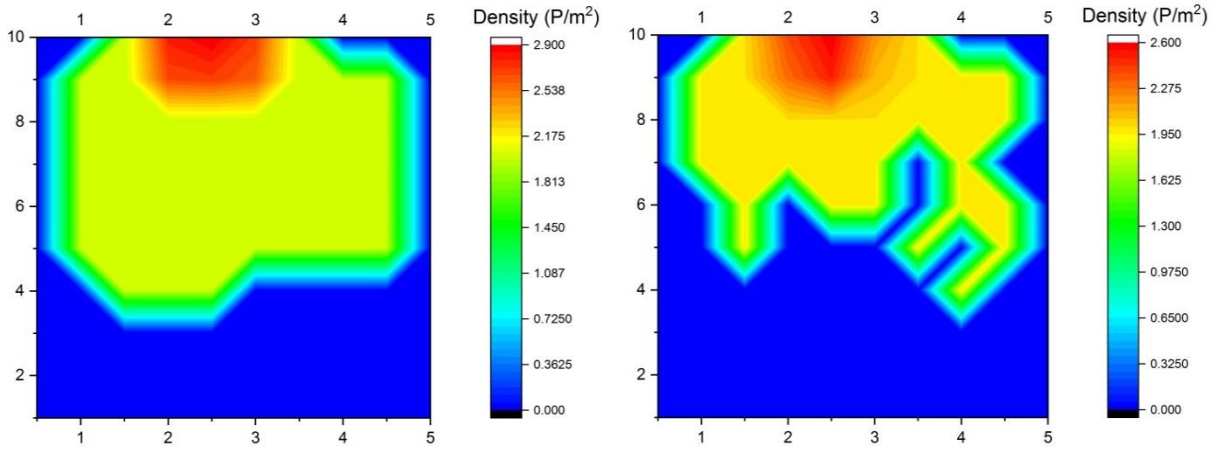

(A) With buffer space (B) Without buffer space

Figure 6.60 Density variations for single door with buffer space (N = 30)

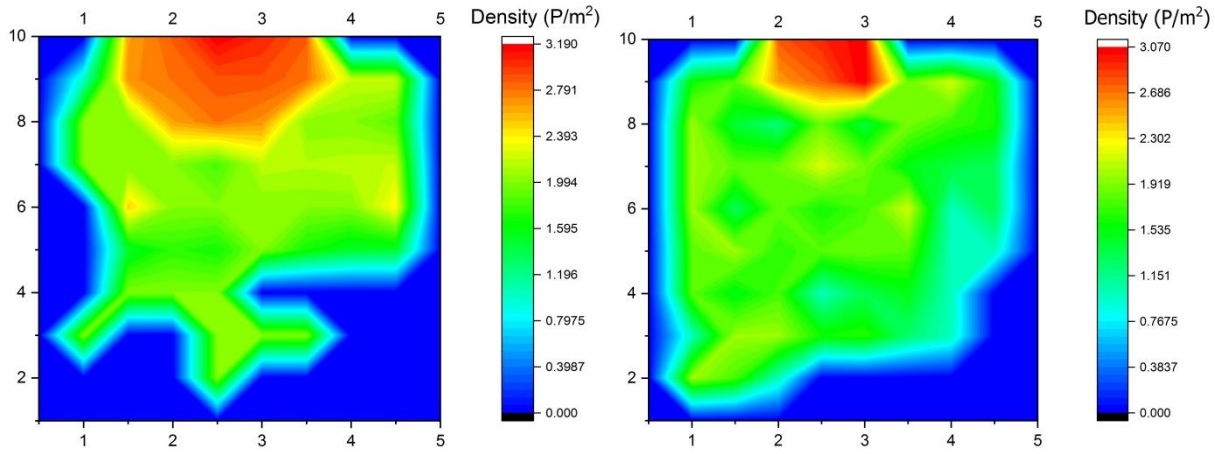

(A) With buffer space (B) Without buffer space

Figure 6.61 Density variations for single door with buffer space (N = 50)

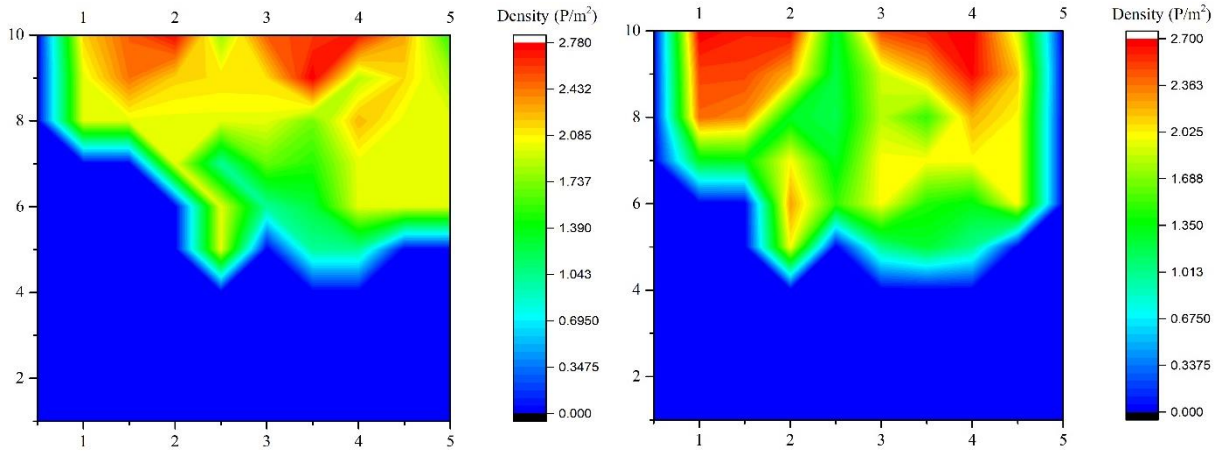

(A) With buffer space (B) Without buffer space

Figure 6.62 Density variations for double doors with buffer space (N = 30)

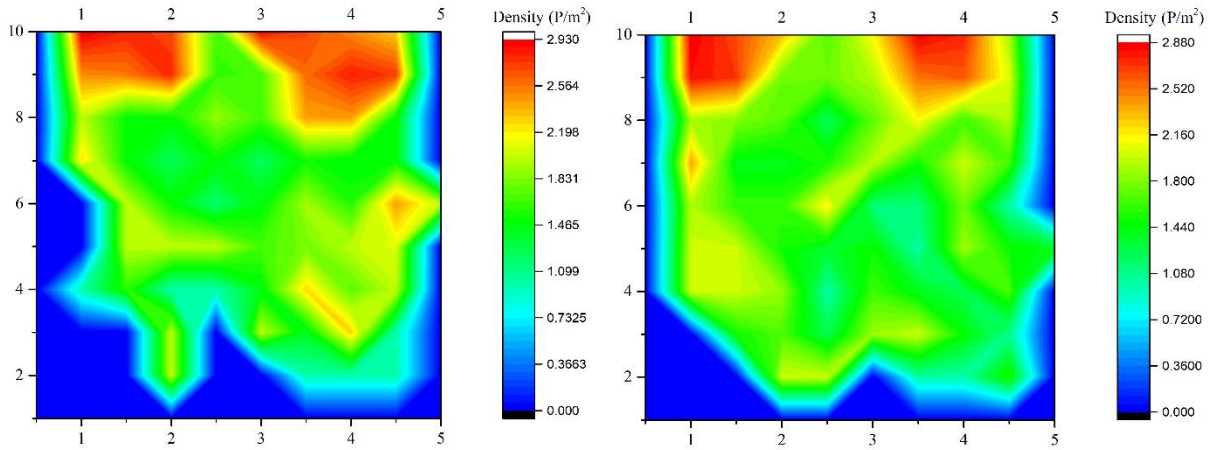

(A) With buffer space (B) Without buffer space

Figure 6.63 Density variations for double doors with buffer space (N = 50)

6.3.5 Door capacity

The observed flow is equal to capacity when congestion occurs. In the present study, for all widths congestion occurred. Figure 6.64 shows the capacity of door for different door widths. The door width has a negative effect, implying that wider doors are less efficiently used and also the capacity observed was low when buffer space was available compared to absence of buffer space. Figure 6.65 shows the capacity for single and double doors. The capacity observed was high in the case of single door compared to double doors.

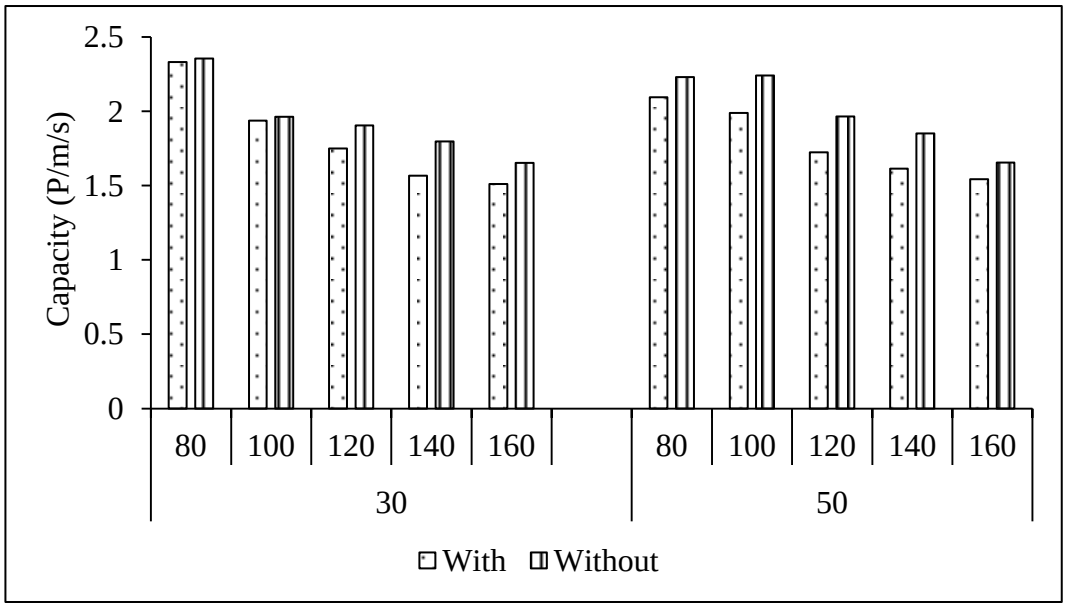

Figure 6.64 Capacity vs door widths

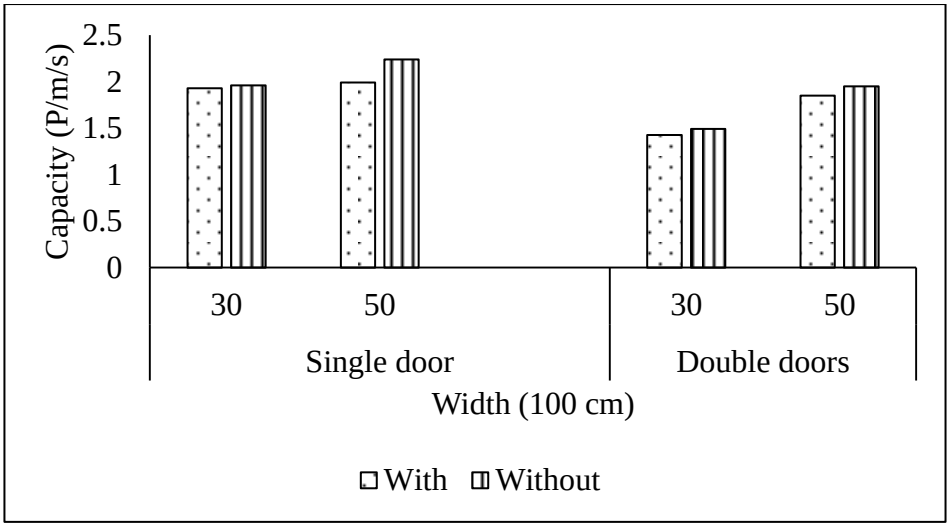

Figure 6.65 Capacity vs door type (single and double)

6.4 Summary

This chapter mainly focussed on analysing the effect of composition and obstacles (bottlenecks) with varying widths on the crowd behaviour. The inclusion of buffer space on crowd dispersion was analysed. Parameters like total time, time gaps, densities and speeds were extracted and analysed in terms of various relations such as total time versus bottleneck width, flow versus bottleneck width and specific flow versus bottleneck width, crowd trajectories, density plots and dynamic layer formations. Total time decreased as the width of the bottleneck increased for both with and without buffer space. The buffer space effect in reduction of total time was more in case of 50 persons than 30 persons. Specific flow was decreasing as the width of bottleneck increased and specific flows were more without buffer space as compared to with buffer space in case where number of persons was fifty. Observations from trajectories have shown a phenomenon called arching, which appears when a crowd with a highly desired velocity tries to pass through a door instead of passing through the door in little time. Five types of distribution were tested to fit a suitable type of distribution for the observed data. From the headway study, it was observed that among the five types of distributions, semi-random distribution is the best fit for the observed headway data. Percentage of free headways and constrained headways can be calculated using semi random distribution. Constrained headways must be less for evacuation of any facility during normal and emergency situations. If the constrained headways were more then evacuation time is more which leads to overcrowding at exits and causes stampedes. Capacities were estimated and comparison of obtained capacities

with other studies has been done. Capacities increase as the width of bottleneck increases because of the dynamic lane formations due to the zipper effect and this increase is stepwise not linear. It can also be observed that, the distance between these lanes is independent of the bottleneck width. Kretz and Muller studies were similar to this study but the only difference is that the formation of dynamic layers has not been considered in their study; which leads to larger capacity prediction. Capacities were estimated for single door and double doors and comparison of capacities for different door widths was done. The capacity is decreasing as the door width increases. Also the capacity observed was less when buffer space was available as compared to absence of buffer space.

7. SUMMARY AND CONCLUSIONS

7.1 Summary

Field data was collected by video-graphic method on different crowded locations. The speed was extracted using TRACKER software and density was measured using foreground detection using background subtraction. Flow was measured using classic equation (Q = K×U). Crowd behavior analysis was studied at microscopic and macroscopic level. In microscopic analysis, factors like gender, age, luggage, density, child carrying, child holding, and group were considered for model development. Statistical analysis was done on crowd speed for the above mentioned factors. Based on statistical results, MLR, ANN, and ANFIS models were developed and compared with field data. In macroscopic analysis, single-regime and multi-regime models were developed for field data. In single-regime concept, Greenshileds model and Underwood model were tested for their fits with observed data. In multi-regime models, K-means clustering was used to calculate the break points. In two regime and three-regime models, four models (L-L, L-E, E-L, and E-E), (L-L-L, E-E-E, E-E-L, and E-L-E) were established respectively. The speed–density relation was modeled using four categories of models and flow–density and speed–flow relations were then established. The Mean Absolute Percentage Error (MAPE) and Root Mean Square Error (RMSE) were used to check the accuracy of model predictions, and the model with the least MAPE and RMSE values was considered to provide the best prediction.

The capacities of corridors were estimated by extracting parameters like total times, time gaps, densities, and speeds. The relationship was established between total times versus bottleneck width, flow versus bottleneck width and specific flow versus bottleneck width. Crowd trajectories, density plots and dynamic layer formations were drawn for different corridor widths. The inclusion of buffer space on crowd dispersion was analysed. Five types of distribution were tested to fit a suitable type of distribution for the observed data. Capacities were estimated and comparison of obtained capacities with other studies was done. The capacities of doors were estimated by extracting the same parameters which was mentioned above and the same same relationships were established. Crowd trajectories and density plots were drawn for different door widths. Capacities were estimated for a single door and double doors and comparison of capacities for different door widths was done. Double doors were provided to observe any herding behavior during the evacuation.

7.2 Conclusions

The conclusions drawn from this study are presented below:

1. In microscopic analysis, the walking speed of male (0.82 m/s) was observed to be more than that of female (0.70 m/s). Also, the speeds of the young were 8.3% and 15.7 % higher compared to those in middle age and the old respectively.
2. The walking speed of people carrying luggage (0.76 m/s) was less compared to people without luggage (0.80 m/s).
3. From statistical tests, it was concluded that gender, age, density and luggage factors significantly affected pedestrian walking behaviour. From the results, it was observed that gender factor had a more significant impact on crowd speed when compared to other factors.
4. At low crowd densities, speed of the crowd was high due to fewer interactions between persons and more space for overtaking. The speed was low at high crowd densities because of more interactions between persons and less space for overtaking.
5. In microscopic analysis, ANFIS model was performing better than MLR and ANN models. This is due to the accurate learning capabilities of neural networks, combined with the simplification and fast learning abilities of fuzzy logic systems.
6. In macroscopic analysis, in **s**ingle-regime model, Greenshiel model was found to be the best compared to Underwood model based on MAPE and RMSE.
7. In two-regime model, among all four models, Model- III (E-L) was best fit model compared to other three models.
8. In three-regime model, among all four models, Model-II (E-E-E was best fit model compared to other three models.
9. In macroscopic analysis, three-regime model was performing better than single and two regime models. In the case of the single-regime and two-regime models, actual field conditions were not effectively represented for the uncongested flow and congested flows and the transition between these two flow regimes.
10. The buffer space effect in reduction of total time is more in the case of 50 persons (10%) than 30 persons (2%) due to overtaking. The overtaking phenomena was observed to be more in the case of 50 persons compared to 30 persons.
11. In terms of capacity in bottleneck analysis, total time was found yo as the width of the bottleneck was increasing for both the cases: with and without buffer space. Specific flow was observed to decrease as the width of the bottleneck increased. Also, specific

flows were found to be more without buffer space, compared to with buffer space in case of fifty persons.

12. Semi-random distribution is the best fit for the observed data due to the consideration of both constrained and free headways whereas in other distributions, either free or constrained headways were considered.
13. Capacities of bottlenecks were observed to be increasing as the width of bottleneck increases because of dynamic lane formations due to the zipper effect and this increase is in a stepwise manner, but not a linear increase.
14. It was observed that when a crowd with a highly desired velocity tries to pass through a door, higher densities are observed at the exit doors leading to arching phenomena. This phenomenon results in stampedes in the case of emergency situations.
15. In capacity of doors analysis, average time gaps and total times are decreasing as the width of the door increased for both the cases with and without buffer space. Also, as the number of persons increased from 30 to 50, the total time also increases in single and double doors.
16. In the case of double doors, it was observed that evacuees chose congested door rather than uncongested due to the herding behavior.

7.3 Contributions

1. Crowd control should be managed by controlling the crowd at entry, regulating the crowd at venue and crowd control at exits. Inflow was calculated based on historical numbers, crowd arrival patterns, type of visitors, etc.
2. Microscopic analysis of crowd behavior would be useful for regulating the crowd at venue to segment visitors by personality, age, special needs etc.
3. Macroscopic analysis of crowd behavior will be helpful in understanding the phases of transformation from uncongested to congested flow.
4. The capacity of a facility is equal to the maximum flow rate. Results of the capacity analysis of bottlenecks are useful in crowd control at exits of the facility.

7.4 Limitations of the study

1. Crowd behavior was analyzed in the form of speed only.
2. This study was limited to normal crowd behavior only.
3. This study was limited to one directional flow (bottlenecks, doors, stairways)

7.5 Scope for further research

1. Abnormal crowd behavior can be analyzed using deep learning algorithms.
2. Cross flows and bi- directional flows can be studied.

REFERENCES

1. Aghabayk, K., Ejtemai, O., Sarvi, M. and Sobhani, A. (2014). "Understanding pedestrian crowd merging behavior". *The Conference on Pedestrian and Evacuation Dynamics, Transportation Research Procedia*, 768 – 773.
2. Aldhaheri, A.R. and Edirisinghe, E.A. (2014). "Detection and Classification of a Moving Object in a Video Stream". *In Proceedings of the International Conference on Advances in Computing and Information Technology*.
3. Alex, S. and Isaac, K.P. (2017). "Development of Delay Models Using Simulation in a Heterogeneous Traffic Condition". *International Journal for Traffic & Transport Engineering*, 7 (1), 52-67.
4. Ali, S. and Shah, M. (2007). "A lagrangian particle dynamics approach for crowd flow segmentation and stability analysis". *In Proceedings of IEEE Conference on Computer Vision and Pattern Recognition*, 1–6.
5. Ali, S.S. and Zafar, M.F. (2009). "A robust adaptive method for detection and tracking of moving objects". *In International Conference on Emerging Technologies*, 262-266.
6. Andrade, E.L., Blunsden, S. and Fisher, R.B. (2006). "Modelling crowd scenes for event detection". *In Proceedings of International Conference on Pattern Recognition*, 175–178.
7. Annunziato, M., Bertini, I., Pannicelli, A. and Pizzuti, S. (2003). "Evolutionary Feed-Forward Neural Networks for Traffic Prediction". *International Congress on Evolutionary Methods for Design, Optimization and Control with Applications to Industrial Problems*.
8. Ardekani, S., Ghandehari, M. and Nepal, S. (2011). "Macroscopic speed-flow models for characterization of freeway and managed lanes". *Institutul Politehnic din Iasi. Buletinul. Sectia Constructii. Arhitectura*, 57.
9. Arora, J.K. and Mosahari, P.V. (2012). "Artificial Neural Network Modelling of Traffic Noise in Agra-Firozabad Highway". *International Journal of Computer Applications*, 56 (2).
10. Askerzade, I.N. and Mahmud, M. (2011). "Design and Implementation of Group Traffic Control System using Fuzzy Logic". *IJRRAS*, 6 (2).

11. Aslani, A. and Mahdavi-Nasab, H. (2013). “Optical Flow Based Moving Object Detection and Tracking for Traffic Surveillance”. *International Journal of Electrical, Computer, Energetic, Electronic and Communication Engineering*, 7 (9).
12. Avidan, S (2004). “Support Vector Tracking”. *IEEE Transactions on Pattern Analysis and machine intelligence*, 26 (8), 1064-1072.
13. Azari, M., Seyfi, A. and Rezaie, A.H. (2011). “Real Time Multiple Object Tracking and Occlusion Reasoning Using Adaptive Kalman Filters”. *Machine Vision and Image Processing*, 1-5.
14. Bahadur, K. (2010). “Review and Evaluation of well-known methods for moving object detection and tracking in videos”. *Journal of Aeronautics and Space Technologies*, 4 (4), 11-22.
15. Bao, H., Wang, B., Yang, S. and Lou, H. (2013). “Crowd Density Estimation Based on Texture Feature Extraction”. *In journal of multimedia*, 8 (4).
16. BenAbdelkader, C., Cutler, R., Nanda, H. and Davis, L. (2001). “Eigen Gait: motion-based recognition of people using image self-similarity”. *In Audio- and Video-Based Biometric Person Authentication, Third International Conference*, 2091, 312–317.
17. Berlonghi, A. (1995). “Understanding and planning for different spectator crowds”. *Safety Science*, 18, 239-247.
18. Bertalmio, M., Sapiro, G. and Randall, G. (2000). “Morphing active contours." *IEEE Trans. on Pattern Analysis and Machine Intelligence*, 22(7), 733-737.
19. Blackman, S.S. (2004). “Multiple Hypothesis Tracking for Multiple Target Tracking”. *IEEE Aerospace and Electronic Systems Magazine*, 19 (1), 5-18.
20. Blackman, S.S. (2004). “Multiple Hypothesis Tracking for Multiple Target Tracking”. *IEEE A&E Systems magazine*, 19 (1), 5-18.
21. Brostow, G.J. and Cipolla, R. (2006). “Unsupervised Bayesian detection of independent motion in crowds”. *In Proceedings of IEEE Conference on Computer Vision and Pattern Recognition, Washington*, 594–601.
22. Buckley, D.J. (1968). “A semi-Poisson model of traffic flow”. *Transportation Science*, 2(2), 107-132.
23. Candamo, J., Shreve, M., Goldgof, D.B., Sapper, D.B. and Kasturi, R. (2010). “Understanding transit scenes: A survey on human behavior-recognition algorithms”. *IEEE Transactions on Intelligent Transportation* Systems, 11(1), 206–224.

24. Candamo, J., Shreve, M., Goldgof, D.B., Sapper, D.B. and Kasturi, R. (2010). "Understanding transit scenes: A survey on human behavior-recognition algorithms". *IEEE Transactions on Intelligent Transportation Systems*, 11(1), 206–224.
25. Cao, S., Zhang, J., Salden, D., Ma, J., Shi, C. and Zhang, R. (2016). "Pedestrian dynamics in single-file movement of crowd with different age compositions". *Physical Review E - Statistical, Nonlinear, and Soft Matter Physics*, 94 (1).
26. Ceder, A. and May, A.D. (1990). "Further Evaluation of Single- and Two-Regime Traffic Flow Models". *54th Annual Meeting of the Transportation Research Board, Transportation Research Record*.
27. Chattaraj, U., Seyfried, A. and Chakroborty, P. (2009). "Comparison of Pedestrian Fundamental Diagram Across Cultures". Advances in Complex Systems, 12 (03), 393-405.
28. Chen, S., Zhang, J., Li, Y. and Zhang, J. (2012). "A hierarchical model incorporating segmented regions and pixel descriptors for video background subtraction". *IEEE Transactions on Industrial Informatics*, 8(1), 118–127.
29. Chen, Y.T., Chu-Song, C., Chun-Rong, H. and Yi-Ping, H. (2007). "Efficient hierarchical method for background subtraction". *Pattern Recognition*, 40, 2706–2715.
30. Cheng, F.C., Huang, S.C. and Ruan, S.J. (2011). "Scene analysis for object detection in advanced surveillance systems using Laplacian distribution model". *IEEE Transactions on Systems, Man, and Cybernetics, Part C (Applications and Reviews)*. 41(5), 589–598.
31. Cheriyadat, A.M. and Radke, R. (2008). "Detecting dominant motions in dense crowds". *In IEEE Journal of Selected Topics in Signal Processing*, 2 (4), 568–581.
32. Chraibi, M. and Seyfried, A. (2010). "Generalized Centrifugal Force Model for Pedestrian Dynamics". *Physical Review E - Statistical, Nonlinear, and Soft Matter Physics*, 82, 4(2).
33. Comaniciu, D. and Meer, P. (2002). "Mean Shift: A robust approach toward feature space analysis". *IEEE Transactions on Pattern Analysis and Machine Intelligence*, 24 (5).
34. Daamen, W. and Hoogendoorn, S. (2010). "Capacity of Doors during Evacuation Conditions". *Procedia Engineering*, 3, 53–66.
35. Daamen, W. and Hoogendoorn, S.P. (2006). "Free speed distributions for pedestrian traffic". *TRB-Annual Meeting, Washington*.

36. Davies, A.C., Yin, J.H. and Velastin, S.A. (1995). “Crowd monitoring using image processing”. *IEE Electronics and Communication Engineering Journal*, 7(1), 37–47.
37. Dias, C., Ejtemai, O., Sarvi, M. and Nirajan, S. (2014). “Pedestrian Walking Characteristics through Angled Corridors: An Experimental Study”. *Transportation Research Record: Journal of the Transportation Research Board*, 41–50.
38. Dias, C., Sarvi, M., Nirajan, S. and Burd, M. (2012). “Turning Angle Effect on Emergency Egress Experimental Evidence and Pedestrian Crowd Simulation”. *Transportation Research Record: Journal of the Transportation Research Board*, 2012, 120–127.
39. Doğan, E., Akgüngör, A.P. and Arslan, T. (2016). “Estimation of Delay and Vehicle Stops at Signalized Intersections using Artificial Neural Network”. *Engineering Review*, 36 (2), 157-165.
40. Dollár, P., Rabaud, V., Cottrell, G. and Belongie, S. (2005). “Behavior recognition via sparse spatio-temporal features”. *In 2nd IEEE Joint International Workshop Visual Surveillance and Performance Evaluation of Tracking Surveillance*, 65–72.
41. Dominguez-Sanchez, A., Cazorla, M. and Orts-Escolano, S. (2017). “Pedestrian Movement Direction Recognition Using Convolutional Neural Networks”. *IEEE Transactions on Intelligent Transportation Systems*, 18 (12).
42. Dougherty, M,S., Kirby, H,R. and Boyle, R.D. (1993). “The use of neural networks to recognise and predict traffic congestion”. *Traffic engineering & control*, 34 (6).
43. Drake, J., Schofer, J. and May, A. (1967). “A Statistical Analysis of speed-density Hypotheses”. *In Vehicular Traffic Science. Proceedings of the Third International Symposium on the Theory of Traffic Flow*, 1967.
44. Drake, J., Schofer, J. and May, A. (1967). “A statistical analysis of speed–density hypotheses in vehicular traffic science”. *In Proceedings of the 3rd International Symposium on the Theory of Traffic Flow, 45th Annual Meeting. Highway Research Board, Washington, DC, USA*, 154, 53–87.
45. Duives, D.C. and Mahmassani, H.S. (2012). “Exit Choice Decisions during Pedestrian Evacuations of Buildings”. *Transportation Research Record: Journal of the Transportation Research Board*, 84–94.
46. Edie, L.C. (1961). “Car following and steady state theory for non-congested traffic”. *Operations Research*, 9(1), 66–76.
47. Efros, A., Berg, A., Mori, G. and Malik, J. (2003). “Recognizing action at a distance”. *In Ninth IEEE International Conference on Computer Vision*, 726–733.

48. Efros, A., Berg, A., Mori, G. and Malik, J. (2003). "Recognizing action at a distance". *In Ninth IEEE International Conference on Computer Vision*, 726–733.
49. El Sherief, M.M., Ramadan, I.M.I. and Ibrahim, A.M. (2016). "Development of traffic stream characteristics models for intercity roads in Egypt". *Alexandria Engineering Journal*, 55, 2765–2770.
50. Elgammal, A., Harwood, D. and Davis, L. (2000). "Non-parametric model for background subtraction". *In 6th European Conference on Computer Vision - Part II*, 751–767.
51. Florio L, and Mussone, L. (1996). "Neural-network models for classification and forecasting of freeway traffic flow stability". *Control Engineering Practice*, 4(2), 153–164.
52. Fouladgar, M., Parchami, M., Elmasriy, R. and Ghaderi, A. (2017). "Scalable Deep Traffic Flow Neural Networks for Urban Traffic Congestion Prediction". *International Joint Conference on Neural Networks*.
53. Fruin, J.J. (1970). "Pedestrian planning and design": A Level of Service Concept.
54. Gopala Krishna, M.T., Ravishankar, M. and Ramesh Babu, D.R. (2011). "Automatic Detection and Tracking of Moving Objects in Complex Environments for Video Surveillance Applications". *In 3rd international conference on Electronics Computer Technology*, 1, 234-239.
55. Greenshields, B.D. (1935). "A study of highway capacity". *In Proceedings of the Highway Research Board. Highway Research Board, Washington, DC, USA*, 14, 448–477.
56. Han, B., Comaniciu, D. and Davis, L. (2004). "Sequential kernel density approximation through mode propagation: Applications to background modeling". *In Asian Conference on Computer Vision*.
57. Heikkilä, M. and Pietäikinen, M. (2006). "A texture-based method for modeling the background and detecting moving objects". *IEEE Transactions on Pattern Analysis and Machine Intelligence*. 28, 657–662.
58. Hoogendoorn, P.S. and Daamen, W. (2005). "Pedestrian Behavior at Bottlenecks". *Journal of Transportation Science*, 39 (2), 147-159.
59. Hoogendoorn, S.P., Daamen, W. and Bovy, P.H.L. (2003). "Microscopic pedestrian traffic data collection and analysis by walking experiments: Behaviour at bottlenecks". *E. R. Galea, ed. Pedestrian and Evacuation Dynamics*, 89-100.

60. Huttenlocher, D.P., Noh, J.J. and Rucklidge, W.J. (1993). “Tracking non-rigid objects in complex scenes”. *In ICCV*, 93–101.
61. Isard, M. and Blake, A. (1998). “CONDENSATION - conditional density propagation for visual tracking". *International Journal of Computer Vision*, 29(1), 5-28.
62. Jabri, S., Duric, Z., Wechsler, H. and Rosenfeld, A. (2000). “Detection and location of people in video images using adaptive fusion of color and edge information”. *In 15th International Conference on Pattern Recognition*, 627–630.
63. Jacobs, H. (1967). “To count a crowd”. *Columbia Journalism Review*, 6, 36–40.
64. Jacques Jr., J.C., Braun, A., Soldera, J., Musse, S.R. and Jung, C.R. (2007). “Understanding people motion in video sequences using Voronoi diagrams”. *Pattern Analysis & Applications*, 10 (4), 321-332.
65. Jang, J.S.R. (1992). “Self-learning fuzzy controllers based on temporal backpropagation”. *IEEE Transactions on Neural Networks*, 3 (5), 714–723.
66. Jeon, H., Jeong, J., Bang, J. and Hwang, C. (2008). “The efficient features for tracking”. *In 20th IEEE International Conference on Tools with Artificial Intelligence*, 241–244.
67. Jiang, M., Huang, J., Wang, X., Tang, J. and Wu, C. (2014). “An Approach for Crowd Density and Crowd Size Estimation”. *In journal of software*, 9 (3).
68. Jo, A., Sano, T. and Ohmiya, Y.I.Y. (2014). “Analysis of crowd flow capacity through a door connected to a crowded corridor”. *Transportation Research Procedia*, 2, 10 – 18.
69. Joshan, J., Athanesious, and Suresh, P. (2012). “Systematic Survey on Object Tracking Methods in Video”. *International Journal of Advanced Research in Computer Engineering & Technology*, 1(8), 242-247.
70. Kale, A., Rajagopalan, A., Cuntoor, N. and Kruger, V. (2002). “Gait-based recognition of humans using continuous HMMs”. *In 5th IEEE International Conference on Automatic Face and Gesture Recognition*, 336–341.
71. Kim, H.B. and and Sim, K.B. (2010). “A Particular Object Tracking in an Environment of Multiple Moving Objects”. *IEEE International Conference on Control, Automation and Systems*.
72. Kim, H.B. and Sim, K.B. (2010). “A Particular Object Tracking in an Environment of Multiple Moving Objects”. *IEEE International Conference on Control, Automation and Systems*.

73. Kim, H.B. and Sim, K.B. (2010). "A Particular Object Tracking in an Environment of Multiple Moving Objects". *IEEE International Conference on Control, Automation and Systems*.
74. Kim, K., Chalidabhongse, T.H., Harwood, D. and Davis, L. (2005). "Real-time foreground–background segmentation using codebook model". *Real-time Imaging*, 11(3), 172–185.
75. Kim, W. and Kim, C. (2012). "Background subtraction for dynamic texture scenes using fuzzy color histograms". *IEEE Signal Processing Letters*, 19(3), 127–130.
76. Ko, T., Soatto, S. and Estrin, D. (2010). "Warping background subtraction". *In IEEE Conference on Computer Vision and Pattern Recognition*, 1331–1338.
77. Kratz, L. and Nishino, K. (2009). "Anomaly detection in extremely crowded scenes using spatio-temporal motion pattern models". *In Proceedings of IEEE Conference on Computer Vision and Pattern Recognition*, 1446–1453.
78. Krbálek, M., Hrabák, P. and Bukáček, M. (2018). "Pedestrian headways - Reflection of territorial social forces". *Physica A*, 490, 38–49.
79. Kretz, T., Grunebohm, A. and Schreckenberg, M. (2006). "Experimental study of pedestrian flow through a bottleneck". *Journal of Statistical Mechanics Theory and Experiment*, 10.
80. Kumar, K., Parida, M. and Katiyar, V.K. (2013). "Short term traffic flow prediction in heterogeneous condition using artificial neural network". *Transport*, 1–9.
81. Kumar, K., Parida, M. and Katiyar, V.K. (2015). "Short Term Traffic Flow Prediction in Heterogeneous Condition using Artificial Neural Network". *Transport*, 30(4), 397–405.
82. Kumar, M., Sarkar, P. and Madhu, E. (2013). "Development of Fuzzy Logic Based Mode Choice Model Considering Various Public Transport Policy Options". *International Journal for Traffic and Transport Engineering*, 3 (4), 408-425.
83. Lam, W.H., Morrall, J.F. and Ho, H. (1995). "Pedestrian flow characteristics in Hong Kong". *Transportation Research Record*, 56-62.
84. Lanza, A. (2011). "Background subtraction by non-parametric probabilistic clustering". *In 8th IEEE International Conference on Advanced Video and Signal-Based Surveillance*, 243–248.
85. Laxman, K.K., Rastogi, R. and Chandra, S. (2010). "Pedestrian flow characteristics in mixed traffic conditions". *Journal of Urban Planning and Development*, 136, 23-33.

86. Lee, D.S. (2005). “Effective Gaussian mixture learning for video background subtraction”. *IEEE Transactions on Pattern Analysis and Machine Intelligence*. 27(5), 827–835.
87. Lee, D.S. (2005). “Effective Gaussian mixture learning for video background subtraction”. *IEEE Transactions on Pattern Analysis and Machine Intelligence*. 27(5), 827–835.
88. Lee, D.S. (2005). “Effective Gaussian mixture learning for video background subtraction”. *IEEE Transactions on Pattern Analysis and Machine Intelligence*. 27(5), 827–835.
89. Lee, Y. (2005). “Pedestrian Walking and Choice Behaviour on Stairways and Escalators in Public”. *Delft University of Technology*.
90. Li, L., Huang, W., Gu, I.H. and Tian, Q. (2004). “Statistical modeling of complex backgrounds for foreground object detection”. *IEEE Transactions on Image Processing*, 13, 1459–1472.
91. Li, X., Wang, K., Wang, W. et al, (2010). “A multiple object tracking method using Kalman filter”. *IEEE International Conference on Information and Automation*, 1862-1866.
92. Liang, W. and Qin, W.J.L. (2007). “Study on Moving Object Tracking Algorithm in Video Images”. *IEEE Conference on Electronic Measurement and Instruments*, 810-816.
93. Liddle, J., Seyfried, A., Klingsch, W., Rupprecht, T., Schadschneider, A. and Winkens, A. (2009). “An experimental study of pedestrian congestions: Influence of bottleneck width and length”. *In Traffic and Granular Flow*.
94. Liddle, J., Seyfried, A., Steffen, B., Klingsch, W., Rupprecht, T., Winkens, A. and Boltes, M. (2011). “Microscopic insights into pedestrian motion through a bottleneck, resolving spatial and temporal variations”. *arXiv:1105.1532*.
95. Lin, H.H., Liu, T.L. and Chuang, J.H. (2009). “Learning a scene background model via classification”. *IEEE Transactions on Signal Processing*. 57(5), 1641–1654.
96. Lipton, A.J., Fujiyoshi, H. and Patil, R.S. (1998). “Moving target classification and tracking from real-time video”. *In Fourth IEEE Workshop on Applications of Computer Vision*, 8–14.
97. Lovreglio, R., Fonzone, A., dell’Olio, L. and Borri, D. (2016). “A study of herding behaviour in exit choice during emergencies based on random utility theory”. *Safety Science*, 82, 421–431.

98. Lovreglio, Ra., Fonzone, A., dell'Olio, L., Borri, D. and Ibeas, A. (2014). "The Role of Herding Behaviour in Exit Choice during Evacuation". *Procedia - Social and Behavioral Sciences*, 160, 390 – 399.
99. Manisha, C., Amudha, S. and Vinaya, G. (2012). "Object Detection and tracking in Video Sequences", *ACEEE International Journal on Signal & Image Processing*, 3 (1).
100. Marana, A., da Costa, L., Lotufo, R. and Velastin, S. (1998). "On the efficacy of texture analysis for crowd monitoring". *International Symposium on Computer Graphics, Image Processing, and Vision, Washington*, 354.
101. Masip, S.C. (2015). "On the use of Convolutional Neural Networks for Pedestrian Detection". *Escola d'Enginyeria (UAB)*.
102. May, A. and Harmut, E. (1967). "Non-integer car-following models". *Highway Research Record*.
103. May, A.D. (1990). "Traffic Flow Fundamentals". *Prentice Hall, Englewood Cliffs, NJ, USA.*
104. Meynberg, O., Cui, S. and Reinartz, P. (2016). "Detection of High-Density Crowds in Aerial Images Using Texture Classification". *In Remote Sensing*, 8, 470.
105. Mohan, A.S. and Resmi, R. (2014). "Video Image Processing for Moving Object Detection and Segmentation using Background Subtraction". *IEEE International Conference on Computational Systems and Communications*, 1 (1), 288-292.
106. Moinuddin, M.M., Faheem, M. and Aquil, M.M. (2017). "Speed, Flow and Headway Modeling of Urban Mixed Traffic Condition". *International Journal of Engineering Research and Industrial Applications*, 10 (2), 35-42.
107. Mondal, S. and Gupta, A. (2019). "Assessment of vehicles headway during queue dissipation at signal-controlled intersection under mixed traffic". *Current Science*, 116 (3).
108. Moridpour, S. (2014). "Evaluating the Time Headway Distributions in Congested Highways". *Journal of Traffic and Logistics Engineering*, 2 (3).
109. Murat, Y.S. and Baskan, O. (2006). "Modelling vehicle delays at signalized junctions: artificial neural networks approach". *Journal of scientific and industrial research*, 65(7), 558–564.
110. Murat, Y.S. and Uludag, N. (2008). "Route choice modeling in urban transportation networks using fuzzy logic logistic regression methods". *Journal of scientific & industrial research*, 67, 19-27.

111. Musse, S.R. and Thalmann, D. (1997). "A Model of Human Crowd Behaviour: Group Inter Relationship and Collision Detection Analysis". *In Computer Animation and Simulations 97, Proceedings of Euro graphics workshop, Budapest, Springer Verlag, Wien*, pp. 39-51.
112. Nagai, R., Fukamachi, M. and Nagatani, T. (2006). "Evacuation of crawlers and walkers from corridor through an exit". *Physica A*, 367, 449-460.
113. Ng, C.B., Tay, Y.H. and Goi, B.M. (2013). "A Convolutional Neural Network for Pedestrian Gender Recognition". *Advances in Neural Networks*, 558-564.
114. Nicolas, A., Bouzat, S. and Kuperman, M.N. (2017). "Pedestrian flows through a narrow doorway: effect of individual behaviours on the global flow and microscopic dynamics". *Transportation Research Part B: Methodological Volume*, 99, 30-43.
115. Nirajan, S., Sarvi, M., Rose, G. and Burd, M. (2011). "Consequence of Turning Movements in Pedestrian Crowds during Emergency Egress". *Transportation Research Record: Journal of the Transportation Research Board*, 97–104.
116. Niyogi, S.A. and Adelson, E.H. (1994). "Analyzing and recognizing walking figures in XYT". *In IEEE Computer Society Conference on Computer Vision and Pattern Recognition*, 469–474.
117. Okuma, K., Taleghani, A., Freitas, N.D. et al. (2004). "A boosted particle filter: Multi target detection and tracking". *Computer Vision*, 28-39.
118. Ouyang, C.S. and Lee, S.J (2000). "A Hybrid Algorithm for Structure Identification of Neuro-Fuzzy Modeling". *IEEE International Conference on Systems, Man, and Cybernetics*, 5.
119. Pappis, C.P. and Mamdani, E.H. (1977). "A fuzzy logic controller for a traffic junction". *IEEE Transactions on Systems, Man and Cybernetics*, 707–717.
120. Piroddi, R. and Vlachos, T. (2006). "A simple framework for spatio-temporal video segmentation and delayering using dense motion fields". *IEEE Signal Processing Letters*. 13(7), 421.
121. Polus, A., Schofer, J. L. and Ushpiz, A. (1983). "Pedestrian flow and level of service". *Journal of Transportation Engineering*, 109, 46-56.
122. Pomares, H., Rojas, I., González, J. and Prieto, A. (2002). "Structure Identification in Complete Rule-Based Fuzzy Systems". *IEEE Transactions on Fuzzy Systems*, 10 (3).
123. Prahara, E. and Prasetya, R.A. (2018). "Speed–volume relationship and headway distribution analysis of motorcycle (case study: Teuku Nyak Arief Road)". *The 4th*

International Seminar on Sustainable Urban Development, Earth and Environmental Science, 106.

124. Quan, S., Zhixing, T. and Songchen, H. (2013). "Hierarchical Code Book for background subtraction in MRF*". Infrared Physics & Technology*, 61, 259–264.
125. Rabaud, V. and Belongie, S. (2006). "Counting crowded moving objects". *In Proceedings of IEEE Conference on Computer Vision and Pattern Recognition*, 705–711.
126. Rahmalan, H., Nixon, M. and Carter, J. (2006). "On crowd density estimation for surveillance". *In Proceedings of Institution of Engineering and Technology Conference on Crime and Security*, 540–545.
127. Rahman, K., Ghani, N.A., Kamil, A.A. and Mustafa, A. (2013). "Weighted Regression Method for the Study of Pedestrian Flow Characteristics in Dhaka, Bangladesh". *Modern Applied Science*, 7, 17-29.
128. Rastogi, R., Ilango, T. and Chandra, S. (2013). "Pedestrian flow characteristics for different pedestrian facilities and situations". *European Transport / Trasporti Europei*, 53
129. Ren, L. and Qu, X. (2015). "Impact Analysis of Headway Distribution on Single Lane Roundabout Entry Capacity". *The 6th International Conference on Engineering, Project, and Production Management*.
130. Ridder, C., Munkelt, O. and Kirchner, H. (1995). "Adaptive Background Estimation and Foreground Detection Using Kalman-Filtering". *Proceedings of International Conference on Recent Advances in Mechatronics*, 193–199.
131. Rojas, I., Pomares, H., Ortega, J. and Prieto, A. (2000). "A self-organized fuzzy system generation from training examples". *IEEE Transactions on Fuzzy Systems*, 8, 23–36.
132. Ronfard, R. (1994). "Region based strategies for active contour models". *International Journal of Computer Vision*, 13(2), 229-251.
133. Roy, R. and Saha, P. (2018). "Headway distribution models of two-lane roads under mixed traffic conditions: a case study from India". *European Transport Research Review*, 10 (3).
134. Saboia, P. and Goldenstein, S. (2012). "Crowd simulation: applying mobile grids to the social force model". *The Visual Computer*, 28(10), 1039–1048.

135. Sadeghpour, M., Sanajou, K. and Öğüt, K.S. (2017). “Determination of Pedestrian Arrival Headway Distribution at Signalized Crosswalks in Istanbul”. *Sigma Journal of Engineering and Natural Sciences*, 8 (4), 325-337.
136. Salvo, G., Amato, G. and Zito, P. (2007). Bus speed estimation by neural networks to improve the automatic fleet management, *European Transport \ Trasporti Europei*, 37, 93-104.
137. Saravanakumar, S., Vadivel, A. and Saneem Ahmed, C.G. (2010). "Multiple human object tracking using background subtraction and shadow removal techniques". *International Conference on Signal and Image Processing*, 79-84.
138. Särkkä, S., Vehtari, A. and Lampinen, J. (2007). "Rao - Blackwellized Particle Filter for Multiple Target Tracking". *Information Fusion*, 8 (1), 2-15.
139. Sato, K. and Aggarwal, J.K. (2004). “Temporal spatio-velocity transform and its application to tracking and interaction”. *Computer Vision and Image Understanding*, 96, 100–128.
140. Sayers, T. (1997). “Fuzzy Logic in Traffic Responsive Signal Control”, *FAC Proceedings Volumes*, 30 (8), 699-703.
141. Seyfried, A., Passon, O., Steffen, B., Boltes, M., Rupprecht, T. and Klingsch, W. (2009). “New Insights into Pedestrian Flow through Bottlenecks”. *Journal of Transportation Science*, 43 (3), 395-406.
142. Seyfried, A., Portz, A. and Schadschneider, A. (2010). “Phase Coexistence in Congested States of Pedestrian Dynamics”. *International Conference on Cellular Automata*, 496-505.
143. Seyfried, A., Steffen, B. and Lippert, T. (2006). “Basics of Modelling the Pedestrian Flow”. *Physica A: Statistical Mechanics and its Applications*, 368 (1-1), 232-238.
144. Sharma, N., Chaudhry, K. and Rao, C.C. (2005). “Vehicular pollution modelling using artificial neural network technique: a review”. *Journal of scientific and industrial research*, 64(9), 637-647.
145. Shimada, A. and Arita, D. (2006). “Dynamic control of adaptive mixture-of-Gaussians background model”. *In IEEE International Conference on Video and Signal Based Surveillance*, 5.
146. Smith B,L. and Demetsky M.J. (1994). “Short-term traffic flow prediction: neural network approach”. *Transportation Research Record*, 1453, 98–104.

147. Stauffer, C. and Grimson, W. (1999). “Adaptive background mixture models for real-time tracking”. *In IEEE Conference on Computer Vision and Pattern Recognition*, 246–252.
148. Steffen, B. and Seyfried, A. (2010). “Methods for measuring pedestrian density, flow, speed and direction with minimal scatter”. *Physica A*, 389, 1902-1910.
149. Stenger, B., Ramesh, V., Paragios, N., Coetzee, F. and Buhmann, J.M. (2001). “Topology free hidden Markov models: application to background modeling”. *In IEEE International Conference on Computer Vision*, pp. 294–301.
150. Streit, R.L. and Luginbuhl, T.E. (1994). “Maximum likelihood method for probabilistic multi-hypothesis tracking”. *In Proceedings of SPIE International Symposium, Signal and Data Processing of Small Targets*, 2335 (24), 394–405.
151. Sun, C.T. (1994). “Rule-Base Structure Identification in an Adaptive-Network-Based Fuzzy Inference System”. *IEEE Transactions on Fuzzy Systems*, 2 (1).
152. Szarvas, M., Yoshizawa, A., Yamamoto, M. and Ogata, J. (2005). “Pedestrian Detection with Convolutional Neural Networks”. *IEEE Proceedings. Intelligent Vehicles Symposium*.
153. Tajima, Y., Nagatani, T. and Adler, J. (2001). “Scaling behavior of crowd flow outside a hall”. *Physica A: Statistical Mechanics and its Applications*, 292(1-4), 545–554.
154. Tanaboriboon, Y. and Guyano, J. (1989). “Level-of-service standards for pedestrian facilities in Bangkok: A case study”. *ITE journal*, 59, 39-41.
155. Tanaboriboon, Y., Hwa, S.S. and Chor, C.H. (1986). “Pedestrian characteristics study in Singapore”. *Journal of Transportation Engineering*, 112, 229-235.
156. Tao, H., Sawhney, H.S. and Kumar, R. (2002). “Object tracking with bayesian estimation of dynamic layer representations". *IEEE Transaction Pattern Analysis and Machine Intelligence*, 24(1), 75-89.
157. Teodorovic, D. and Kikuchi, S. (1990). “Transportation route choice model using fuzzy inference technique”. *In Proceedings of IEEE Computer Society Press*, 140–145.
158. Tsai, D.M. and Lai, S.C. (2009). “Independent component analysis-based background subtraction for indoor surveillance”. *IEEE Transactions on Image Processing*. 18(1), 158–167.

159. Underwood, R.T. (1961). “Speed, volume and density relations”. *In Quality and Theory of Traffic Flow: A Symposium. Bureau of Highway Traffic, Yale University, New Haven, CT, USA*, 141–188.
160. Virkler, M. R. and Elayadath, S. (1994). “Pedestrian speed-flow-density relationships”. *Transportation Research Record*, 1438, 57-58.
161. Wang, J., Bebis, G. and Miller, R. (2006). “Robust video-based surveillance by integrating target detection with tracking”. *In IEEE Computer Vision and Pattern Recognition Workshop*, 137.
162. Wang, L., Ning, H.Z. and Hu, W.M. (2002). “Gait recognition based on procrustes statistical shape analysis”. *In International Conference on Image Processing*, 433–436.
163. Wang, L.R.Z. (1996). “An Algorithm of Extracting Fuzzy Rules Directly from Numerical Examples by Using FNN”. *IEEE International Conference on Systems, Man and Cybernetics. Information Intelligence and Systems*.
164. Wang, X., Ma, X. and Grimson, W.E.L. (2009). “Unsupervised activity perception in crowded and complicated scenes using hierarchical Bayesian models”. *In IEEE Transactions on Pattern Analysis and Machine Intelligence*, 31 (3), 539–555.
165. Wei, L., Jianhua, W. and Qin, L. (2007). “Study on Moving Object Tracking Algorithm in Video Images”. *IEEE Conference on Electronic Measurement and Instruments*, 810-816.
166. Wei, L., Jianhua, W. and Qin, L. (2007). “Study on Moving Object Tracking Algorithm in Video Images”. *IEEE Conference on Electronic Measurement and Instruments*, 810-816.
167. Weidmann, U. (1993). “Transporttechnik der Fufiganger. Schriftenreihe des IVT 90”. *ETH Zurich*.
168. Weifeng, Y. and Hai, T.K. (2011). “A model for simulation of crowd behaviour in the evacuation from a smoke-filled compartment”. *Physica A*, 390, 4210–4218.
169. Weinland, D., Ronfard, R. and Boyer, E. (2006). “Free viewpoint action recognition using motion history volumes”. *Computer Vision Image Understanding*, 104(2–3), 249–257.
170. Welch, G. and Bishop, G. (2006). “An introduction to the Kalman Filter”. *In University of North Carolina at Chapel Hill, Department of Computer Science. Tech. Rep*.

171. Wolf, P.R. and Dewitt, B. A. (2000). "Elements of Photogrammetry with Applications", *in GIS, 3rd edn. McGraw-Hill, New York, NY, USA.*
172. Xiaofei, J. and Honghai, L. (2010). "Advances in view-invariant human motion analysis: a review". *IEEE Transactions on Systems, Man, and Cybernetics, Part C (Applications and Reviews)*, 40(1), 13–24.
173. Yang, C., Duraiswami, R. and Davis, L. (2005). "Fast Multiple Object Tracking via a Hierarchical Particle Filter". *IEEE International Conference on Computer Vision*, 212-219.
174. Yeh, C.Y., Jeng, W.H.R. and Lee, S.J. (2011). "Data-Based System Modeling Using a Type-2 Fuzzy Neural Network with a Hybrid Learning Algorithm". *IEEE Transactions on Neural Networks*, 22(12), 2296-2309.
175. Yi, Z. and Liangzhong, F. (2010). "Moving Object Detection Based on Running Average Background and Temporal Difference". *In International Conference on Intelligent Systems and Knowledge*, 270-272.
176. Yusupbekov, N.R., Marakhimov, A.R., Igamberdiev, H.Z. and Umarov, Sh.X. (2016). "An Adaptive Fuzzy-Logic Traffic Control System in Conditions of Saturated Transport Stream". *The Scientific World Journal*, 1-9.
177. Zadeh, L.A. (1965). "Fuzzy sets". *Information and Control*, 8 (3).
178. Zhang, J. and Seyfried, A. (2013). "Comparison of bidirectional pedestrian flows by experiments". *arXiv:1312.2475*.
179. Zhang, J., Klingsch, W., Schadschneider, A. and Seyfried, A. (2011). "Transitions in pedestrian fundamental diagrams of straight corridors and T-junctions". *Journal of Statistical Mechanics: Theory and Experiment*.
180. Zhang, J., Klingsch, W., Schadschneider, A. and Seyfried, A. (2012). "Ordering in bidirectional pedestrian flows and its influence on the fundamental diagram". *Journal of Statistical Mechanics: Theory and Experiment*.
181. Zhang, T., Liu, Z., Lian, X. and Wang, X. (2010). "Study on Moving-Objects Detection Technique in Video Surveillance System". *IEEE Control and Decision Conference*, 2375 – 2380.
182. Zhang, W., Zhong, X. and Xu, F.Y. (2006). "Detection of moving cast shadows using image orthogonal transform". *In 18th International Conference on Pattern Recognition*, 626–629.
183. Zhao, L. and Thorpe, C.E. (2000). "Stereo-and neural network-based pedestrian detection". *IEEE Trans Intelligent Transportation System*, 1(3), 148 154.

184. Zheng, W., Lee, D.H. and Shi, Q. (2006). “Short-Term Freeway Traffic Flow Prediction: Bayesian Combined Neural Network Approach”. *Journal of Transportation Engineering*, 114-121.
185. Zhiqiang, W., Xiaopeng, J. and Peng, W. (2006). “Real-time moving object detection for video monitoring systems”. *Journal of Systems Engineering and Electronics*, 17 (4), 731 -736.
186. Zhong, H., Shi, J. and Visontai, M. (2004). “Detecting unusual activity in video”. *In IEEE Computer Society Conference on Computer Vision and Pattern Recognition*, 819–826.
187. Zhong, H., Shi, J. and Visontai, M. (2004). “Detecting unusual activity in video”. *In IEEE Computer Society Conference on Computer Vision and Pattern Recognition*, 819–826.

PUBLICATIONS

International Journals:

1. **Yugendar, Poojari** and Ravi Shankar, K.V.R. (2018) "Crowd behaviour analysis at mass gathering events" *Journal of KONBiN*, Volume 46, 2018, Issue 1, pp 5-20. (**Scopus**) (**Published**)
2. **Yugendar, Poojari** and Ravi Shankar, K.V.R. (2018) "Analysis of crowd flow parameters using Artificial Neural Network" *Journal of Transport and Telecommunication Engineering*, 2018, volume 19, no. 4, 335-345. (**Scopus**) (**Published**)
3. **Yugendar, Poojari** and Ravi Shankar, K.V.R. (2018) "Multi Regime modelling of large congregation" *The Institution of Civil Engineers – Transport*, https://doi.org/10.1680/jtran.18.00077. (**SCI**) (**Published**)
4. **Yugendar, Poojari** and Ravi Shankar, K.V.R. "The Effect of Physical Factors on Crowd Walking Behavior at Religious Gatherings", *Quality & Quantity, International Journal of Methodology*, volume 53, issue 6, November, 2019, 2969-2982. (**Published**) (**SCOPUS**)
5. **Yugendar, Poojari** and Ravi Shankar, K.V.R. "Neuro-Fuzzy based crowd speed analysis at mass gathering events" *Jordan Journal of Civil Engineering*, volume 13, issue 3, 2019. (**Published**) (**SCOPUS**)
6. **Yugendar, Poojari** and Ravi Shankar, K.V.R. "Experimental Study on Crowd Flow Behaviour through Bottlenecks" *Transportation Letters*, the International Journal of Transportation and Research. (**Under Review**) (**SCI**)
7. **Yugendar, Poojari** and Ravi Shankar, K.V.R. "Experimental Study on Estimation of Door Capacity under Emergency Situations, *Iranian Journal of Science and Technology, Transactions of Civil Engineering.* (**Under Review**) (**SCI**)

International Conferences:

1. **Yugendar, Poojari** and Ravi Shankar, K.V.R. (2019) "Experimental Study on Crowd Flow Behaviour through Bottlenecks" *98th Annual Meeting, Transportation Research Board*, Washington Convention Centre, Washington DC, USA.
2. **Yugendar, Poojari** and Ravi Shankar, K.V.R. (2016) "Crowd behaviour analysis through video surveillance", *12th Transportation Planning and Implementation methodologies for Developing Countries*, 19-21 December, 2016, Bombay, India.

National Conferences:

1. Anand, Punuri, **Yugendar, Poojari** and Ravi Shankar, K.V.R (2018) "Crowd Behavior Analysis and Tracking using Tracker", *5th Colloquium Transportation Systems Engineering and Management*, National Institute of technology, Warangal, India.
2. Govinda, Lalam., Eswar, Sala., **Yugendar, Poojari** and Ravi shankar, K.V.R. (2018) " Tool Kit to Evaluate the Mid-Block in Perception to Pedestrian Crossings Behavior" *5th Colloquium Transportation Systems Engineering and Management*, National Institute of technology, Warangal, India.